NICOLAUS COPERNICUS UNIVERSITY IN TORUŃ

FACULTY OF BIOLOGICAL AND VETERINARY SCIENCES

Liliana Siekacz

A millennium-long blue ring record in bristlecone pine (*Pinus longaeva* D.K. Bailey) - establishment and paleoclimatic interpretation

Dissertation for a doctoral degree

Supervisors:

Dr. Charlotte Pearson, Associate Professor, University of Arizona

Dr hab. Marcin Koprowski, prof. UMK

Toruń 2024

Acknowledgments

As I bring the chapter of my doctoral studies to a close, I do so filled with the deepest sense of gratitude for the opportunities and support I have received along the way. It is with sincere appreciation that I take this moment, as I open the thesis, to acknowledge those who have been instrumental in this journey.

First and foremost, I wish to express my deepest thanks to my supervisors.

I am profoundly grateful to Dr. hab. Marcin Koprowski for offering me the opportunity to conduct my research under his guidance within the Department of Ecology and Biogeography. You fostered a safe and supportive academic environment, so different from the one I experienced in my previous position, allowing me the freedom to independently explore my research interests, for which I am truly appreciative.

My heartfelt thanks also go to Dr. Charlotte Pearson for giving me the honor of working under her supervision and for her unwavering belief in me. Your steadfast commitment has been fundamental to the successful completion of my doctoral dissertation. I'm grateful for the opportunity to conduct the laboratory part of my work at your institution, the Laboratory of Tree Ring Research (University of Arizona), one of the world's leading dendrochronological laboratories, where I was wholeheartedly welcomed and given support and access to the research facilities. It so happened that my research visit there took place during the most strict part of the Covid-19 lockdown, your presence and aid were invaluable for me. I thank you for your constant support and patience, for the countless hours of videoconferences during which, I could consult you on my research ideas, and discuss the many questions and challenges that arose in the research process and the doctoral studies. Your thoughtful feedback and mentorship have substantially contributed to the refinement of my work and the resultant articles that comprise this thesis. I'm deeply grateful for your help and mentoring, for your unbreakable positive attitude that spread the light in the darkest moments and hardest challenges of my doctoral journey. Your kindness, your invaluable insights, your contagious passion and optimism, your expertise and wisdom, the open-door policy - constitute for me the role model both in my academic and personal life, from which I will continue to strive to learn.

I would like to thank Dr. Matthew Salzer for entrusting me with access to his extensive and invaluable collection of bristlecone pine samples, developed over many

years of fieldwork campaigns. It has been a great privilege for me to work with such a remarkable and iconic species.

I want to express my deepest gratitude to my Family.

To my parents, Katarzyna and Ryszard, I owe my deepest gratitude. Through your example, you instilled in me the core values of hard work and perseverance, shaping me into the person I am today. You always encouraged learning and curiosity, kept your fingers crossed for me, and motivated me to embrace life challenges and never give up. The safe, stable, and happy home environment you created for us has always been a sanctuary through all life challenges and a place to recharge my batteries. For your love and dedication, for being both my greatest supporters and harshest critiques right when this was needed – I offer my heartfelt thanks.

To my brothers, Mikołaj and Marcin, for simply being who they are—I cannot imagine what life would have been like if I had been an only child for longer than the first eight years of my life.

Last but not least, I want to thank my academic colleagues and dear friends, Paweł Matulewski and Agata Buchwał , for always offering me their kind words of support and encouragement.

This work was supported by the project Universitas Copernicana Thoruniensis In Futuro – modernization of the Nicolaus Copernicus University as part of the Integrated University Program (project no. POWR.03.05.00-00-Z302/17-00), and by the National Science Center under my Preludium grant no. 2019/35/N/ST10/04366. Additionally, Dr. Charlotte Pearson contributed both financial and equipment support at various stages of this work.

Table of contents

List of abbreviations

BR/BRs – blue ring/rings

BRn – blue ring number

FR/FRs – frost ring/rings

EWFR/EWFRs – earlywood frost ring/rings

LWFR/LWFRs – latewood frost ring/rings

MXD – maximum latewood density

RW/RWs – ring width/ ring widths

RWI – ring width index

Abstract

The study of past climates, known as paleoclimatology, plays a crucial role in understanding the Earth's climate system and predicting future climate changes. Within this field, dendroclimatology - using tree rings to infer past climatic conditions - has proven to be a particularly valuable method. Tree rings provide annual records of climate variability, and their width, density, and composition can reflect past temperature, precipitation, and other environmental factors.

Bristlecone pine (*Pinus longaeva*), known for its longevity and resilience in harsh climates grows, at high elevations in the White Mountains of California and other high mountain ranges of Nevada and Utah, making it a particularly sensitive indicator of environmental changes. This sensitivity, coupled with its long lifespan, makes it an ideal candidate for studying past climate variability over millennia. Upper tree line populations correlate with temperature, while lower tree line stands offer a resource for precipitation reconstructions.

The discovery of "blue rings" in this and other species opens possibilities to add a new layer of information to climate reconstructions derived from these trees.

The formation of blue rings (BRs) is a temperature-dependent process in which cooler temperatures during and after the late growing season disrupt the lignification of cell walls, resulting in underlignified cells that appear bluish when stained with Safranine and Astrablue. To address the need for more precise tools to reconstruct past climate conditions, particularly short-term and subtle temperature variations that are not well captured by other proxies, this study developed the use of blue rings as a sensitive thermal indicator in bristlecone pine, arguing that they may offer a more accurate proxy for past cooling episodes than traditional tree ring indicators.

Previous studies have established a strong connection between growth minima, frost rings, and growing season cooling and frost episodes. This connection has been particularly useful in reconstructing volcanic eruptive histories causing cooling episodes.

However, traditional dendroclimatological methods have limitations in their ability to capture short-term and subtle climatic fluctuations. While frost rings provide valuable information, they are less sensitive to milder cooling events or late-season temperature drops. Tree ring widths, on the other hand, are less capable to accurately capture

interannual and intra-annual temperature variations due to strong autocorrelation resulting from biological memory, aggregating climate signals from the entire growing season and even from previous seasons. Tree ring width-based temperature reconstructions frequently exhibit a lagged and smoothed-out climate response to abrupt cooling following volcanic eruptions compared to other proxies. This research addresses the need for a more sensitive and reliable proxy that can capture these subtle, high-frequency variations, thereby improving the accuracy of paleoclimatic reconstructions, complementing traditional dendroclimatological proxies.

Specifically, this study investigates whether blue rings in bristlecone pine can serve as a more sensitive proxy for late-season cooling events by developing a comprehensive blue ring time series from 83 cores and covering almost two millennia. By comparing blue ring occurrence with available climatic data from 1895 to 2008, we first investigate the connection between temperature, topography and blue ring formation. Further, across the timespan of the past eleven centuries, we explore the association between blue rings and historical volcanic eruptions, and analyze how the information contained in blue rings is distinct from, and complementary to frost ring, TRW, and MXD-based paleoclimate inferences.

We find that blue rings in Bristlecone pines are significantly influenced by late-season temperature drops, particularly in September. However, apart from the influence of September, our findings also reveal that blue rings form as a result of a more complex interplay of climatic factors, with lower temperatures in April, June, and August and higher temperatures in February and October also playing a role. The occurrence and intensity of blue rings decrease gradually with elevation below the upper tree line, indicating that topography and elevation modulate their formation.

We established a strong, statistically significant connection between BR formation and volcanic activity. These results suggest a causal link between volcanic eruptions and BR formation through volcanically induced cooling with tropical eruptions showing the strongest correlation.

Not all BR signals are linked to significant volcanic eruptions, just as not all RW and/or MXD minima correspond to known volcanic events. This is because not every cold summer in a particular location can be attributed to volcanic activity, and similarly, not all eruptions lead to cooler summers. While BRs offer a sensitive record of cooling episodes,

they can also be a noisy proxy, with many low BR signal years reflecting localized cold snaps rather than large-scale cooling.

Our results demonstrate that blue rings tend to form more often in wider or neutral rings and frequently precede negative pointer years or growth minima. This suggests that BRs can provide valuable insights into late-season or post-growing season cooling events, which would no longer affect the ring width of that year. Longer cooling periods, such as those linked to climatically effective volcanic eruptions, can impact climatic conditions after the completion of radial growth and into the following seasons. As a result, while these events may cause a delayed response in ring widths, BRs can signal the onset of such events earlier. Moreover, BRs are better suited than ring widths to record cooling episodes, as they form when a sudden temperature drop halts the lignification process, leaving a permanent mark of underlignified cells. In contrast, ring widths are influenced by biological memory and autocorrelation, which can delay the cooling evidence and smooth out its magnitude.

Finally, we demonstrate how a multiproxy approach - integrating frost rings, ring widths, maximum latewood density (MXD), ice-core data, and BRs - can enhance our understanding of the climate system's response to volcanic eruptions.

Overall, the study expands the understanding of the factors that influence blue ring formation. While previous research has suggested a link between blue rings and temperature, this study provides a more detailed analysis of the specific climatic conditions that lead to their formation. By using a large dataset of tree cores and applying statistical modeling techniques, the research offers a comprehensive assessment of the factors that influence blue ring formation, including temperature, elevation, and topography. Although earlier studies established a tentative connection between blue ring formation and volcanic activity, we reinforced this connection with a larger dataset and longer timeline, and highlighted specific nuances that BRs can contribute to our knowledge of the timing and spatial extent of climatic consequences of specific eruptions.

The use of blue rings as a proxy for past cooling events could enhance the accuracy of climate reconstructions improving our understanding of how climate has changed over millennia providing an additional layer of information about abrupt short-term events that might otherwise not be captured by tree ring-based reconstructions. BRs could also help in untangling the complex interactions between volcanoes, climate, and human activity at sub-annual resolution. This is because societal resilience or vulnerability is highly reliant

on agricultural productivity, which can be influenced by short-term weather extremes that are usually not reflected in the traditional TRW and MXD chronologies. This better understanding of past climate variability could lead to better predictions of future climate trends, particularly in relation to volcanic activity and other large-scale climate forcings, with possible abrupt consequences for societies.

Streszczenie

Paleoklimatologia – nauka zajmująca się badaniem zmian klimatu w przeszłości Ziemi, odgrywa kluczową rolę w zrozumieniu systemu klimatycznego obecnie oraz przewidywaniu przyszłych zmian klimatycznych. W tej dziedzinie dendroklimatologia – nauka wykorzystująca słoje drewna do wnioskowania o przeszłych warunkach klimatycznych – stanowi szczególnie cenne źródło. Słoje drzew dostarczają rocznych zapisów zmienności klimatu, a ich szerokość, gęstość i skład mogą odzwierciedlać przeszłe temperatury, opady i inne czynniki środowiskowe.

Sosna długowieczna (*Pinus longaeva*), znana ze swojej długowieczności i odporności w trudnych warunkach klimatycznych, rośnie na dużych wysokościach w Górach Białych w Kalifornii i innych wysokich pasmach górskich w Nevadzie i Utah, co czyni ją szczególnie wrażliwym wskaźnikiem zmian środowiskowych. Ta wrażliwość w połączeniu z niezwykle długim wiekem jakie osiągają osobniki tego gatunku sprawia, że jest ona idealnym źródłem materiałów do badania przeszłej zmienności klimatu na przestrzeni tysiącleci. Sekwencje przyrostowe populacji z górnej granicy lasu korelują z temperaturą, podczas gdy drzewostany dolnej granicy lasu oferują źródło do rekonstrukcji opadów.

Odkrycie obecności „niebieskich pierścieni" w tym i innych gatunkach drzew otwiera możliwość dodanie nowej warstwy informacji do rekonstrukcji klimatu uzyskanych z tych drzew.

Formowanie się niebieskich pierścieni jest procesem zależnym od temperatury, w którym niższe temperatury w trakcie i po późnym sezonie wegetacyjnym przerywają proces lignifikacji, co skutkuje wytworzeniem nie w pełni zlignifikowanego drewna, które można rozpoznać po niebieskim zabarwieniu ścian komórkowych na preparatach cienkich drewna zabarwionych Safraniną i Astrablue. Aby sprostać potrzebie bardziej precyzyjnych narzędzi do rekonstrukcji przeszłych warunków klimatycznych, w szczególności krótkotrwałych i subtelnych wahań temperatury, które nie są dobrze odzwierciedlane przez inne źródła, w niniejszej pracy opracowano zastosowanie niebieskich pierścieni jako czułego wskaźnika niższych temperatur w chronologii sosny długowiecznej, argumentując, że mogą one oferować dokładniejszy znacznik przeszłych epizodów ochłodzeń niż tradycyjne metody dendrochronologiczne.

Wcześniejsze badania wykazały silny związek między minimami wzrostu, oraz pierścieniami mrozowymi a ochłodzeniem i przymrozkami w trakcie sezonu wegetacyjnego. Ten związek okazał się szczególnie przydatny w rekonstrukcji historii erupcji wulkanicznych powodujących niektóre z epizodów ochłodzenia.

Jednak tradycyjne metody dendroklimatologiczne są obciążone ograniczeniami w zakresie zdolności do uchwycenia krótkoterminowych i subtelnych wahań temperatury. Podczas gdy słoje mrozowe dostarczają cennych informacji, są one mniej wrażliwe na łagodniejsze zjawiska ochłodzenia lub spadki temperatury na końcu i po sezonie wegetacyjnym. Z drugiej strony szerokości słojów drewna są mniej zdolne do uchwycenia wahań temperatury w skali rocznej i ponad rocznej ze względu na silną autokorelację wynikającą ze zjawiska pamięci biologicznej, jako że przyrosty roczne agregują sygnał warunków wzrostu w skali całego sezonu wegetacyjnego a czasem nawet poprzednich sezonów. Rekonstrukcje temperatury oparte na szerokościach przyrostów rocznych często wykazują opóźnioną i wygładzoną odpowiedź klimatu w postaci ochłodzeń będących skutkiem efektywnych klimatycznie erupcji wulkanicznych w porównaniu z innymi wskaźnikami. Niniejszy projekt odpowiada na potrzebę opracowania bardziej czułego wskaźnika, który mógłby uchwycić bardziej subtelne wahania temperatury o większej częstotliwości, zwiększając tym samym dokładność rekonstrukcji klimatycznych, uzupełniając tradycyjne wskaźniki dendroklimatyczne.

W szczególności, w niniejszej pracy zajęto się zbadaniem, czy niebieskie pierścienie w sośnie długowiecznej mogą służyć jako bardziej czuły wskaźnik epizodów ochłodzeń pod koniec sezonu wegetacyjnego poprzez opracowanie kompleksowego szeregu czasowego niebieskich pierścieni z 83 wywiertów drewna sosny długowiecznej, pokrywających prawie dwa tysiąclecia. Porównując występowanie niebieskich pierścieni z dostępnymi danymi klimatycznymi z lat 1895–2008, najpierw zbadano związek między temperaturą, topografią i powstawaniem niebieskich pierścieni. Ponadto, na przestrzeni ostatnich jedenastu stuleci, zbadano związek między niebieskimi pierścieniami a historycznymi erupcjami wulkanów i przeanalizowano, w jakim zakresie informacje zawarte w niebieskich pierścieniach różnią się od i uzupełniają informacje na temat zmian klimatu w przeszłości pochodzące z pierścieni mrozowych, chronologii szerokości przyrostów rocznych drewna oraz chronologii maksymalnej gęstości drewna późnego.

W niniejszej pracy odkryto, że na formowanie się niebieskich pierścieni w sośnie długowiecznej istotny wpływ mają spadki temperatury pod koniec sezonu wegetacyjnego, szczególnie we wrześniu. Jednak poza wpływem temperatur września zaobserwowano

również bardziej złożone współdziałanie czynników klimatycznych z kilku miesięcy, w tym niższe temperatury w kwietniu, czerwcu i sierpniu oraz wyższe temperatury w lutym i październiku. Występowanie i intensywność niebieskich pierścieni stopniowo maleje wraz ze spadkiem wysokości poniżej górnej linii granicy lasu, wskazując, że topografia terenu i wysokość nad poziomem morza również modulują ich powstawanie.

Znaleziono silny, i statystycznie istotny związek między powstawaniem niebieskich pierścieni a aktywnością wulkaniczną. Wyniki te wskazują na związek przyczynowo skutkowy między erupcjami wulkanów a powstawaniem niebieskich pierścieni poprzez ochłodzenie wywołane przez wulkanizm, przy czym erupcje tropikalne wykazują najsilniejszą korelację.

Nie wszystkie lata wykazujące niebieskie pierścienie są powiązane ze znaczącymi erupcjami wulkanicznymi, tak jak nie wszystkie minima szerokości przyrostów rocznych i/lub maksymalnej gęstości drewna późnego (MXD) odpowiadają znanym wydarzeniom wulkanicznym. Dzieje się tak, ponieważ nie każde zimne lato w danym miejscu można przypisać aktywności wulkanicznej, i podobnie nie wszystkie erupcje prowadzą do letnich ochłodzeń. Niebieskie pierścienie oferują wrażliwy zapis epizodów ochłodzenia, ale mogą stanowić zaszumione źródło informacji, z wieloma latami o niskim udziale niebieskich przyrostów odzwierciedlającymi lokalne przymrozki, a nie wielkoskalowe ochłodzenie.

Nasze wyniki pokazują, że niebieskie pierścienie mają tendencję do tworzenia się częściej w szerszych lub neutralnych pierścieniach przyrostów rocznych i często poprzedzają lata wskaźnikowe lata ujemne lub minima wzrostu. Sugeruje to, że mogą one dostarczać cennych spostrzeżeń na temat epizodów ochłodzenia pod koniec sezonu lub po sezonie wegetacyjnym, które nie miałyby już wpływu na szerokość przyrostu w danym roku. Dłuższe okresy ochłodzenia, takie jak te związane z klimatycznie efektywnymi erupcjami wulkanicznymi, mogą wpływać na warunki klimatyczne po zakończeniu wzrostu radialnego i w kolejnych sezonach. W rezultacie, podczas gdy ochłodzenia te mogą powodować opóźnioną reakcję szerokości przyrostów, niebieskie pierścienie mogą sygnalizować początek takich zdarzeń wcześniej. Co więcej, niebieskie pierścienie stanowią lepszy indykator ochłodzeń niż szerokości przyrostów rocznych, ponieważ powstają, gdy nagły spadek temperatury zatrzymuje proces lignifikacji, pozostawiając trwały ślad w postaci nie w pełni zlignifikowanych komórek drewna. Natomiast szerokości przyrostów w skutek zjawiska pamięci biologicznej oraz autokorelacji, mogą wskazywać na ochłodzenie z opóźnieniem oraz wygładzać jego wielkość.

Ostatecznie pokazano również, w jaki sposób podejście integrujące wiele źródeł — w tym pierścienie mrozowe, szerokości przyrostów, maksymalną gęstość drewna późnego, dane z rdzeni lodowych i niebieskie przyrosty — może zwiększyć naszą wiedzę na temat reakcji systemu klimatycznego na erupcje wulkaniczne.

Praca ta poszerza wiedzę na temat czynników wpływających na powstawanie niebieskich pierścieni. Podczas gdy wcześniejsze badania sugerowały związek między niebieskimi pierścieniami a temperaturą, niniejsza praca przedstawia bardziej szczegółową analizę konkretnych warunków klimatycznych, które prowadzą do ich powstawania. Dzięki wykorzystaniu dużej ilości wywiertów z drzew i zastosowaniu technik modelowania statystycznego, praca przedstawia kompleksową analizę czynników wpływających na powstawanie niebieskich pierścieni, w tym temperatury, wysokości i topografii. Chociaż wcześniejsze badania wskazały na wstępny związek między powstawaniem niebieskich pierścieni a aktywnością wulkaniczną, tutaj wzmocniono ten związek na większym zestawie danych i dłuższej osi czasu oraz zilustrowano konkretne przykłady nowych informacji, jakie niebieskie pierścienie mogą wnieść do naszej wiedzy na temat czasu i zasięgu przestrzennego skutków klimatycznych konkretnych erupcji.

Wykorzystanie niebieskich pierścieni jako wskaźnika przeszłych epizodów ochłodzenia może zwiększyć dokładność rekonstrukcji klimatu, poprawiając zrozumienie tego, jak klimat zmieniał się na przestrzeni tysiącleci, zapewniając dodatkową warstwę informacji o nagłych, krótkoterminowych zdarzeniach, które w przeciwnym razie mogłyby nie zostać uchwycone przez rekonstrukcje oparte na szerokościach przyrostu drzew. Mogą one również pomóc w rozwikłaniu złożonych interakcji między wulkanizmem, klimatem i działalnością człowieka w rozdzielczości ponad rocznej. Wynika to z faktu, że odporność lub podatność społeczeństw w dużym stopniu zależy od produktywności rolnictwa, na którą mogą wpływać krótkoterminowe ekstrema pogodowe, które zwykle nie są odzwierciedlone w tradycyjnych chronologiach szerokości przyrostów rocznych oraz maksymalnej gęstości drewna późnego. Lepsze zrozumienie przeszłej zmienności klimatu może przyczynić się do trafniejszych prognoz przyszłych trendów klimatycznych, szczególnie w odniesieniu do aktywności wulkanicznej i innych czynników klimatycznych o dużym zasięgu, których nagłe skutki mogą mieć wpływ na społeczeństwo.

Introduction

In climates with distinct seasonality, trees undergo a cycle of growth and a subsequent dormancy period each year, that results in the deposition of a layer of xylem – a radial annual growth increment with a characteristic internal structure. Changes in environmental conditions affect the pace of cambial division and further cell development, this results in the dimensional characteristics of annual increments that vary from one year to another. This variability is correlated with the climate parameter that is the most growth-limiting factor for a particular site, for example, at upper treeline and high latitude sites, the temperature is usually the dominant growth-limiting factor, whereas moisture availability dominates tree growth in arid environments. Trees as long-lived organisms, that lay down a ring of xylem each year, can record these environmental conditions in the parameters characterizing the growth rings, such as the ring width, the wood density, cellular dimensional parameters, the isotopic or elemental composition. Typically, in trees at a given site, the characteristics of radial growth increments retain the same pattern of signal of the dominant growth limiting factor. This offers the potential to reconstruct long histories of environmental variation from tree rings. This is achieved by using a set of dendrochronological methods that start from the specific tree ring parameter measurement and employ statistics to bring together large datasets of growth ring characteristics from trees. Individual and age-related trends are removed and groups of matching patterns from trees at the site level are combined together to build representative chronologies. These can then be used to reconstruct the dominant growth limiting factor at multi-centennial and even multimillennial scales. Super-imposed on these longer-term records are various markers for unusual, sudden onset events such as growing season frosts or geomorphic disturbances that can affect the dimensional and structural properties of individual tree rings. This can result in features such as ‘frost rings’ (LaMarche and Hirschboeck, 1984) intra-annual density fluctuations (Nabais et al., 2014), traumatic resin ducts (Stoffel, 2008), scars (Stoffel et al., 2005). Chronologies of these tree ring anomalies can be used to reconstruct the history of more specific conditions leading to their formation.

Blue rings, the object of this study, are continuous bands of axial tracheids characterized by reduced lignin content. They can be found both in earlywood and latewood (Crivellaro et al., 2018; Piermattei et al., 2015). If cell wall lignification is disrupted, the underlignified cells are left behind in the tree ring structure. Blue rings take

their name from the double staining by which they are revealed, when transverse thin-sections of the tree ring series are stained with safranin - staining cell walls richer in lignin red, and astrablue - staining cell walls richer in cellulose blue. Underlignified cells are displayed as blue/ish (compared to pink normally lignified cells) bands of cells in a radial file of cells constituting a tree ring. The double-staining procedure allows us to comprehensively track the effects of incomplete lignification in a tree ring at a cellular level.

Understanding the factors affecting lignification as well as the timing of this process within the developmental stages of xylem structure has further implications regarding the interpretation of the blue ring record, therefore it is necessary to provide background information related to the process of wood formation. Xylogenesis is a development process of new fully operational xylem tissue, which performs several functions in woody plants such as mechanical support, water and nutrient transport, storage of water, carbohydrates, and other compounds, as well as protection from pathogens by storing and distributing defensive compounds (Kozlowski and Pallardy, 1997). In conifers on average wood consists in c. 90% of tracheids performing mechanical support and water conduction functions, and in c. 10% of parenchyma cells, that are responsible for storage and radial transport of various compounds. Tracheid cells have to die off at the end of their development to be able to perform their functions, whereas parenchyma cells remain alive for a couple of years (Bollhöner et al., 2012). Conifer cell walls are generally composed of 40-50% of cellulose, 20-35% hemicelluloses, and 15-35% of lignin (Saranpää, 2003). Lignin is the last structural element to be incorporated into the cell wall, it impregnates the main network of cellulose and hemi-cellulose matrix forming chemical bonds with non-cellulosic carbohydrates (Donaldson, 2001) and due to its chemical structure provides hydrophobicity, rigidity, and durability (Barnett and Jeronimidis, 2003; Zhong and Ye, 2009).

The xylem formation process consists of five major stages: (1) the division of a cambial cell that creates a new xylem cell; (2) the enlargement of the newly formed xylem cell; (3) the deposition of cellulose and hemi-cellulose to build the secondary cell wall; (4) the impregnation of the cell walls with lignin; and finally, (5) the programmed cell death (Rathgeber et al., 2016).

Much effort has been invested in exploring the molecular mechanisms, as well as the biochemical and biophysical pathways that trigger and regulate xylogenesis. This includes examining phytohormones and gene expression patterns involved in controlling

the process of cell division, xylem chemical constituents' synthesis, its structural development and the programmed death of the tracheary elements (Cosgrove, 2005; Du and Groover, 2010; Mutwil et al., 2008; Perrot-Rechenmann, 2010; Ursache et al., 2013; Vanholme et al., 2010; Zhong and Ye, 2015).

This introduction, however, is going to delve in more detail into the external climatic factors affecting wood formation since these are of interest for studies of past climate change and of direct relevance to the focus of this thesis. External environmental conditions affecting specific stages of xylogenesis result in the formation of xylem with specific characteristics, which once quantified, can then be used to reconstruct these causal environmental conditions. External factors initiating and controlling cambial reactivation, cell enlargement, and cell wall thickening are relatively well understood. Intra-annual kinetics of xylem structure development in several coniferous species have revealed (Cuny et al., 2014) the intricate connections between the duration and rate of each phase of xylogenesis and the structural properties of the tree rings under normal conditions. The onset of cambial cell division in conifers is proven to be driven mostly by the photoperiod and thermal conditions (temperature, winter chilling, and spring forcing) (Begum et al., 2013; Delpierre et al., 2019; Huang et al., 2020; Rossi et al., 2007) as well as moisture availability (Ren et al., 2015; Ziaco et al., 2018) in drought limited sites. Drought stress can affect cell enlargement since turgor is the main driving force of cell enlargement (Abe et al., 2003), hence multiple studies linked intra-annual density fluctuations and false rings to moisture availability during the growing season (Arzac et al., 2021; Gao et al., 2021; Morino et al., 2021; Nabais et al., 2014; Versace et al., 2021), however it may also be controlled by temperature even months before the cells are formed (Eckstein, 2013). Cell wall thickening can also be affected by temperature (Castagneri et al., 2017; Fonti et al., 2013; Panyushkina et al., 2003) as well as moisture availability since it was observed that turgor can also impact the biosynthesis of secondary cell walls (Proseus and Boyer, 2006). Both cell enlargement and secondary cell wall deposition are also modulated by the rate and duration of each of the phases (Cuny et al., 2014). The first three phases of xylogenesis (cambial reactivation, cell enlargement, and cell wall thickening), which have their expression in the total radial growth of a tree in a particular year are mainly affected by temperature and/or moisture availability. Thus ring widths and other tree ring dimension-related parameters such as quantitative wood anatomy or MXD measurements are used to infer past climatic conditions of a site, temperature in high latitude and altitude temperature limited sites (Briffa et al., 2013; Büntgen et al., 2006; Esper et al., 2012; Salzer et al.,

2014a) and precipitation in drought limited areas (Salzer and Kipfmueller, 2005; Touchan et al., 2008). Discrete structural tree ring anomalies like frost rings (Glerum and Farrar, 1966; LaMarche and Hirschboeck, 1984) traumatic resin ducts (Bollschweiler et al., 2008; Matulewski et al., 2021), etc. can also be used to infer about past conditions and disturbances affecting the tree growth.

Blue rings studied in this work are not related to dimensional or structural characteristics of a tree ring, blue rings in essence are a visual manifestation of a biochemical response of a tree to external conditions leading to a reduction of a lignin content in parts of a tree ring.

Lignification is initiated by unknown factors at the cell corners in the primary wall and further spreads through the secondary wall towards the cell lumen. As it starts within the region furthest from the protoplast, and thus it's been suggested that there are initiation sites bound to specific regions of the cell wall, which begin the polymerization process. The identification of these has, however, so far remained elusive. The process of lignification in the middle lamella and primary wall typically commences after the initiation of secondary wall formation, whereas lignification of the secondary wall typically begins upon the completion of secondary wall formation (Donaldson, 2001). Coniferyl alcohol, sinapyl alcohol, p-coumaryl alcohol, the monomers of lignin are synthesized in the cytoplasm and released into the cell wall as monolignols or monolignol glucosides. Lignification is influenced by the surrounding carbohydrate matrix, which affects the shape and orientation of lignin lamellae (Atalla and Agarwal, 1985; Donaldson, 1994). Wall porosity regulates lignin concentration across cell wall regions, with the porous middle lamella and primary wall allowing more lignin deposition compared to the dense secondary cell wall (Fujino and Itoh, 1998). Lignin fills the voids in the carbohydrate matrix, binding chemically with hemicelluloses providing compression strength and waterproofing of conductive elements within the xylem.

The main inspiration to undertake the study of blue rings in my doctoral thesis in February 2020 was the work published by Piermattei et al., (2015) first describing this new, visually distinct tree ring anomaly in conifers. Lignin deposition in wood cell walls had previously been the topic of several studies (Donaldson, 2001, 1993, 1992, 1991; Gindl, 2001; Gindl et al., 2001, 2000; Trendelenburg, 1939) and (Gindl et al., 2000) demonstrated that lignin concentration of the terminal latewood cells in *Picea abies* (L.) Karst in alpine growing conditions correlates with autumn (September-October) temperature. However, Piermattei et al., (2015) first described that the conifer cell walls

with reduced lignin content can easily be distinguished with the use of double staining of wood thin-sections with safranine and astra blue dyes, proposed to name the discovered anomaly as “blue rings” and connected the observed blue stained underlignified bands of cells in *Pinus nigra* rings to not only be related to autumn temperature but more precisely with identified episodes of lower than usual air temperature toward the end of the local growing season (mid-late October). This work brought the topic of lignification to renewed attention for tree ring scientists from a paleoclimatic perspective for at least two reasons. First, although wood anatomical thin-section preparation is a laborious process, the implementation of a double staining technique to detect rings with reduced lignin content, made the detection and differentiation of these from normally lignified structures more efficient, and applicable for long tree ring series. Second, the hypothesized fine time resolution sensitivity to ephemeral cooling episodes of only a few days, offered a means to explore past cooling episodes with sub-annual resolution, raising the possibility of extracting a new layer of information unavailable from traditional ring width studies. It has to be taken into account however, that the detection of underlignified cells with the double staining procedure is only a qualitative indication and provides no quantitative information on the actual lignin content.

Since then, a number of studies have undertaken research utilizing BRs both in contemporary and past climate change studies. In the contemporary context BRs have been employed to study cold adaptation in assisted migration trials, investigating the influence of projected climate change on forest productivity and wood quality (Matisons et al., 2020; Montwé et al., 2018). Several studies have also utilized BRs as evidence and record of past cooling episodes (Büntgen et al., 2022; Helama et al., 2019; Piermattei et al., 2020; Tardif et al., 2020). Greaves et al., (2022)examined the continuity of BR formation within a tree stem. Montwé et al., (2018) in a study of cold signatures such as frost rings and BRs in Lodgepole pine (*Pinus contorta* Dougl. ex. Loud.) revealed that BRs and earlywood frost rings (EWFR) are linked to a late initiation of the growing season, an early end of the growing season, and a generally cool growing season. In a similar study, Matisons et al., (2020) analyzed the relationship between BRs and minimal summer temperature (July-September) in Scots pine (*Pinus sylvestris* L.) but found it to be very limited and inconsistent across the trials and provenances studied. While these studies have established a general link between reduced lignification and temperature, their findings are based on relatively short time series and/or low sample depths. Such exploratory findings based on relatively short contemporaneous sequences and low sample replication have limited

applications in a paleoclimatic context necessitating greater sample depth and longer time series to truly assess the full potential of blue rings as a paleoclimatic proxy.

In this study we present the chronology of BR occurrence in bristlecone pine (*Pinus longaeva* D.K. Bailey) for the period 164-2014, with a sample depth of 10 from 897 AD onwards, reaching 50 in 1428 AD, and a maximum of 83 from 1890 AD onwards. This is the longest and best replicated BR study to date.

Upper tree line chronologies from bristlecone pine, the world's longest living trees (Schulman, 1958; Schulman and Ferguson, 1956) have provided multimillennial insights into past temperature variations, and are well known for their sensitivity to volcanic forcing on climate (Salzer et al., 2014a, 2014b; Salzer and Hughes, 2007) and the cross-correlation of frost rings (structural damage in tree rings (Glerum and Farrar, 1966; Schweingruber, 2007) caused by a sudden, short-term onset of growing season frosts) with volcanic markers in ice core records (LaMarche and Hirschboeck, 1984; Sigl et al., 2015). These characteristics make the species a highly prospective object for detailed investigation of the potential new paleoclimatic proxy, that BRs might become, opening the door to gain relevant new paleoclimatic insights of subannual resolution that can be extended over most of the Holocene.

Preliminary explorations of blue rings in bristlecone pine (Tardif et al., 2020) confirmed their presence and have indicated that BRs may result from a late growing season start and a cool summer, with an associated interruption of lignification in the late growing season due to cool temperatures affecting the rate and duration of cell wall deposition. This work highlighted possibilities that blue rings in bristlecone pine may offer a more sensitive proxy for subtle changes in climate due to volcanism and other forcings than the well-established frost-ring record. However limited low sample depth and its concentration on only two short, discrete time intervals around 536 and 1965 CE warrants further comprehensive examination of BR record in bristlecone pine to explore the climatic parameters leading to BR formation and to develop a blue-ring climatic proxy which might eventually produce paleoclimatic information spanning several millennia.

In this study, we comprehensively research the thermal and topographical factors leading to and modulating BR formation in bristlecone pine, as well as establish the connection between BRs and volcanic eruptions and show how BR chronologies can be used to expand and complement our knowledge about past volcanic eruptions and their climatic effects.

Aim, hypothesis and objectives of the study

The overarching aim of my doctoral thesis was to investigate the environmental conditions affecting blue ring formation in bristlecone pine and to examine how the blue ring record can enhance our knowledge of the timing and spatial extent of past cooling episodes, particularly those associated with climatically effective volcanic eruptions.

The foundational hypothesis of this study is that blue rings in bristlecone pine might provide a more sensitive way to study the cooling effects of past volcanic eruptions than conventionally used tree ring parameters.

The specific objectives of the study are as follows:

1. Identify and investigate the key climatic parameters leading to blue ring formation. (P1)
2. Determine if and how elevation and topography modulate the blue ring record. (P1)
3. Evaluate the natural variability of the blue ring record and assess its paleoclimatic potential and limitations in bristlecone pine. (P1)
4. Create a blue ring record for bristlecone pine covering the last millennium. (P2)
5. Evaluate the relationship between blue ring formation and volcanic activity. (P2)
6. Analyze the relationship between blue rings and ring widths and determine if blue rings bring additional information about cooling episodes compared to traditional ring width chronologies. (P2)
7. Demonstrate on a set of selected volcanic eruption cases how bristlecone pine blue ring chronology brings additional information, in terms of, timing and spatial extent of climatic effects of volcanic eruptions compared to selected published traditional tree ring parameters (frost rings, ring widths, MXD) and derived climate reconstructions. (P2)

Publication list

1.	Siekacz, L., Pearson, C., Salzer, M., Soja-Kukieła N., Koprowski M. Blue rings in Bristlecone pine as a high resolution indicator of past cooling events. Climatic Change 177, 123 (2024). https://doi.org/10.1007/s10584-024-03773-8	IF – 4.8 $IF_{5\text{-year}}$ – 5.4 MNiSW – 140
2.	Submitted to: Science of the Total Environment Siekacz, L., Pearson, C., Salzer, M., Wojtasik J., Koprowski M. A 1100-year record of blue rings in Bristlecone pine provides new insights into volcanic forcing	IF – 8.2 $IF_{5\text{-year}}$ – 8.6 MNiSW – 200

Publication 1 - Blue rings in Bristlecone pine as a high resolution indicator of past cooling events

Climatic Change (2024) 177:123
https://doi.org/10.1007/s10584-024-03773-8

Blue rings in Bristlecone pine as a high resolution indicator of past cooling events

Liliana Siekacz[1] · Charlotte Pearson[2,3,6] · Matthew Salzer[2] · Natalia Soja-Kukieła[4] · Marcin Koprowski[1,5]

Received: 7 December 2023 / Accepted: 19 June 2024

Abstract

This study develops the use of 'blue rings' (BR), reflecting incomplete cell wall lignification, as a sensitive thermal indicator in bristlecone pine (*Pinus longaeva* D.K. Bailey). Using double-stained anatomical thin-sections, we explore the climatic and topographical constraints governing BR formation by developing a time-series from 83 cores and comparing BR occurrence with the full temporal span of available climatic data (1895–2008 CE). Lignification is temperature-dependent and continues at a cellular level post-radial growth completion. As BRs reflect incomplete lignification, they can serve as a higher resolution and more sensitive proxy for past cooling than previously established tree-growth indicators. Results indicate that blue ring formation is primarily induced by low September temperatures and responds more sensitively to cooling than the well-established frost-ring record. Additionally, the occurrence and intensity of blue rings decreases gradually below the upper tree line. Bristlecone pine BRs are demonstrated to have significant capacity to enhance the reconstruction of past cooling events in North America connected with both localized and hemispheric scale forcing over multi-millennial timescales. Given its unmatched longevity, the species offers an unparalleled potential for Holocene length climate reconstruction. Findings also highlight the potential for blue rings to provide a more nuanced understanding of past temperature fluctuations across multi-millennial timescales.

Keywords Blue rings · Lignification · Dendroclimatology · *Pinus longaeva* · Temperature reconstruction · Wood anatomy

✉ Liliana Siekacz
lilsie@doktorant.umk.pl

[1] Department of Ecology and Biogeography, Nicolaus Copernicus University, Lwowska 1, 87-100, Toruń, Poland

[2] Laboratory of Tree-Ring Research, The University of Arizona, 1215 E. Lowell St, 85721 Tucson, AZ, USA

[3] Geosciences, The University of Arizona, 1040 E. 4Th Street, 85721 Tucson, AZ, USA

[4] Centre for Statistical Analysis, Nicolaus Copernicus University, Chopina 12/18, 87-100, Toruń, Poland

[5] Centre for Climate Change Research, Nicolaus Copernicus University, Lwowska 1, 87-100 Torun, Poland

[6] Anthropology, The University of Arizona, 1009 E. South Campus, 85721 Tucson, AZ, USA

Published online: 19 July 2024

1 Introduction

The environmental constraints of cell wall lignification and the ecological interpretation of varying lignification levels in tree rings require further exploration. A range of early studies using UV microscopic lignin analysis first indicated a connection between the lower lignification of cell walls and lower temperatures (Trendelenburg 1939; Donaldson 1991; Gindl et al. 2000), highlighting the possibility that microscopic study of the lignification process could provide a very real capacity to track seasonal temperature change across a single year's growth. Gindl et al. (2000) went on to demonstrate that lignin concentration in the terminal latewood cells of Norway spruce (*Picea abies* (L.) H. Karst) correlated with autumn (September–October) temperature under alpine growing conditions. Recent advances in wood anatomical thin-section making techniques (Gärtner and Schweingruber 2013) have facilitated the further progress of such studies. In particular, the technique of double staining of transverse micro-sections of tree-ring series with Safranin, which stains red the cell walls which are richer in lignin, and Astrablue, which stains blue the cell walls which are richer in cellulose (coined 'blue rings' by Piermattei et al. 2015), has revealed a faster and more comprehensive way to track the lignification process at a cellular level in long tree ring records (Gerlach 1969; Schweingruber 2007). If lignification is disrupted, the unlignified cells are left behind in the wood structure to create time-series for the development of proxy records. Piermattei et al. (2015) found continuous layers of unlignified axial tracheids both in the earlywood and latewood of Black pine (*Pinus nigra* Arnold) from an advancing tree line in the central Apennines (Italy), and attributed BR occurrence in the last formed latewood cells to a temperature drop at the end of the local growing season (at that growth location, this was the end of October). Crivellaro et al. (2022), in a study covering large latitudinal (40°S and 80°N), and altitudinal (0–6150 m asl) gradients, and analyzing 1770 species of trees, shrubs, and herbaceous plants (with vascular cambium), argues that in the context of global tree line positioning, cell wall lignification is also temperature driven. Montwé et al. (2018) studied BRs and physical damage from frost in lodgepole pine (*Pinus contorta* Dougl. ex. Loud.), revealing that BRs and earlywood frost rings (EWFR) (structural damage characterized by the presence of collapsed/crushed/abnormal tracheids with lateral expansion and displacement of the rays (Glerum and Farrar 1966; Schweingruber 2007), can also be linked to a late initiation of the growing season, an early end of the growing season, and a generally cool growing season. Matisons et al. (2020) analyzed the relationship between BR and minimal summer temperature (July–September) in Scots pine (*Pinus sylvestris* L.) and found it very limited and inconsistent among analyzed trials and provenances. Despite establishing the connection between reduced lignification and temperature, all these studies were limited to relatively short time series and/or low sample depth. Such findings based on short contemporaneous sequences have limited application in a paleoclimatic context. Greater sample depth and longer time-series are required to truly assess the full potential of blue rings as a paleoclimatic proxy.

Upper tree line chronologies from bristlecone pine (*Pinus longaeva* D.K. Bailey) offer potential for constructing far longer than average time-series (Schulman et al. 1955; Schulman 1958) and have well demonstrated potential for multi-millennial reconstructions of temperature, which connect to both regional climate and wider scale volcanic forcing (Salzer and Hughes 2007; Salzer et al. 2014a). In particular, the presence of frost rings in this species has been correlated with the impact of explosive volcanism on climate (LaMarche and Hirschboeck 1984) and has been used to improve chronological

frameworks for the subsequent deposition of volcanic marker horizons in ice core records (Sigl et al. 2015). All of this provides a strong basis to further develop a thermo-lignification record in bristlecone pine, with potential to span much of the Holocene and to expand detailed investigations of volcanic forcing.

Preliminary exploration of BRs in bristlecone pine (Tardif et al. 2020) indicated a likely BR correlation with a late start to the growing season and a cool summer, highlighting the potential for BRs in bristlecone pine to offer a more sensitive proxy for subtle changes in climate due to volcanism and other forcings than the well-established frost-ring record. This study was, however limited by low sample depth and concentrated on only two short, discrete time intervals around 536 and 1965 CE. In order to comprehensively explore the specific climatic parameters, timing, and conditions leading to BR occurrence in bristlecone pine, a comprehensive investigation of BR occurrence across multiple trees and the longest possible time frame for which temperature data are available is required. In this study, BR sequences were created from 83 bristlecone pine cores from the Sheep Mountain/Patriarch Grove area of the Ancient Bristlecone Pine Forest in the White Mountains of California for the period 1895–2014 and 1981–2014, for which respectively monthly and daily climatic data were available. This dataset is the longest and best replicated developed so far with a focus on the investigation of specific climatic conditions leading to BR formation. It also provides the opportunity not only to better evaluate the natural variability of such data, but to present a more comprehensive analysis of the potential for, and limitations of, developing a multi-millennial BR record from bristlecone pine. Additionally, it provides an opportunity to explore the influence of topographic setting in a complex upper tree line ecotone, providing data to better inform future sampling campaigns targeted at producing representative BR chronologies.

The main aims of this study are threefold: (1) to investigate climatic parameters leading to BR formation, (2) to answer if and how elevation and topography modulates the BR record, 3) to evaluate the natural variability of the BR record and assess its paleoclimatic potential and limitations in bristlecone pine.

2 Materials and methods

2.1 Samples and study area

A set of 83 cores were selected from a collection of Great Basin Bristlecone pine (*Pinus longaeva* D. K. Bailey) samples acquired over a series of field campaigns in the Sheep Mountain and Patriarch Grove area of the Ancient Bristlecone Pine Forest in the White Mountains of California (37.5 W, 118.2 N) see Fig. 1.

The trees sampled (Salzer et al. 2014a) spread over an area of roughly 3 km^2 of rugged mountainous terrain consisting of predominantly dolomitic substrate. They cover an elevational transect between 3512 and 3320 m. a. s. l. that is 192 m in vertical distance between the highest and the lowest situated tree. Cores from trees along two distinct transects, (the RW of which have been previously analyzed by (Salzer et al. 2014b) one south facing (SF) and one north facing (NF), were selected to explore the impact of exposure on BR occurrence. Samples from three other bristlecone pine chronologies from the White Mountains: Cottonwood Upper (CWU), Sheep Mountain (SHP) and Patriarch Lower (PAL), were also selected in order to extend the vertical distance covered by the samples to assess any

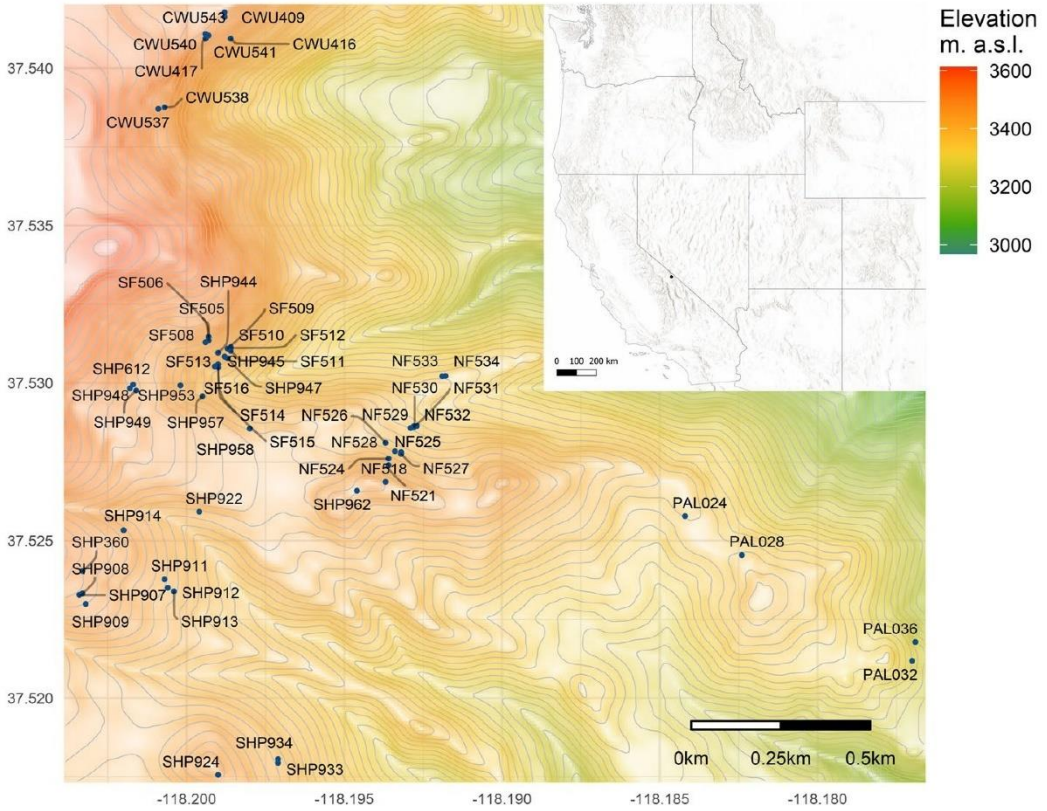

Fig. 1 Locations of sampled trees in the White Mountains of California. Inset map shows the general location of the study area in the western United States. Please note that trees SHP972 and SHP975 are not shown on this map, as these were located circa 3 km to the north from the main group of sampled trees shown

impact of altitude or distance from upper tree line on BR formation. These cores were also assigned as predominantly south or north facing based on the topographic position of the sampled trees.

To explore BR continuity around the stem where possible, we included two cores per tree. The strip-bark nature of bristlecone growth is such that for more mature trees there are often only a few sampling locations on the tree where the cambium is active (Brunstein 2006; Boyce and Lubbers 2011), imposing some limitations on the sampling strategy. Suitability for sectioning also required selection of cores with relatively consistent internal structure to facilitate effective sectioning of the material to avoid any distortion of the tracheid wall dimensions. The final selection of 83 cores suitable for this study includes 44 cores representing double sampled trees and a further 39 representing a single sampling from a tree (Table S1).

2.2 Laboratory preparation

Cores used for this study were previously air dried, glued into wooden core mounts, sanded, and measured following standard dendrochronological procedures (Stokes 1996; Salzer et al. 2014b). For this study, cores were separated from their mounts by soaking in a tray filled with near boiling water until they detached from the core mounts. Subsequently

each core was cut into shorter 4-6 cm long diagonally overlapping segments that could be reassembled with ease to perform accurate cross-dating on the finished sections. The cores were not cut into equal length segments because each core was individually assessed under the microscope to ensure maximum ring overlap on both sides of the split. The order of the sectioned pieces was noted to enable final reassembly of each core when the sectioning process was over. All core elements were next cut into c.10-15 µm thick thin-sections using a GSL1 microtome (Gärtner et al. 2014).

Thin-sectioning was followed by staining in a mixture of Safranine and Astrablue to reveal lignified cell walls in red and emphasize underlignified cell walls in blue. Stains were prepared following the procedure by Gärtner and Schweingruber (2013), where 0.5 g of Astrablue powder is dissolved in 100 ml of distilled water and 2 ml acetic acid, and 0.1 g of Safranin powder is dissolved in 100 ml of distilled water. Finally both stains were mixed in a 1:1 proportion. Each thin-section was placed in the stain bath for 3–4 min, after which it was washed with water and then ethanol at gradually increasing concentrations of 50%, 75%, 99,8% to remove the surplus stain from intercellular spaces and to dehydrate the section. Finally, each section was embedded in Canada Balsam under a cover glass and oven dried for 24 h in 60 °C. Laboratory preparation of 83 cores resulted in 612 permanent thin-sections. These were then digitized to facilitate ring width measurement and cross-dating. Thin-sections were photographed with a digital camera (CANON EOS 700D) coupled to a microscope under 40 times magnification. In total 29,105 high resolution pictures were taken, which were subsequently stitched in PTGui software (http://www.ptgui.com) to create high-resolution images of entire thin-sections. A control photo of an according scale was taken for each microscope magnification to ensure accurate analysis. Care was taken to achieve a representative overlap (20–30%) between single photos to secure reliable stitching results. Finally, ring widths of thin-sections representing every core were measured in ImageJ software (https://imagej.nih.gov/ij/index.html), and ring width sequences visually cross-dated and confirmed using CDendro software (http://www.cybis.se/forfun/dendro/) against the previously dated cores. The cell structure of the sections was surveyed using both the high-resolution digital images and the stained slides at 40×and 100x magnification. Underlignified tracheids (Fig. 2), were noted and assigned calendar dates for each observed BR. Earlywood Frost Rings (EWFR) and Latewood Frost Rings (LWFR) were also observed and assigned calendar dates.

2.3 Climate indices and statistical analysis

To assess the association between temperature and BR occurrence, mean-monthly temperature data were obtained for the grid pertaining to Sheep Mountain (Location: 37.5470 lat, -118.2179 lon, Spatial resolution 4 km, PRISM Climate Group, Oregon State University, http://prism.oregonstate.edu). Mean-monthly temperatures in the PRISM (Parameter-elevation Regressions on Independent Slopes Model) dataset are available for the period starting in January 1895; therefore, our analysis covers years 1895–2014 (2014 being the latest year in which our group of samples were collected). Our complete dataset, unusually large for thin-section analysis, with a sample depth of 83 cores, and temporal coverage of 120 years (for which temperature data was available), allowed us to implement a modeling approach to analyze the association between BRs and temperature. Our dataset consists of a time-series (non-independent setting) representing observations within individual cores that vary in their sensitivity to BR formation. Therefore we decided to fit a generalized linear mixed-effects model (GLMM), to account for these dependencies in the

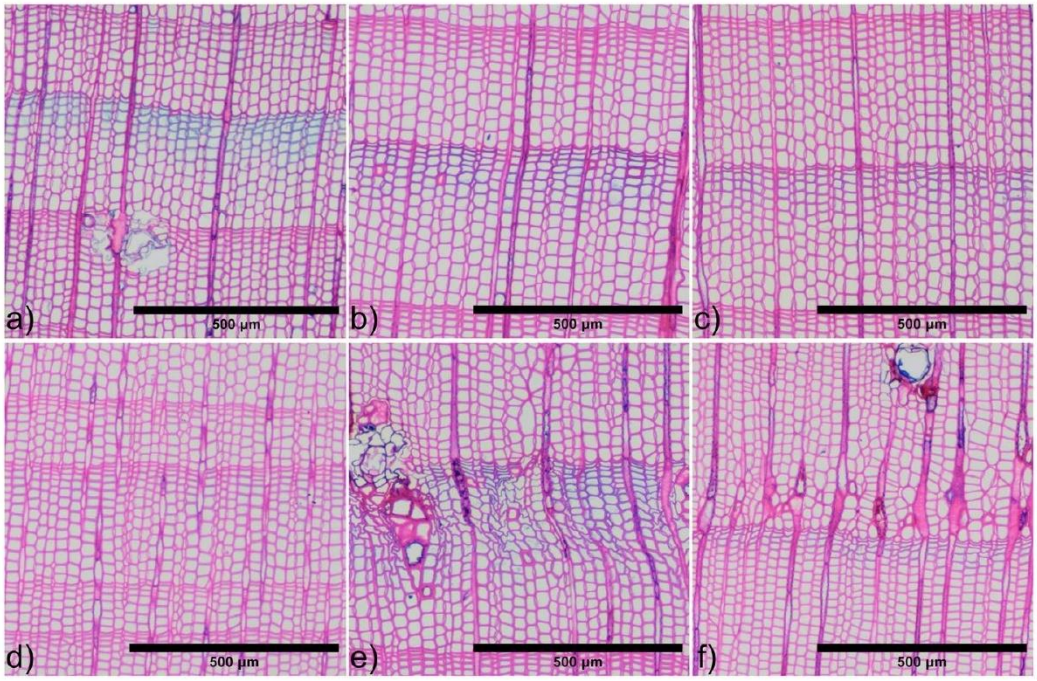

Fig. 2 Observed anatomical abnormalities: **a**) blue ring type 1 (BR-1), **b**) blue ring type 2 (BR-2), **c**) blue ring type 3 (BR-3), **d**) blue ring type 4 (BR-4), **e**) BR-1 along with deformed cells of late-wood frost ring, **f**) BR-3 followed by a lesser early-wood frost ring. Please note the difference between cell distortion in a) which occurred during sectioning due to the reduced strength of the cell walls due to lower lignin content, and the frost deformation of cells during life of the tree in e) and f). It is possible to clearly distinguish between the two effects through microscopic examination of the uncut sample, and the fact that procedural deformation produces a more uniform effect at a cellular level

data. We treat each core as a random effect, allowing the intercept of the model to vary among cores. The response variable is binary, representing the absence (0) or presence (1) of BR in a particular year, in a particular sample. The independent variables are mean-monthly temperatures of respective years, and the vertical distance from the upper tree line in meters (hereafter referred to as DTL). Samples analyzed are from trees growing on predominantly southerly or northerly exposed slopes of the temperature determined upper tree line (Bruening et al. 2017). Upper tree line elevation differs on both these slopes, so the distance from the respective upper tree line elevation of 3511 m on the southern slope, and 3475 m on the northern slope (Salzer et al. 2014b) was calculated for each core analyzed. To account for the independence of observations in our model we included only one sample per tree, resulting in a sample depth reduction to 61 individual cores. In order to fit the model, we used a manual step-wise, step-down, backward elimination procedure. We initially constructed the model with all available explanatory variables (mean temperature for every month and DTL); subsequently, we built a model retaining only variables significant at $p < 0.01$ from the first model. The final model included 7 significant explanatory variables: mean monthly temperatures of February, April, June, August, September, October, and DTL. Data analysis was conducted in R, v. 4.1.3 (R Core Team, 2024), using the package "lme4" for mixed modeling (Bates et al. 2015). The model specification was as follows: BR_event ~ feb_tmean + apr_tmean + jun_tmean + aug_tmean + sep_tmean + oct_tmean + DTL + (1|core) and the model was estimated using ML and BOBYQA optimizer.

Mean-daily temperature data were obtained for the grid pertaining to Sheep Mountain (Location: 37.5470 lat, -118.2179 lon, Spatial resolution 4 km, PRISM Climate Group, Oregon State University, http://prism.oregonstate.edu) for the full period available, that is 1981–2014, to explore the association between BRs and daily temperatures.

2.4 Topographic indices and statistical analysis

In order to further assess the association between BR occurrence and topographic variables, DTL and exposure, we calculated BR frequency per tree for the period 1793–1998, the longest period continuously covered by the highest number of samples (61 in total). We then applied simple linear regression between BR frequency and DTL, and used the non-parametric Mann–Whitney U test to compare cores from southerly- and northerly-exposed trees. BR frequency was calculated per tree, not per core in this case, because two cores coming from the same tree are influenced by the same DTL and slope exposure.

In order to assess if trees growing in cooler topographic locations might be more susceptible to record BRs driven by colder temperatures (as suggested by Bunn et al. 2011; Bruening 2016; Bruening et al. 2018) as compared to trees in surrounding areas, topoclimate variables—mean-monthly temperatures derived by Bruening et al. (2017, 2018) for each tree location were used. We again used the non-parametric Mann–Whitney U test to check for significant differences in topoclimate variables between BR-recording and non-recording trees in years of BR formation.

3 Results

3.1 Blue ring typology

Careful examination allowed us to develop a classification of blue ring intensity (Table 1) for use in this study, based on observations of the full range of variability, such as: numbers of rows of under lignified tracheids; the degree of lignification of the tracheid walls; the thickness of the latewood cell walls compared to the latewood of surrounding rings: and the overall intensity of the blue color ensuing from the proportion of underlignified cell walls.

The BRs that we observed in this study appear exclusively in the latewood, predominantly in its outermost part consisting of the 2–5 outermost cells of a radial file. A few of the most intensive examples included blue in up to 50% of ring width, and these were usually coupled with LWFRs (Fig. 2e).

In cases of particularly strong BRs (BR-1, BR-2) tracheid shapes can be distorted during thin-section preparation because of lowered lignin content (which provides rigidity and mechanical strength). In such cases, careful microscopic examination can distinguish strong BRs from frost rings, because in BRs only the tracheid and ray shapes are distorted during microtome preparation, whereas FRs are also characterized by lateral expansion and displacement of rays (Fig. 2).

In total (1895–2014, 9357 rings), we identified only 203 BRs (0.022) of which BR-1: 0 (0.0), BR-2: 18 (0.002), BR-3: 67 (0.007), BR-4: 118 (0.013). BR-1 type are extremely rare and in fact present only in very strong BR years in the earlier part of the dataset, for which temperature data were not available for comparison. In this dataset, frost rings occur

Table 1 BR intensity classification

Blue Ring Type	Characterization	Example shown
BR-1	Strongly blue in section, multiple rows of underlignified tracheids, complete sections of tracheid walls are underlignified, underlignified latewood cell walls are visibly thinner compared to the latewood of the surrounding rings, and in some cases the initiation of cell wall lignification can be observed in cell wall corners (pink). In some instances they appear coupled with LWFRs	Figure 2a,e, Fig. S1a
BR-2	Less blue in section compared to type 1, the lignification process progressed further from cell corners with only the inner portion of the tracheid walls appearing blue	Figure 2b, Fig.S1b
BR-3	Less blue in section compared to type 2, with only the very thin innermost cell wall part appearing blue	Figure 2c,f, Fig.S1c
BR-4	Slight bluish tint in section visible in the latewood cells, present in the same year in at least 2 samples*	Figure 2d, Fig.S1d

*A similar effect could also potentially be produced by insufficiently washed-out stain from intercellular spaces. This type was only assigned where the effect was present in the same year in at least two samples, as it is unlikely for two separate samples to independently show this stain-washing effect in the same year

even more rarely, only a single LWFR was observed in the period of analysis (0.0001), and EWFR in 19 rings (0.002).

Our data indicate that BR and EWFR in bristlecone pine are independent markers, with only 2 EWFRs out of 19 following BRs. Blue rings in bristlecone pine at our growth locations form in years with lower-than-normal temperatures during the late part of the growing season, while EWFRs probably mark early cambial reactivation and cold snaps at the beginning of the growth season. A Mann–Whitney U Test was performed on mean monthly temperatures for the period 1895–2014 and confirmed that mean May temperatures were significantly higher ($p = 0.002$) (Table S2, Fig. S2) in years with EWFRs. Such early-season warmth possibly induces an earlier-than-normal onset of cambial activity and resultant frost damage from subsequent spring cold snaps. Analysis of daily temperatures for the period 1981–2014 confirms that in EWFR years (1984, 1992, 2007) minimal daily temperatures rose above 0°C already in May and were later followed by period of below-zero temperatures likely leading to the observed frost damage (Fig. S3).

3.2 Temperature constraints of blue ring formation

Model input for the period 1895–2014 includes 61 samples from independent trees, in total 6848 observations. The model's total explanatory power is substantial, with a conditional $R2 = 0.796$, and the part related to the fixed effects (marginal R2) is 0.558. The model fit parameters indicate an optimal fit. Both the C-value (0.9681743) and Somers' D_{xy} (0.9363487) show a good fit between predicted and observed occurrences of BRs. If the C-value is 0.5, the predictions are random, while the predictions are perfect if the C-value is 1. C-values above 0.8 indicate real predictive capacity (Baayen 2008). Somers' D_{xy} is a value that represents a rank correlation between predicted probabilities and observed responses. Somers' D_{xy} values range between 0, which indicates complete randomness, and 1, which indicates perfect prediction (Baayen 2008).

The model indicates that mean-monthly temperatures in February, April, June, August, September, and October significantly influence BR formation, along with distance from upper tree line (DTL) (Table 2).

The higher the average monthly temperature in February, the higher the odds of a BR forming later in the year (Table 2, Fig. 3a). Whereas, lower temperatures in April raise the probability of lignification being disrupted later in the growing season, leaving behind an underlignified band of cells in the latewood of that particular year (Table 2, Fig. 3b).

We observe a negative relationship between June mean temperature and BR formation (Table 2, Fig. 3c); the cooler June is, the higher the odds of BR formation. It is possible that June, as the month when cambial activity starts, might also be partly defining how long cambial activity can be sustained, that is, the length of the growing season. A cool June may lead to the latest formed tracheids being challenged to fully lignify when cold snaps in September and/or October arrive. This interplay is clear when we look at the predicted likelihood of BR formation in September and October under different temperature scenarios for June (Fig. S5). Lower temperatures in June delay the onset of xylogenesis. Thus, the lignification of latewood tracheids could still be ongoing in September/October when colder temperatures arrive, disrupting the lignification completely and leading to the formation of a BR.

We do not observe any significant relationship between mean July temperature and BR occurrence. We suggest that, however much cooler, temperatures in July across our period of

Table 2 Parameters of generalized linear mixed-effects model (GLMM)

Predictors	BR event			
	Log-Odds	*CI*	*Statistic*	*p*
(Intercept)	8.36 ***	6.42 – 10.31	8.44	3.266e-17
February mean temp	0.26 ***	0.14 – 0.37	4.29	1.817e-05
April mean temp	-0.33 ***	-0.45 – (-0.21)	-5.26	1.406e-07
June mean temp	-0.82 ***	-0.97 – (-0.67)	-10.57	3.976e-26
August mean temp	-0.39 ***	-0.55 – (-0.23)	-4.83	1.396e-06
September mean temp	-1.12 ***	-1.32 – (-0.93)	-11.29	1.514e-29
October mean temp	0.15 ***	0.07 – 0.24	3.44	5.799e-04
DTL	-0.03 **	-0.04 – (-0.01)	-3.04	2.361e-03
Random Effects				
σ^2	3.29			
$\tau_{00\ symbol}$	3.82			
ICC	0.54			
$N_{\ symbol}$	61			
Observations	6848			
Marginal R^2 / Conditional R^2	0.558 / 0.796			
AIC	856.487			

* $p < 0.05$ ** $p < 0.01$ *** $p < 0.001$

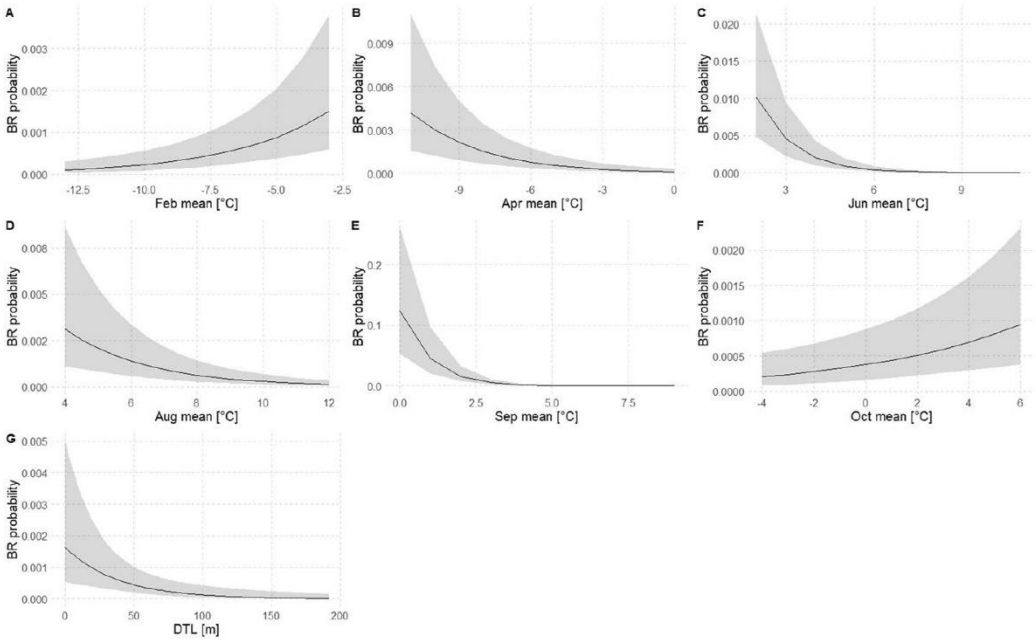

Fig. 3 Generalized linear mixed-effects model (GLMM) results presented as predicted probabilities of BR formation for each predictor significant in the model, plotted along observed ranges of predictors. BR probability is shown according to: **a**) February mean temperatures, **b**) April mean temperatures, **c**) June mean temperatures, **d**) August mean temperatures, **e**) September mean temperatures, **f**) October mean temperatures, **g**) DTL. Please note the highest effect of September mean monthly temperature on the probability of BR formation. Note the different y-axis in each subplot

study (1895–2014) never dropped to the level where they might disrupt the lignification process of newly forming early-wood tracheids. This is further supported by the observation that we also do not see BRs in earlywood across our period of study, just in the last tracheids of the latewood towards the very end of the growth season.

The effect of the mean temperature in August is negative (Table 2, Fig. 3d), cooler temperatures increase the likelihood of BR occurrence.

Model results indicate that the strongest relationship exists between September temperatures and the occurrence of BRs (Table 2, Fig. 3e). On average, cambial activity in bristlecone pine ceases when mean daily temperatures drop below 6 °C (Ziaco et al. 2016). This threshold is normally reached at our site by approximately the 17th of September (Fig. S6). While this date will vary somewhat, we can extrapolate that the production of new tracheids stops and lignification of the lastly formed cells occurs around mid-September.

Mean October temperatures appear to have a positive effect on the likelihood of BR occurrence (Table 2, Fig. 3f). A 1 °C increase in mean October temperature increases the odds of BR formation by 16%. In some years, favorable conditions for cambial activity, with average daily temperatures above 6 °C, can still occur for some part of October (Fig. S6), effectively extending the time window when lignification can occur into periods where sudden temperature drops are likely, if not inevitable. In this scenario, late cambial activity leads to a late start to the lignification process and a subsequent thermally induced lignification disruption and the formation of a BR. Such situations are not very frequent and therefore the effect of October temperatures in our model is relatively low. We suggest that the influence of June and October mean temperatures impacts BR formation by effectively either delaying or extending the time window of favorable conditions for xylogenesis.

There are cases when BR formation is most probably induced by short temperature decreases at scale of a couple of days as observed by Piermattei et al. (2015). This kind of short-term temperature variation is not well captured by average monthly temperatures. Daily temperature records for the study area are only available from 1981 onwards (PRISM), and for this most recent period in our dataset, we observed only two BR events, one in 1982 (17 out of 82 samples) and one in 1998 (4 of 82 samples). We compared the relationship of BR occurrence with mean daily temperatures during these two event years (Fig. S7). The result for the 1982 growth season indicates that BR formation was mainly influenced by temperature in June and September. A short growth season characterized 1982, with < 6 °C mean daily temperatures occurring until 11th of July and cold snaps with below-zero mean daily temperatures still occurring up to the 1st of July. The growth season ended with temperatures dropping below 6 °C on the 11th of September. In contrast, the beginning of the growth season in 1998 was not characterized by such harsh conditions, as indicated by the weaker BR signal present in only 4 out of 82 upper tree line (DTL-14 ± 15 m) samples. Cambial activity likely started around the 19th of June; however, temperature dropped below 6 °C for a couple of days beginning on the 10th of September, which might have induced a lignification shutdown and the limited BR formation seen in the dataset.

Modeled temperature results also revealed a weak but significant negative effect in relation to distance from the upper tree line (Table 2, Fig. 3g), with a one meter increase in DTL decreasing the odds of BR formation by 3%. This potential topographic influence was further explored using different techniques.

3.3 Topographic influence on BR occurrence

We observe a significant ($p=0.01$) negative relationship between BR frequency and DTL (Fig. S4). Although the observed relation explains only 9% in the variance of the dataset, DTL constitutes the strongest common topographic constraint of BR occurrence. A non-parametric Mann–Whitney U test between BR frequency on southerly and northerly exposed slopes shows that there is no significant ($W=435$, $p=0.83$) difference between the distribution of BR frequencies on both exposures (Fig. S4). We therefore found no evidence for exposure influencing the trees' susceptibility to BR formation.

Results across 79 cores (1793–1998), arranged in an ascending order of DTL show that the further below the tree line the tree is located, the less severe the temperature impact of a given event (Fig. 4). We observe a buffering effect with distance below the upper tree line, which is balanced against the severity of the cold snap. More extreme low-temperature departures result in stronger and more BRs in the higher portion of the elevational transect, with weaker and fewer BRs present in trees further down from the upper tree line.

Examining the pairs of cores from the same tree (Fig. S8), we can observe that BRs are often not continuous around the stem. Usually, one of the pair of cores records more BRs and of higher class than the other. This may be due to stem exposure, where the side of the trunk that is not exposed to direct solar radiation remains slightly cooler than the sun-exposed side, and thus the non-exposed side is prone to record more and stronger BRs.

We performed non-parametric Mann–Whitney U test between BR-recording and non-recording trees in every BR year for DTL and mean monthly temperatures (topoclimate

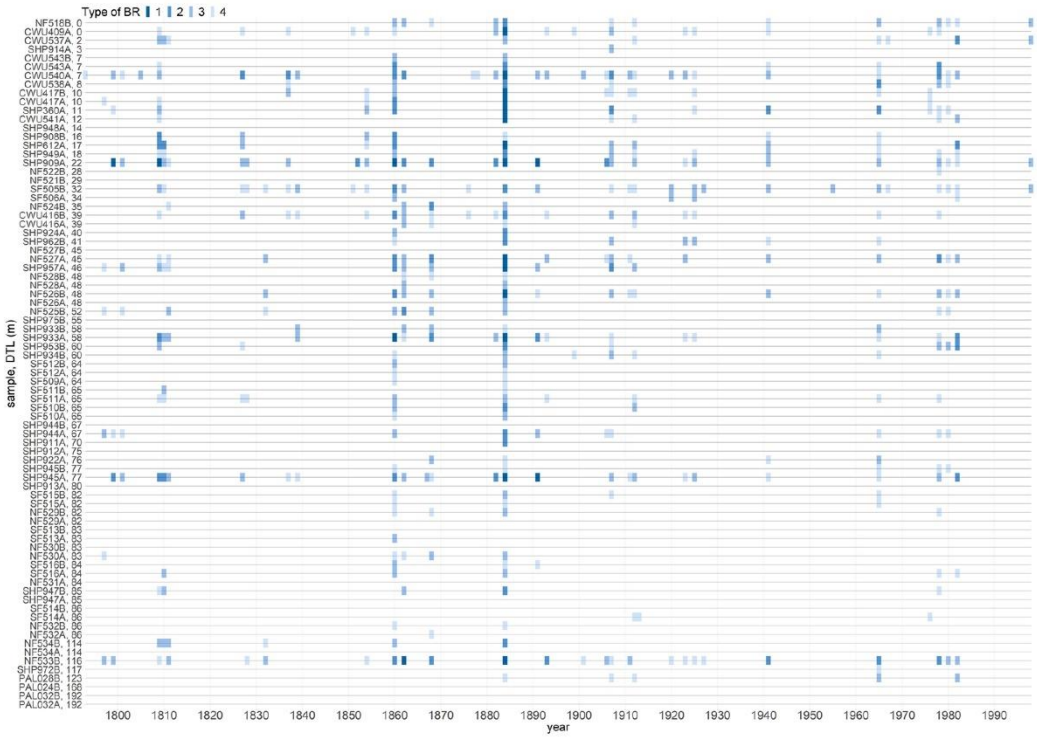

Fig. 4 BR chronology of 79 cores continuously covering the period 1793–1998, arranged in an ascending order of DTL. Please note that the further below the upper tree line the tree is located the fewer BRs it forms and that the BRs formed in a particular year become less intense with increasing DTL

variables derived by Bruening et al. (2017)) of each month for the period 1793–1998 continuously covered by 61 trees (Table 3). We identified 47 BR event years (1793, 1797, 1799, 1801, 1805, 1809, 1810, 1811, 1818, 1827, 1828, 1832, 1837, 1839, 1851, 1852, 1854, 1860, 1862, 1868, 1876, 1877, 1878, 1882, 1884, 1891, 1893, 1899, 1901, 1906, 1907, 1911, 1912, 1913, 1920, 1923, 1925, 1927, 1941, 1955, 1965, 1967, 1976, 1978, 1980, 1982, 1998). We observed significant ($p <= 0.01$) differences only for June in 1907, July 1907 and November 1868 and for DTL in 1907, 1941, 1809, 1837. This shows that the BR sensitivity of particular trees cannot be sufficiently explained by obtained topoclimate variables.

Table 3 Results of the Mann–Whitney test (two-sided) of differences in DTL and topoclimatic variables calculated for each tree location between BR-recording and non-recording trees for 47 BR event years between 1793–1998. The median and interquartile range (IQR) are indicated. Note that the number of observations per group varies for each year analyzed. Only results significant at least at the level of $p \leq 0.05$ are listed, results significant at $p \leq 0.01$ are bolded

Variable	Year	n BR	n non-RB	Median (IQR) BR	Median (IQR) non-BR	*p* value
DTL	1907	26	34	35.5 (11–60) m	67.5 (37–84) m	**0.002**
	1941	16	44	20 (7–45) m	64 (37–83) m	**0.005**
	1809	22	36	27 (11–60) m	66 (40–83) m	**0.007**
	1837	8	51	16 (7–32) m	60 (34–83) m	**0.008**
	1998	4	55	12 (0–22) m	58 (29–82) m	0.014
	1854	9	50	17 (11–32) m	62 (35–83) m	0.016
	1925	13	47	32 (11–41) m	64 (35–83) m	0.023
	1884	44	14	48 (16–70)m	81.5 (34–117)m	0.033
	1882	7	52	22 (0–58)m	60 (29–83) m	0.034
	1827	10	49	27 (16–60) m	60 (34–83) m	0.045
January temperature	1868	16	43	-6.7 (-6.9-(-6.1)) °C	-5.8 (-6.5-(-5.5)) °C	0.013
	1862	16	43	-6.7 (-6.9-(-5.9)) °C	-5.8 (-6.7-(-5.5)) °C	0.047
	1811	10	48	-6.8 (-6.9-(-5.8)) °C	-6.1 (-6.7-(-5.5)) °C	0.048
April temperature	1907	26	34	-2.3 (-2.5-(-1.9)) °C	-2.0 (-2.3-(-1.8)) °C	0.033
May temperature	1907	26	34	1.7 (1.5–2.0) °C	1.9 (1.7–2.1) °C	0.019
	1809	22	36	1.7 (1.5–1.9) °C	1.9 (1.7–2.1)°C	0.028
June temperature	1907	26	34	7.0 (6.8–7.2) °C	7.2 (7.1–7.5) °C	**0.007**
	1809	22	36	7.0 (6.8–7.2) °C	7.2 (7.0–7.5) °C	0.026
July temperature	1907	26	34	10.8 (10.6–10.9) °C	11.0 (10.8–11.2) °C	**0.005**
	1809	22	36	10.8 (10.6–10.9) °C	11.0 (10.7–11.2) °C	0.012
August temperature	1907	26	34	10.7 (10.4–10.8) °C	10.9 (10.7–11.0)°C	0.010
	1809	22	36	10.7 (10.4–10.8) °C	10.9 (10.7–11.0) °C	0.016
September temperature	1907	26	34	7.1 (6.9–7.4) °C	7.4 (7.1–7.6) °C	0.024
November temperature	1868	16	43	-1.7 (-2.1-(-1.2)) °C	-1.0 ± (-1.7-(-0.7)) °C	**0.006**
	1862	16	43	-1.7 (-2.1-(-1.1)) °C	-1.0 (-1.7-(-0.7)) °C	0.025
	1811	10	48	-1.8 (-2.1-(-1.1)) °C	-1.2 (-1.7-(0.8)) °C	0.046

4 Discussion

4.1 Blue ring typology

At a cellular level, our observations of the lignification process were compatible with previous studies (Saleh et al. 1967), which observed that cell corners in the primary wall lignify first and subsequently lignification continues in the middle lamella of the radial and then tangential walls. Results in this study demonstrate that in varying stages of incomplete lignification, radial walls are visibly more strongly lignified than tangential walls (Fig. S1).

BR were present only in the latewood portion of the ring for our time-series (1793–2014) as observed by Montwé et al. (2018) and Matisons et al. (2020), but not by Piermattei et al. (2015) who reported BR in both the terminal portion of the ring and within the earlywood portion.

The fact that in our dataset, LWFR occur less frequently than EWFR, is in contrast to earlier studies, which report EWFR to occur less frequently than LWFR in bristlecone (LaMarche 1979; LaMarche and Hirschboeck 1984; Brunstein 1995). However, this difference may originate from differing sample preparation in earlier studies, where frost rings were noted on polished core surface, and less obvious EWFRs might have gone unrecognized. Detailed microscopic analysis based on thin-sections allows us to recognize even the slightest abnormalities in wood structure.

Our analysis shows that BR and EWFR are independent markers of two separate events. This is contrary to indications by Montwé et al. (2018), on a far more limited dataset, that BRs capture a cold event at the end of the growing season which leads to cambial damage and irregular growth upon re-activation in the following spring. In bristlecone pine at our growth locations, BRs form in years with lower-than-normal, but not below freezing temperatures during the late part of the growing season that are sufficient to cease lignification without damaging the cambium. In contrast EWFRs probably mark early cambial reactivation and cold snaps at the beginning of the growth season.

Studies of lodgepole pine (*Pinus contorta* Dougl. ex. Loud.) (Montwé et al. 2018) and Scots pine (*Pinus sylvestris* L) (Matisons et al. 2020) have reported higher proportions of BRs and FRs than this study. While this could be a species specific difference, the trees used in these earlier studies were not growing in their natural proveniences and so may have been over sensitized. However, Greaves et al. (2022) also reported higher BR proportion for Scots pine (*Pinus sylvestris* L) growing within its seed source location and far from the thermal limits of Scots pine growth. As bristlecone pine is highly adapted for survival in its marginal habitat, we conclude that BRs are formed very rarely, only during highly extreme conditions, and the bristlecone BR record therefore constitutes a more reliable record of years with adverse climatic conditions. Both earlier studies (Montwé et al. 2018; Matisons et al. 2020) also reported higher proportions of BRs compared to frost rings, which is in agreement with our results. This implies that BRs represent a more sensitive reaction of tree growth to adverse thermal conditions than FR, which require below freezing temperatures to form. This is particularly important in the context of bristlecone pine given the previously described and longstanding association of FRs with explosive volcanism (LaMarche and Hirschboeck 1984; Brunstein 1996; Salzer and Hughes 2007). Blue ring records might allow early or late growth season distinction for specific eruptive events (LaMarche and Hirschboeck 1984; Gurskaya 2014; Barbosa et al. 2019). A long BR record could augment FR records of past

eruptions (Piermattei et al. 2020; Büntgen et al. 2022) and could considerably enhance paleoclimatic and cultural histories related to eruptive events as well as their influence upon regional circulation patterns.

We did not observe any relationship between juvenility and an increased probability of BR formation, as noted by Matisons et al. (2020) and Montwé et al. (2018), related to weaker insulation of the cambium (Payette et al. 2010; Montwé et al. 2018), the lower height, and weaker heat absorption of smaller trees (Kidd et al. 2014) because all cores used in this study came from mature trees.

4.2 Temperature constraints of blue ring formation

Connections between mean-monthly June, August, September, and October temperatures and BR occurrence confirm preliminary observations (Montwé et al. 2018; Matisons et al. 2020; Tardif et al. 2020) that BRs form due to late initiation of the growing season, an early end of the growing season, and a generally cool growing season. Although limited by the lack of longer sequences of daily temperature data, we were also able to support the suggestion made by Piermattei et al. (2015), that there is a connection between short-term temperature decreases (at the scale of several days) at the end of the growing season and the occurrence of BRs, based on our observations of the 1982 BR event. Further analysis of the relationship between short-term temperature decreases and BR formation is necessary to fully confirm this association in settings where daily temperature records are available.

We were also able to develop a deeper understanding of the previously hypothesized temperature response, revealing some additional subtleties to be expanded on in future studies. The observed connection between February and April mean temperatures and BR occurrence seems initially surprising, as the cambial activity of bristlecone pine in other growth locations has been observed to start when mean daily temperatures reach around 6 °C (Ziaco et al. 2016), which, at our sampling site occurs on average around 13th of June (Fig. S6). Therefore, the lignification process, the last phase of xylogenesis, should not be directly affected by temperatures occurring before the onset of the cambial activity itself. However, ecophysiological models of the onset of cambial activity can potentially explain this connection. Delpierre et al. (2019) compared various models, including temperature threshold, temperature and photoperiod thresholds, heat-sum, chilling influenced heat-sum, and regression line models, and found that a chilling influenced heat-sum model provides the highest accuracy predictions of the onset of cambial activity. This was based on a large observational dataset spreading through a broad altitudinal, and latitudinal gradient of four different coniferous species. The model considers the complex interplay of chilling and forcing temperatures in interaction with the photoperiod and attempts to address the influence of ecodormancy and endodormancy phenological phases on the resumption of cambial activity. During the endodormancy phase, cambial activity is prevented by the tree's internal physiology, even if favorable external conditions arise the tree does not respond. Whereas during ecodormancy, the cambium remains inactive until favorable external conditions occur, at which point it reactivates. This model provides a potential means to explain our observed connection between BRs and temperatures in February and April, outside of the growth period. In the model, chilling temperatures and forcing temperatures counterbalance each other, and this interaction modulates the onset date of cambial activity. The resulting hypothesis is that the cambium should require a lower accumulation of forcing temperatures during ecodormancy, when it has been exposed to increasingly cold temperatures during the endodormancy phase. Chilling accumulation was modeled to start

shortly after the winter solstice, whereas forcing accumulation starts around the vernal equinox. In the context of our results, this would imply that warmer February temperatures would encompass the chilling accumulation phase and lead to lower chilling temperature accumulation. Further, lower April temperatures shortly after the theoretical start of the forcing accumulation period (vernal equinox), would lead to lower and slower forcing temperature accumulation. This, coupled with higher threshold requirements due to lower chilling accumulation, could lead to later resumption of cambial activity. Consequently, further xylogenesis phases, including lignification, might be delayed towards the end of the growing season, when advection of colder air masses is more likely to occur, further disrupting lignification resulting in underlignified bands of cells in the latewood of a particular year observed as BRs.

Greaves et al. (2022) found only the very strong 1976 BR, present in most of their samples, to be related to a cold end of the growing season. They found the remaining BR years displayed an irregular distribution between and within trees and could not assign these to any specific temperature signal. They concluded that these weaker BRs might be related to other biotic and abiotic stresses. Our modeling approach, based on a long chronology and high sample depth spread along an altitudinal gradient, allowed us to capture a broader picture of interacting thermal conditions during February, April, June, August, September and October, and BR formation modulated by DTL. It is worth noting that the site location studied by Greaves et al. (2022) is not near the thermal limit for Scots pine growth, and therefore the BR signal might have been less consistent. Our samples all come from trees growing close to the temperature-limited upper tree line, where adverse thermal conditions are the main common growth-limiting factor, and BR formation is an observed response to that temperature influence. At different sites, limited by different factors, BR may potentially constitute a compound response to different stressors. Therefore, future studies should target trees coming from a wide range of micro-environmental settings to further assess the consistency of BR formation in trees subjected to different stressors and to aid its ecological interpretation.

4.3 Topographic influence on BR occurrence

Topography influences ring-width patterns in bristlecone pine. Ring widths from the lower forest border correlate with precipitation (Hughes and Funkhouser 1998), whereas at the upper forest border, the correlation is with temperature (LaMarche 1970). The trees used in this study are from the more complex interface zone between the upper and lower tree line (Salzer et al. 2009, 2014b; Kipfmueller and Salzer 2010; Bunn et al. 2011). Ring-width analysis of trees within this zone has shown that near the climatically-determined upper tree line, relatively small differences in elevation of the order of 60–80 vertical meters, alter the factor most limiting to tree-ring growth. Trees growing in a narrow elevational band near the tree line show a pattern of growth consistent with temperature limitation, while trees below this band show a pattern of growth more similar to lower forest border precipitation-sensitive trees. It was also discovered that in a small subset of the trees growing below the upper tree line, but rooted in particular locations on the landscape vulnerable to cold-air pooling, ring-width patterns were more similar to the temperature-sensitive patterns found in the highest trees (Bunn et al. 2011). The BR data in this study add further evidence of this fine-scale spatial sensitivity of bristlecone pine to temperature close to the upper tree line and indicates that this sensitivity may be at even finer scales than previously shown. The BR classification

system developed in this study provided useful additional insights in this context. It revealed that the further below the tree line a tree is located, not only are fewer BRs observed, but those that are, are of lower intensity. Although the microscopic examination of each blue ring occurrence to assign an intensity classification made the analysis more time-consuming, this effort proved to be worthwhile, providing valuable information. It was particularly important to note the presence of even the least intense BR types, BR-3 and BR-4, as these are the more abundant types of this generally rare phenomenon (BR-3 occurred 67 times and BR-4 120 times out of 205 BRs observed for the 1895–2014 period). Omitting these less intense types would lead to ignoring a large portion of the information available from this new proxy. We would recommend that future studies invest in efforts to incorporate BR intensity in their observations, with the caveat that such an approach relies upon a highly standardized and precise thickness of micro-sections to ensure direct comparability of all features.

Outliers from this general DTL dependent pattern, like core NF533B (Fig. 4), which was located in the lower portion of the elevational transect (DTL 116 m) and exhibits a proportion of BRs more consistent with samples from the higher locations, might illustrate the effect of cold air pooling (Bunn et al. 2011). Core NF533B comes from a tree situated on a slight plateau in the NF transect (Fig. 1) which supports this hypothesis. However, cores NF534A and B, from a tree located approximately 10 m from NF533B, both exhibit a much lower proportion of BRs (Fig. 4). It is possible that much larger topographically induced temperature differences experienced by trees exist than previously reported (Bruening 2016; Bruening et al. 2017), or there may be some individual tree level factors, like the genetic susceptibility of particular trees to BR formation, that play a role. The former would be in accordance with the observed lack of regular significant differences between topoclimate variables of trees recording and not recording BRs (Table 3); the latter is supported by observations made for *Pinus radiata* lignification by Donaldson (1993). Work by Salzer et al. (2014b) indicated that trees on the SF slope grew faster than their NF slope counterparts; thus, we expected that SF trees, having somewhat better conditions for growth, might be less responsive in terms of BRs. However, we found no evidence of exposure affecting the probability of BR formation.

Tardif et al. (2020) looked for significant differences in topoclimate variables between BR recording and non-recording trees for 4 BR years they analyzed (536, 1965, 1978, 1982), with sample depth 12, 31, 29, 29 respectively, and found significant differences in elevation, seasonal mean temperature, length of the growing season, and mean May and September temperatures. Our analysis, based on much larger sample depth and including more BR event years than Tardif et al. (2020), shows a much deeper complexity of interactions between topoclimate and BR sensitivity. We observed significant ($p \leq 0.01$) differences only for June in 1907, July 1907, and November 1868 and for DTL in 1907, 1941, 1809, 1837. This shows that the BR sensitivity of particular trees cannot be sufficiently explained by obtained topoclimate variables. In BR event years 1965 and 1982, common for both this study and that of Tardif et al. (2020), contrary to Tardif et al. (2020), we did not find significant differences between any of the analyzed variables. This difference might be due to smaller sample depth analyzed by Tardif et al. (2020) or simply site-specific differences between the White Mountains (this study) and Pearl Peak, Ruby Mountain Range, Nevada (Tardif et al. 2020).

Future studies aimed at constructing the most representative record of BRs possible in bristlecone pine should target trees located close to the upper tree line and involve collection of at least two cores per tree in order to capture a full record of BR years. Trees at lower elevation should also be sampled to provide information about the severity of

particular event years, as the strongest BR events are captured also in trees situated further from the upper tree line.

Additional benefits may be gained from experimental designs to assess the daily temperature thresholds for BR formation; because taking into account that BRs are a very rare phenomenon, it would be very difficult to capture BR formation in observational studies under natural conditions.

A recent study (Björklund et al. 2021), focused on elucidating the differences between different approaches to obtaining maximum latewood density signals (X-ray, Blue Intensity, and quantitative wood anatomy) has shown that incomplete lignification (as represented by BR years) is not captured in X-ray and Blue Intensity methods. We suggest that BR chronologies may have additional value to constitute an independent record of past temperature in the late part of the growing season, not otherwise captured by densitometric techniques. Overall, results demonstrate excellent potential for the future development of BR proxy records from bristlecone pine, and indicate this approach will provide a more sensitive paleotemperature proxy to complement and inform ring width and/or densitometric techniques.

Supplementary Information The online version contains supplementary material available at https://doi.org/10.1007/s10584-024-03773-8

Acknowledgements LS thanks Joanna Karłowska-Pik, Krzysztof Leki and Jakub Wojtasik for useful discussions during the model-building phase of work. The Laboratory of Tree Ring Research is thanked for its support and for making the laboratory facilities available to the leading author during the laboratory preparation phase of work, which took place during the most challenging phase of the COVID pandemic. Heartfelt thanks to the Pearson-Brewer family for the warmest welcome and invaluable support during the research visit.

Authors' contributions L.S. and C.P. conceived the study, M.S. contributed and crossdated the samples, and contributed to manuscript revision, L.S performed laboratory work, conducted analyses, interpretation, visualization and led the writing, N.S-K. contributed to statistical modeling, C.P contributed to interpretation and writing, M.K contributed to manuscript revision.

Funding This work was supported by: National Science Centre 2019/35/N/ST10/04366 to L.S.,
The National Science Foundation's P2C2 program 1902625 and 1203749 to M.S.,
Project nr POWR.03.05.00–00-Z302/17 "Universitas Copernicana Thoruniensis In Futuro" (2018–2022) co-financed from the European Social Fund-the Operational Programme Knowledge Education Development. Module 5. Interdisciplinary PhD School "Academia Copernicana" to L.S.,
The Malcolm H. Wiener Foundation and the University of Arizona to C.P.

Data availability All the data and materials supporting the findings of this study are available from the corresponding author upon reasonable request.

Declarations

Conflict of interest The authors declare that they have no conflict of interest.

References

Baayen RH (2008) Analyzing Linguistic Data: A Practical Introduction to Statistics using R. Cambridge University Press

Barbosa AC, Stahle DW, Burnette DJ, et al (2019) Meteorological Factors Associated With Frost Rings in Rocky Mountain Bristlecone Pine At Mt. Goliath, Colorado. Tree Ring Res 75 101 https://doi.org/10.3959/1536-1098-75.2.101

Bates D, Mächler M, Bolker B, Walker S (2015) Fitting Linear Mixed-Effects Models Using lme4. J Stat Softw 67 https://doi.org/10.18637/jss.v067.i01

Björklund J, Fonti MV, Fonti P et al (2021) Cell wall dimensions reign supreme: cell wall composition is irrelevant for the temperature signal of latewood density/blue intensity in Scots pine. Dendrochronologia (verona) 65:125785

Boyce RL, Lubbers B (2011) Bark-stripping patterns in bristlecone pine (Pinus aristata) stands in Colorado, USA1. J Torrey Bot Soc 138:308–321

Bruening JM, AG, Bunn et al (2017) Fine-scale modeling of bristlecone pine treeline position in the Great Basin, USA. Environ Res Lett 12:14008

Bruening JM, Bunn AG, Salzer MW (2018) A climate-driven tree line position model in the White Mountains of California over the past six millennia. J Biogeogr 45:1067–1076. https://doi.org/10.1111/jbi.13191

Bruening JM (2016) Fine-scale topoclimate modeling and climatic treeline prediction of Great Basin bristlecone pine (Pinus longaeva) in the American southwest

Brunstein FC (1996) Climatic significance of the bristlecone pine latewood frost-ring record at Almagre Mountain, Colorado, U.S.A. Arct Antarct Alp Res 28:65–76. https://doi.org/10.2307/1552087

Brunstein FC (2006) Growth-form characteristics of ancient Rocky Mountain bristlecone pines (Pinus aristata). Colorado. https://doi.org/10.3133/sir20065219

Brunstein FC (1995) Bristlecone pine frost-ring and light-ring chronologies, from 569 BC to AD 1993, Colorado

Bunn AG, Hughes MK, Salzer MW (2011) Topographically modified tree-ring chronologies as a potential means to improve paleoclimate inference: A letter. Clim Change 105:627–634. https://doi.org/10.1007/s10584-010-0005-5

Büntgen U, Crivellaro A, Arseneault D et al (2022) Global wood anatomical perspective on the onset of the Late Antique Little Ice Age (LALIA) in the mid-6th century CE. Sci Bull (beijing) 67:2336–2344. https://doi.org/10.1016/j.scib.2022.10.019

Crivellaro A, Piermattei A, Dolezal J et al (2022) Biogeographic implication of temperature-induced plant cell wall lignification. Commun Biol 5:767. https://doi.org/10.1038/s42003-022-03732-y

Delpierre N, Lireux S, Hartig F et al (2019) Chilling and forcing temperatures interact to predict the onset of wood formation in Northern Hemisphere conifers. Glob Chang Biol 25:1089–1105

Donaldson LA (1991) Seasonal changes in lignin distribution during tracheid development in Pinus radiata D. Don Wood Sci Technol 25:15–24. https://doi.org/10.1007/BF00195553

Donaldson LA (1993) Lignin distribution in wood from a progeny trial of genetically selected Pinus radiata D. Don Wood Sci Technol 27:391–395. https://doi.org/10.1007/BF00192226

Gärtner H, Schweingruber F (2013) Microscopic preparation techniques for plant stem analysis. Verlag Dr, Kessel, Remagen-Oberwinter

Gärtner H, Lucchinetti S, Schweingruber FH (2014) New perspectives for wood anatomical analysis in dendrosciences: The GSL1-microtome. Dendrochronologia (verona) 32:47–51. https://doi.org/10.1016/j.dendro.2013.07.002

Gerlach D (1969) Botanische mikrotechnik. Georg Thieme Verlag

Gindl W, Grabner M, Wimmer R (2000) The influence of temperature on latewood lignin content in treeline Norway spruce compared with maximum density and ring width. Trees - Structure and Function 14:409–414. https://doi.org/10.1007/s004680000057

Glerum C, Farrar JL (1966) Frost Ring Formation in the Stems of Some Coniferous Species. Can J Bot 44:879–886. https://doi.org/10.1139/b66-103

Greaves C, Crivellaro A, Piermattei A et al (2022) Remarkably high blue ring occurrence in Estonian Scots pines in 1976 reveals wood anatomical evidence of extreme autumnal cooling. Trees. https://doi.org/10.1007/s00468-022-02366-1

Gurskaya MA (2014) Temperature conditions of the formation of frost damages in conifer trees in the high latitudes of Western Siberia. Biol Bull 41:187–196

Hughes MK, Funkhouser G (1998) Extremes of moisture availability reconstructed from tree rings for recent millennia in the Great Basin of western North America. The impacts of climate variability on forests 99–107. https://doi.org/10.1007/BFb0009768

Kidd KR, Copenheaver CA, Zink-Sharp A (2014) Frequency and factors of earlywood frost ring formation in jack pine (Pinus banksiana) across northern lower Michigan. Ecoscience 21:157–167
Kipfmueller KF, Salzer MW (2010) Linear trend and climate response of five-needle pines in the western United States related to treeline proximity. Can J for Res 40:134–142
LaMarche VC Jr (1979) (1974) Paleoclimatic Inferences from Long Tree-Ring Records: Intersite comparison shows climatic anomalies that may be linked to features of the general circulation. Science 183:1043–1048. https://doi.org/10.1126/science.183.4129.1043
LaMarche VC, Hirschboeck KK (1984) Frost rings in trees as records of major volcanic eruptions. Nature. https://doi.org/10.1038/307121a0
LaMarche Jr VC (1970) Frost-damage rings in subalpine conifers and their application to tree-ring dating problems. Smith, JH G, and Worrall, J(eds), Tree-ring Analysis with Special Reference to Northwest America University of British Columbia Faculty of Forestry Bulletin 99–100
Matisons R, Gärtner H, Elferts D et al (2020) Occurrence of 'blue' and 'frost' rings reveal frost sensitivity of eastern Baltic provenances of Scots pine. For Ecol Manage 457:117729. https://doi.org/10.1016/j.foreco.2019.117729
Montwé D, Isaac-Renton M, Hamann A, Spiecker H (2018) Cold adaptation recorded in tree rings highlights risks associated with climate change and assisted migration. Nat Commun 9:1–7. https://doi.org/10.1038/s41467-018-04039-5
Payette S, Delwaide A, Simard M (2010) Frost-ring chronologies as dendroclimatic proxies of boreal environments. Geophys Res Lett 37:1–6. https://doi.org/10.1029/2009GL041849
Piermattei A, Crivellaro A, Carrer M, Urbinati C (2015) The "blue ring": anatomy and formation hypothesis of a new tree-ring anomaly in conifers. Trees 29:613–620. https://doi.org/10.1007/s00468-014-1107-x
Piermattei A, Crivellaro A, Krusic PJ et al (2020) A millennium-long 'Blue Ring' chronology from the Spanish Pyrenees reveals severe ephemeral summer cooling after volcanic eruptions. Environ Res Lett 15:124016. https://doi.org/10.1088/1748-9326/abc120
R Core Team (2024) R: A language and environment for statistical computing. R Foundation for Statistical Computing, Vienna, Austria
Saleh TM, Leney L, Sarkanen K V (1967) Radioautographic studies of cottonwood, Douglas fir and wheat plants
Salzer MW, Hughes MK (2007) Bristlecone pine tree rings and volcanic eruptions over the last 5000 yr. Quat Res 67:57–68. https://doi.org/10.1016/j.yqres.2006.07.004
Salzer MW, Hughes MK, Bunn AG, Kipfmueller KF (2009) Recent unprecedented tree-ring growth in bristlecone pine at the highest elevations and possible causes. Proc Natl Acad Sci 106:20348–20353
Salzer MW, Bunn AG, Graham NE, Hughes MK (2014a) Five millennia of paleotemperature from tree-rings in the Great Basin, USA. Clim Dyn 42:1517–1526
Salzer MW, Larson ER, Bunn AG, Hughes MK (2014) Changing climate response in near-treeline bristlecone pine with elevation and aspect. Environ Res Lett 9:114007. https://doi.org/10.1088/1748-9326/9/11/114007
Schulman E (1958) Bristlecone pine, oldest known living thing. Nat Geogr Mag 113:355–372
Schulman E, Ferguson C, (1956) Millenia-old pine trees sampled in 1954 and, (1955). In: Schulman E (ed) Dendroclimatic Changes in Semiarid America. University of Arizona Press, Tucson AZ, pp 136–138
Schweingruber FH (2007) Wood structure and environment. Springer Science \& Business Media
Sigl M, Winstrup M, McConnell JR et al (2015) Timing and climate forcing of volcanic eruptions for the past 2,500 years. Nature 523:543–549. https://doi.org/10.1038/nature14565
Stokes MA (1996) An introduction to tree-ring dating. University of Arizona Press
Tardif JC, Salzer MW, Conciatori F et al (2020) Formation, structure and climatic significance of blue rings and frost rings in high elevation bristlecone pine (Pinus longaeva DK Bailey). Quat Sci Rev 244:106516. https://doi.org/10.1016/j.quascirev.2020.106516
Trendelenburg (1939) Das Holz als Rohstoff. Lehmanns, Munich
Ziaco E, Biondi F, Rossi S, Deslauriers A (2016) Environmental drivers of cambial phenology in Great Basin bristlecone pine. Tree Physiol 36:818–831. https://doi.org/10.1093/treephys/tpw006

Supplementary data

Table S1 Characteristics of cores used in the study

Table S2 Results of the Mann-Whitney test (two sided) of differences in mean monthly temperatures between EWFR recording and non-recording trees for the period 1895-2014. The median and IQR are indicated. Results significant at p <= 0.01 are bolded

Figure S1 High magnification microphotographs of a) BR-1, b) BR-2, c) BR-3, d) BR-4. Please note the increasing level of cell wall lignification of different BR intensity types. Lignification process clearly starts in cell wall corners and continues along first radial walls and then tangential walls. In varying stages of incomplete lignification, radial walls are visibly more strongly lignified that tangential walls

Figure S2 Boxplots presenting Mann-Whitney test results for mean monthly temperatures of EWFR and non-EWFR years (period 1895-2014). EWFR years: 1895, 1897, 1928, 1938, 1950, 1954, 1979, 1984, 1992, 2007. Please note that May mean monthly temperature is significantly higher for EWFR years suggesting that earlier cambial reactivation may lead to EWFR formation due to subsequent spring frost events

Figure S3 Daily mean temperatures for the period 1981-2014. EWFR years 1984, 1992, 2007. Please note temperatures raising above 6°C already in May, followed by period of below 0°C temperatures probably leading to EWFR formation

Figure S4 Significant (p=0.02) negative linear relationship between BR frequency and DTL. Mann-Whitney test indicates lack of statistically significant (p=0.83) difference of BR frequency distribution between southerly and northerly exposed trees

Figure S5 Generalized linear mixed-effects model (GLMM) results. Predicted probability of BR formation in September and October under different temperature scenarios for June. Please note the interaction between beginning of growth season (June) temperatures and end of growth season (September, October). Lower temperatures in June delay the onset of xylogenesis, increasing the probability of BR formation in September and October

Figure S6 Daily mean temperatures in the period 1981-2014. Please note when on average mean daily temperatures rise above and drop below 6°C – the approximate threshold for cambial activity in bristlecone pine

Figure S7 Daily mean temperature for the period 1981-2014 and BR years 1982, 1998. Please note cold snaps in June and September 1982 and September 1998 probably leading to BR formation

Figure S8 BR chronology of 22 pairs of cores coming from double-cored trees continuously covering the period 1793-1998. Please note that in many cases BRs are not continuous around the stem appearing only in one of the pair of cores, in other cases BR intensity varies around the stem with BRs of higher intensity class in one core than in the second

Table S1 Characteristics of cores used in the study

Core	Start year	End year	Length	Elevation	DTL	Exposition
CWU409A	1595	2014	420	3512	0	S
CWU416A	1625	2014	390	3473	39	S
CWU416B	1500	1999	500	3473	39	S
CWU417A	1538	2014	477	3502	10	S
CWU417B	1626	2014	389	3502	10	S
CWU537A	1438	2014	512	3510	2	S
CWU538A	1775	2014	240	3504	8	S
CWU540A	1730	2014	285	3505	7	S
CWU541A	1671	2007	337	3500	12	S
CWU543A	1750	2014	265	3505	7	S
CWU543B	1306	2014	709	3505	7	S
NF518B	1793	2009	217	3475	0	N
NF521B	1221	2008	788	3446	29	N
NF522B	1547	2008	462	3447	28	N
NF524B	1178	2009	814	3440	35	N
NF525B	1198	2009	811	3423	52	N
NF526A	1181	2009	822	3427	48	N
NF526B	1132	2009	876	3427	48	N
NF527A	902	2009	1103	3430	45	N
NF527B	897	2009	977	3430	45	N
NF528A	954	2002	1049	3427	48	N
NF528B	875	1999	1125	3427	48	N
NF529A	1500	2009	510	3393	82	N
NF529B	1259	2009	751	3393	82	N
NF530A	1545	2009	465	3392	83	N
NF530B	1469	2009	541	3392	83	N
NF531A	1675	2009	335	3391	84	N
NF532A	1378	2009	632	3389	86	N
NF532B	1068	2009	942	3389	86	N
NF533B	871	2009	1139	3359	116	N
NF534A	1166	2009	844	3361	114	N
NF534B	1579	2000	422	3361	114	N
PAL024B	681	2001	1321	3344	168	S

PAL028B	787	1998	1212	3352	123	N
PAL032A	164	2005	1842	3320	192	S
PAL032B	515	2006	1492	3320	192	S
PAL036A	322	1956	1635	3309	166	N
SF505B	1625	2008	384	3480	32	S
SF506A	1672	2009	338	3478	34	S
SF508B	1813	2009	190	3475	37	S
SF509A	1196	2008	813	3448	64	S
SF510A	1044	2009	966	3447	65	S
SF510B	1064	2009	946	3447	65	S
SF511A	1330	2009	680	3447	65	S
SF511B	1182	2009	828	3447	65	S
SF512A	1324	2009	686	3448	64	S
SF512B	1154	2009	856	3448	64	S
SF513A	1345	2009	665	3429	83	S
SF513B	1014	2009	996	3429	83	S
SF514A	1183	2009	827	3426	86	S
SF514B	1315	2009	695	3426	86	S
SF515A	1291	2009	719	3430	82	S
SF515B	794	2009	1216	3430	82	S
SF516A	1034	2009	950	3428	84	S
SF516B	1034	2009	976	3428	84	S
SHP360A	1229	2005	777	3501	11	S
SHP612A	1546	2005	460	3495	17	S
SHP907A	1583	2005	423	3498	14	S
SHP908B	1738	2005	268	3496	16	S
SHP909A	1667	2005	339	3490	22	S
SHP911A	1332	2005	674	3442	70	S
SHP912A	1691	2005	315	3437	75	S
SHP913A	1713	2005	293	3432	80	S
SHP914A	1172	2005	834	3472	3	N
SHP922A	1170	2005	836	3436	76	S
SHP924A	1113	2005	893	3472	40	S
SHP933A	1405	2005	601	3417	58	N
SHP933B	1616	2005	390	3417	58	N
SHP934B	1180	2005	821	3415	60	N

SHP944A	1328	2005	678	3445	67	S
SHP944B	1199	2005	807	3445	67	S
SHP945A	1392	2005	614	3435	77	S
SHP945B	1015	2005	991	3435	77	S
SHP947A	583	2005	1423	3427	85	S
SHP947B	1556	2005	450	3427	85	S
SHP948A	1712	2005	294	3498	14	S
SHP949A	1440	2005	566	3494	18	S
SHP953B	1428	2005	578	3452	60	S
SHP957A	1734	2005	272	3429	46	N
SHP958A	1886	2005	120	3438	37	N
SHP962B	1281	2005	725	3471	41	S
SHP972B	1527	2005	479	3395	117	S
SHP975B	1495	2005	511	3457	55	S

Table S2 *Results of the Mann-Whitney test (two sided) of differences in mean monthly temperatures between EWFR recording and non-recording trees for the period 1895-2014. The median and IQR are indicated. Results significant at* ***p <= 0.01 are bolded***

Month	n EWFR	n non-EWRF	Median (IQR) EWFR	Median (IQR) non-EWFR	*p* value
January	10	110	-7.0 (-9.3-(-5.5)) °C	-7.0 (-8.3-(-6.3)) °C	0,861
February	10	110	-6,9 (-9.0-(-6.2)) °C	-7,6 (-9.0-(-6.4)) °C	0,468
March	10	110	-6,3 (-8.4-(-5.4)) °C	-6,2 (-8.1-(-5.1)) °C	0,955
April	10	110	-3,0 (-4.6-(-2.1)) °C	-4,3 (-5.4-(-2.8)) °C	0,125
May	10	110	2,5 (0.8-3.4) °C	0.0 (-1.9-1.3) °C	**0,002**
June	10	110	5,8 (5.4-6.2) °C	6.0 (4.7-7.4) °C	0,917
July	10	110	10,1 (8.6-10.8) °C	10.0 (8.9-10.7) °C	0,958
August	10	110	9,4 (9-10.3) °C	9.0 (8.2-10.1) °C	0,428
September	10	110	6,3 (5.3-7) ± 1 °C	5,4 (4.4-6.7) °C	0,171
October	10	110	1,2 (-0.2-2.1) °C	0,7 (-0.3-2.1) °C	0,772
November	10	110	-3.0 (-4.1-(-1.1)) °C	-3.0 (-4.3-(-1.7)) °C	0,625
December	10	110	-7,2 (-7.8-(-4.1)) °C	-6,3 (-8.0-(-5.1)) °C	0,887

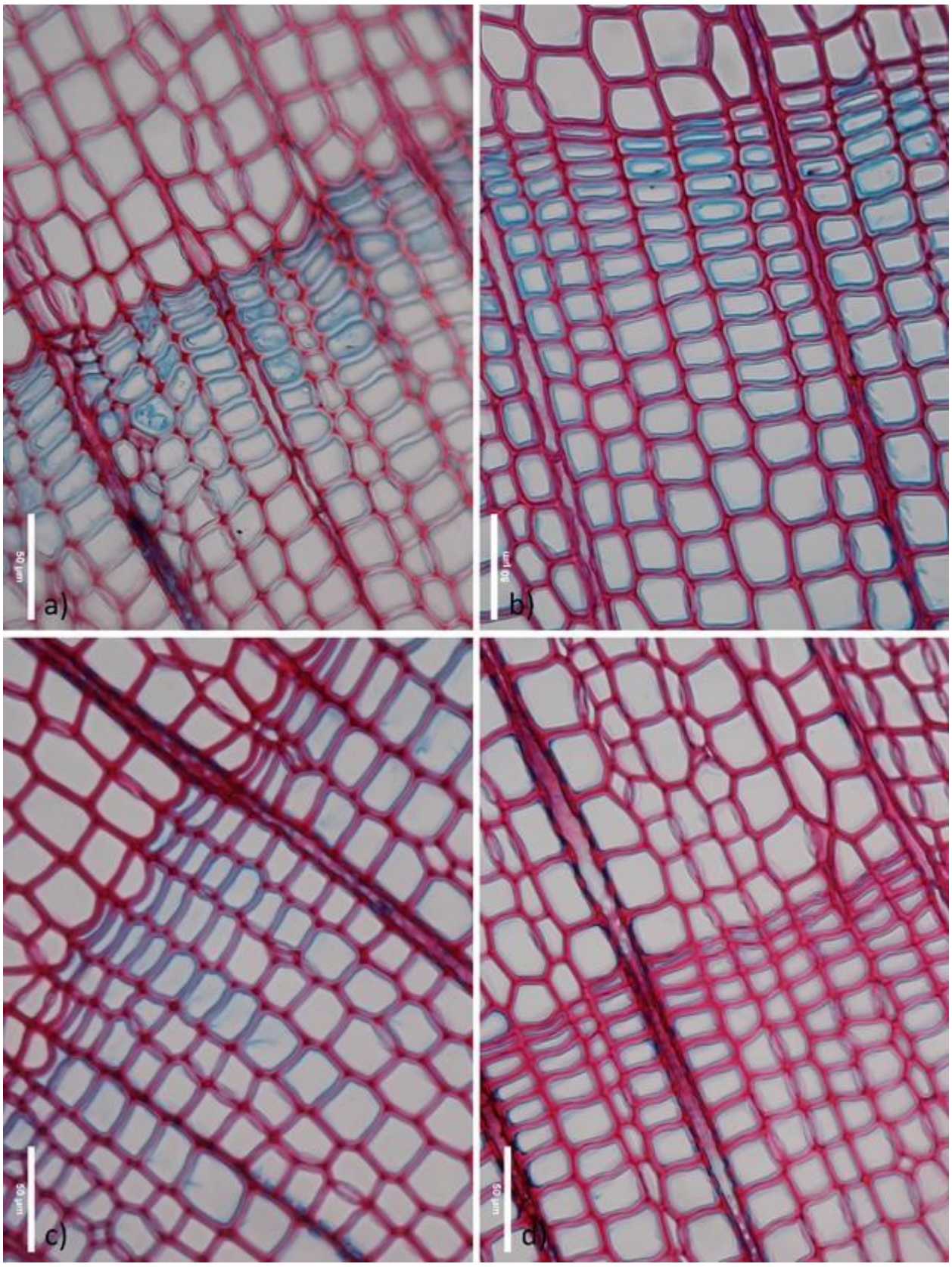

Figure S1 High magnification microphotographs of a) BR-1, b) BR-2, c) BR-3, d) BR-4. Please note the increasing level of cell wall lignification of different BR intensity types. Lignification process clearly starts in cell wall corners and continues along first radial walls and then tangential walls. In varying stages of incomplete lignification, radial walls are visibly more strongly lignified that tangential wall

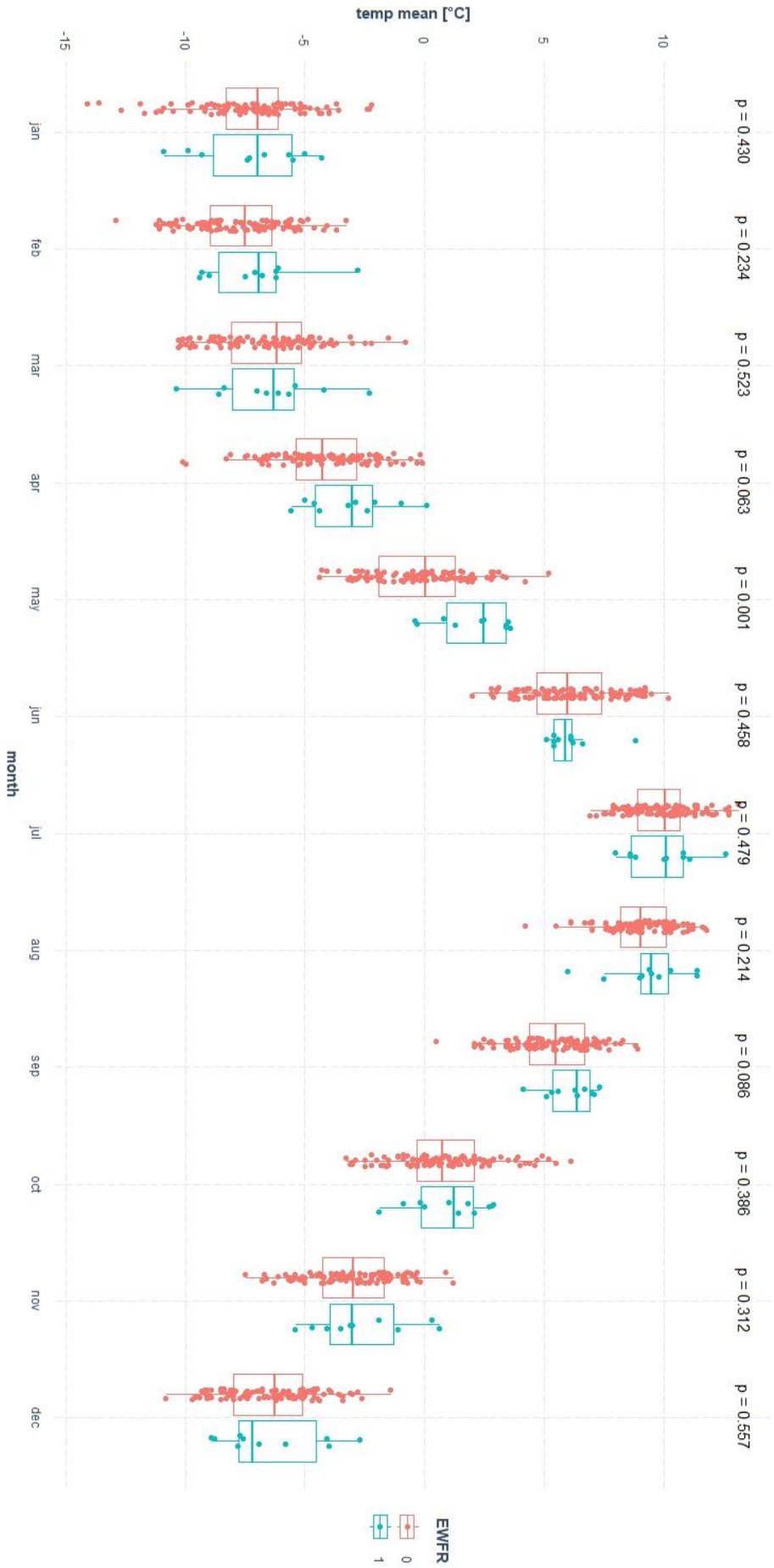
temp mean [°C]
-15
-10
-5
0
5
10
month
jan
feb
mar
apr
may
jun
jul
aug
sep
oct
nov
dec
p = 0.430
p = 0.234
p = 0.523
p = 0.063
p = 0.001
p = 0.458
p = 0.479
p = 0.214
p = 0.086
p = 0.386
p = 0.312
p = 0.557
EWFR
1
0

Figure S2 Boxplots presenting Mann-Whitney test results for mean monthly temperatures of EWFR and non-EWFR years (period 1895-2014). EWFR years: 1895, 1897, 1928, 1938, 1950, 1954, 1979, 1984, 1992, 2007. Please note that May mean monthly temperature is significantly higher for EWFR years suggesting that earlier cambial reactivation may lead to EWFR formation due to subsequent spring frost events

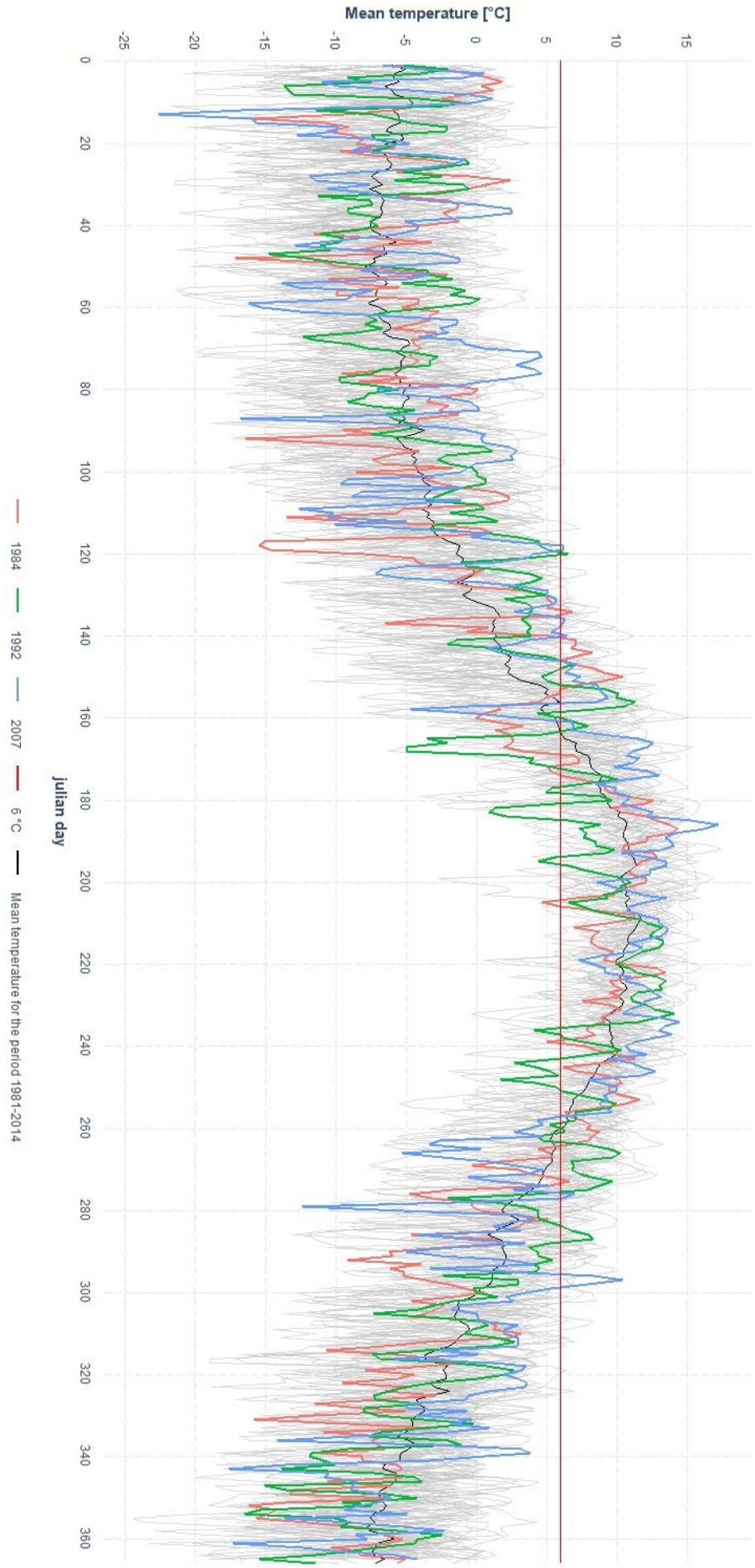
Mean temperature [°C]
-25
-20
-15
-10
-5
0
5
10
15
0
20
40
60
80
100
120
140
160
180
200
220
240
260
280
300
320
340
360
julian day
1984
1992
2007
6 °C
Mean temperature for the period 1981-2014

Figure S3 Daily mean temperatures for the period 1981-2014. EWFR years 1984, 1992, 2007. Please note temperatures raising above 6°C already in May, followed by period of below 0°C temperatures probably leading to EWFR formation

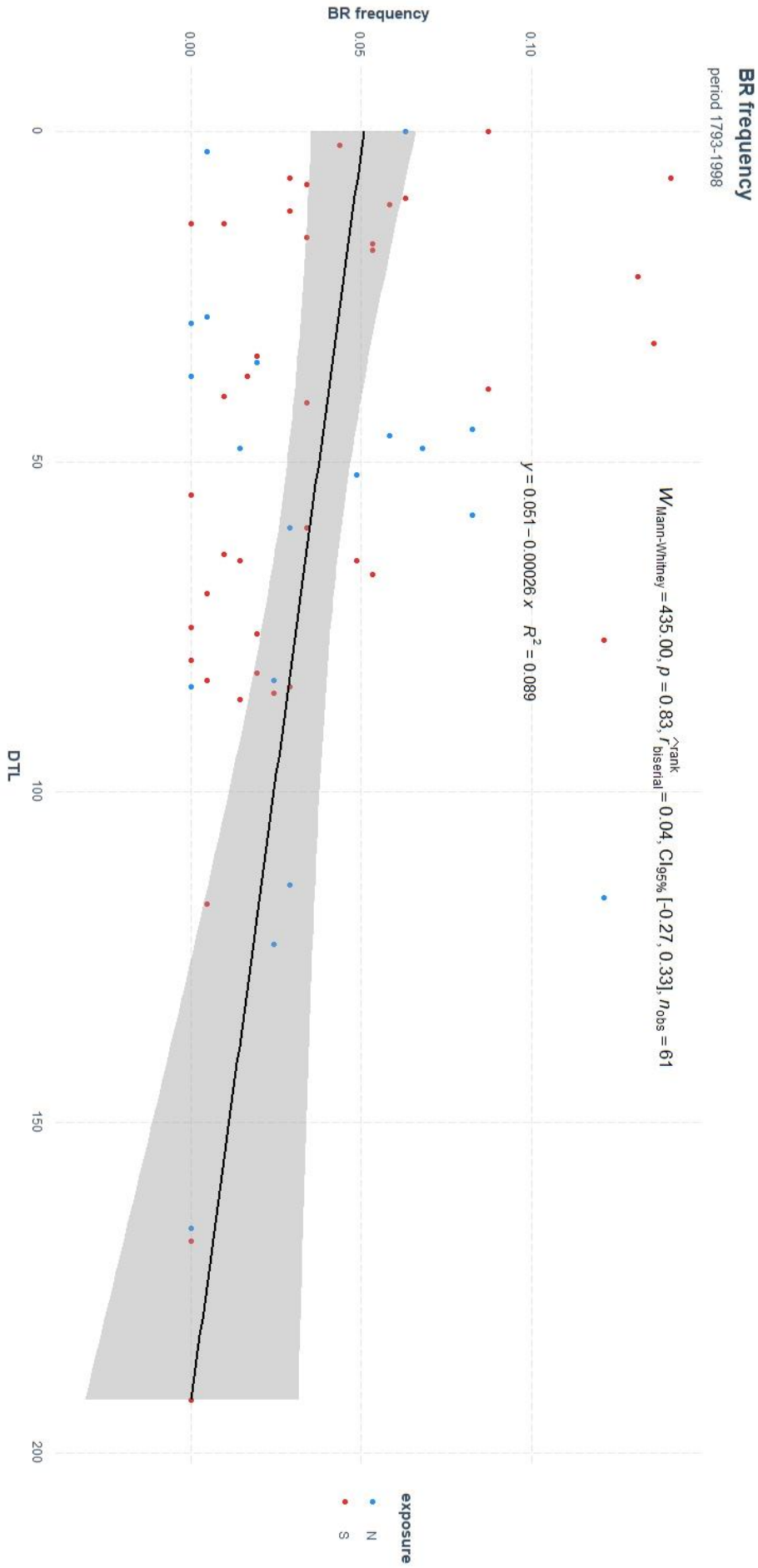
BR frequency
period 1793-1998
BR frequency
0.00
0.05
0.10
0
50
100
150
200
DTL
$y = 0.051 - 0.00026\,x \quad R^2 = 0.089$
$W_{\text{Mann-Whitney}} = 435.00,\ p = 0.83,\ \hat{r}^{\text{rank}}_{\text{biserial}} = 0.04,\ \text{CI}_{95\%}\ [-0.27, 0.33],\ n_{\text{obs}} = 61$
exposure
N
S

Figure S4 Significant (p=0.02) negative linear relationship between BR frequency and DTL. Mann-Whitney test indicates lack of statistically significant (p=0.83) difference of BR frequency distribution between southerly and northerly exposed trees

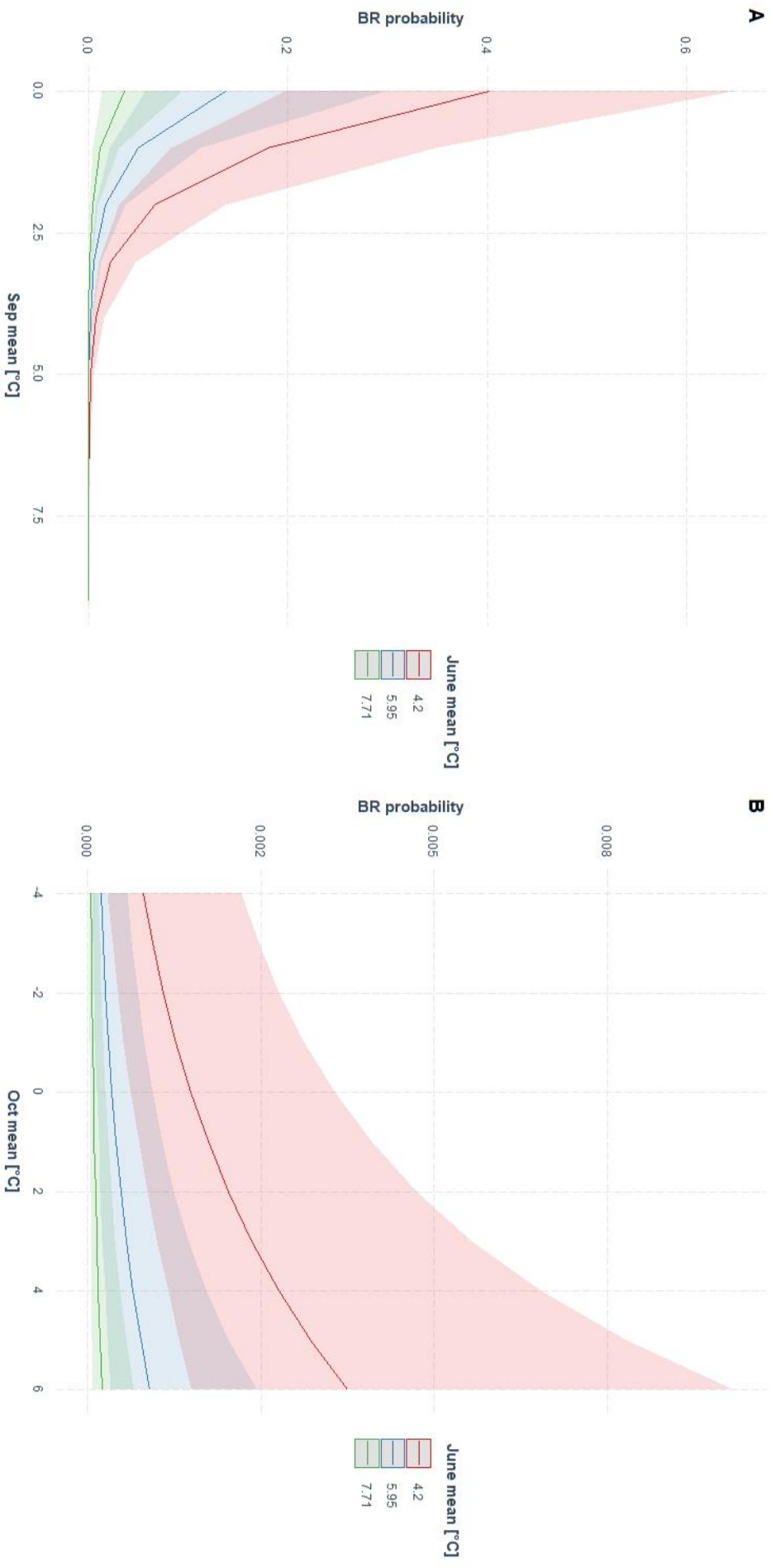
A
BR probability
0.0
0.2
0.4
0.6
Sep mean [°C]
0.0
2.5
5.0
7.5
June mean [°C]
4.2
5.95
7.71
B
BR probability
0.000
0.002
0.005
0.008
Oct mean [°C]
-4
-2
0
2
4
6
June mean [°C]
4.2
5.95
7.71

Figure S5 Generalized linear mixed-effects model (GLMM) results. Predicted probability of BR formation in September and October under different temperature scenarios for June. Please note the interaction between beginning of growth season (June) temperatures and end of growth season (September, October). Lower temperatures in June delay the onset of xylogenesis, increasing the probability of BR formation in September and October

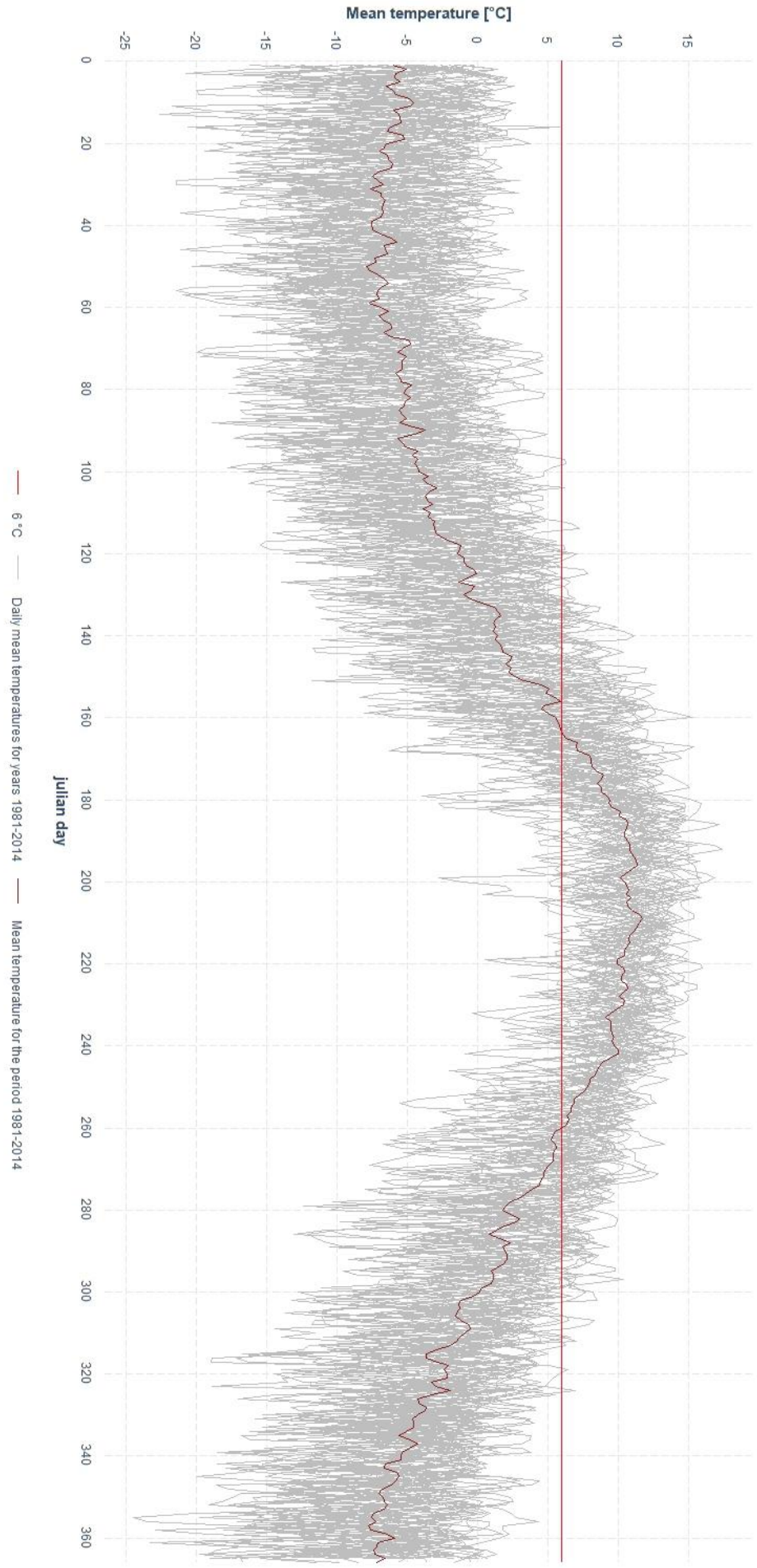
Mean temperature [°C]
-25
-20
-15
-10
-5
0
5
10
15
0
20
40
60
80
100
120
140
160
180
200
220
240
260
280
300
320
340
360
julian day
6 °C
Daily mean temperatures for years 1981-2014
Mean temperature for the period 1981-2014

Figure S6 Daily mean temperatures in the period 1981-2014. Please note when on average mean daily temperatures rise above and drop below 6°C – the approximate threshold for cambial activity in bristlecone pine

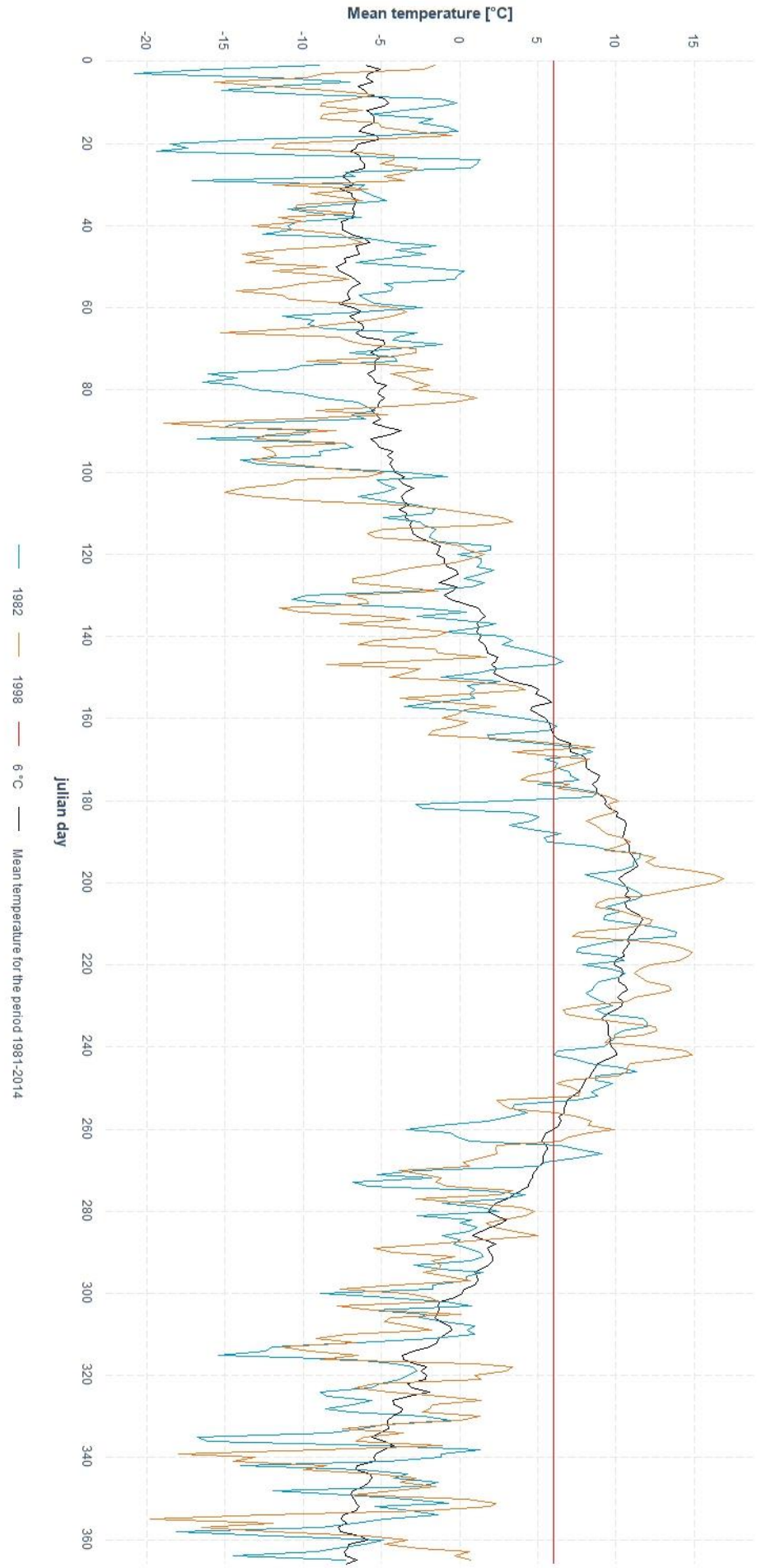
Mean temperature [°C]
-20
-15
-10
-5
0
5
10
15
0
20
40
60
80
100
120
140
160
180
200
220
240
260
280
300
320
340
360
julian day
1982
1998
6 °C
Mean temperature for the period 1981-2014

Figure S7 Daily mean temperature for the period 1981-2014 and BR years 1982, 1998. Please note cold snaps in June and September 1982 and September 1998 probably leading to BR formation

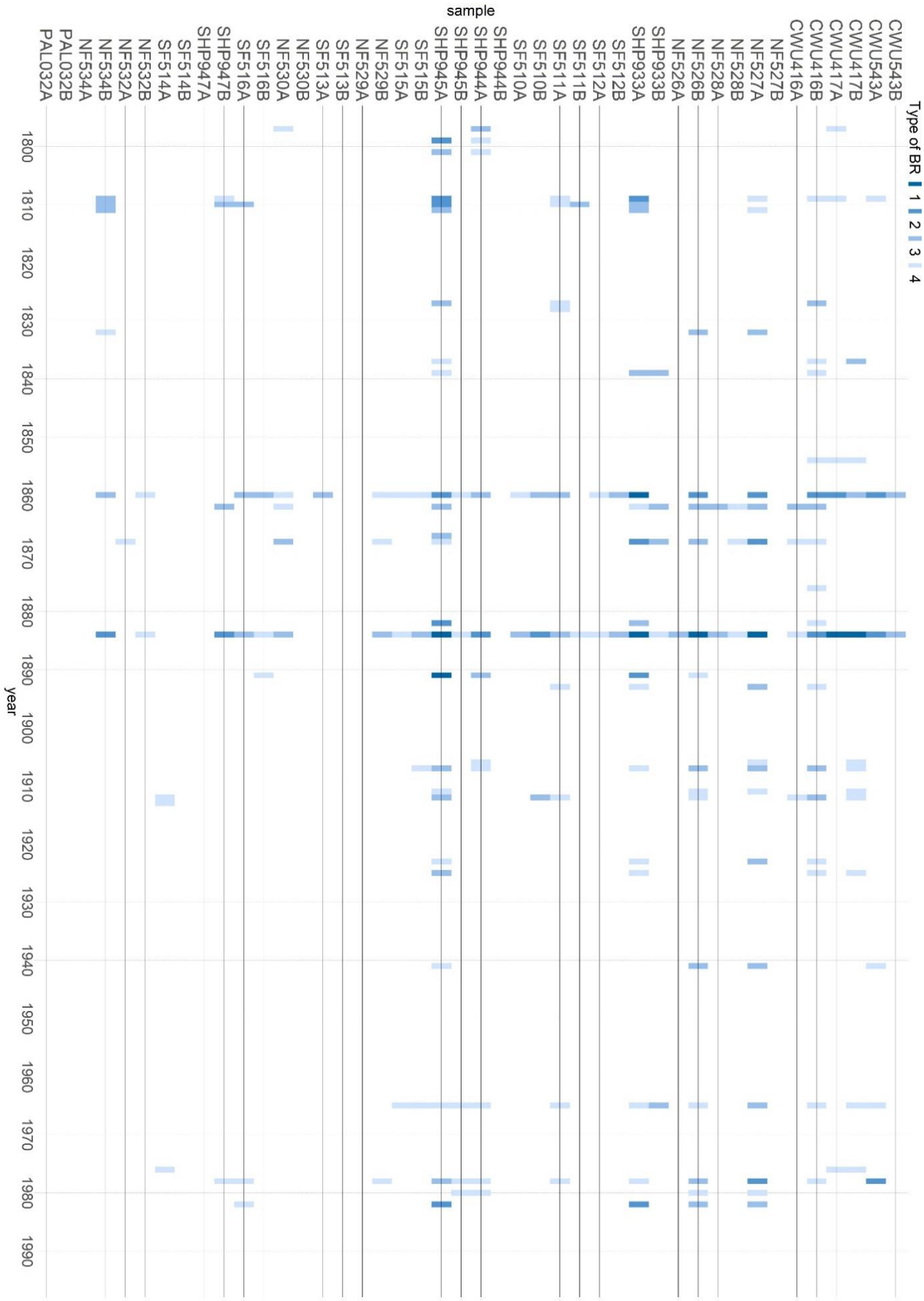

Figure S8 BR chronology of 22 pairs of cores coming from double-cored trees continuously covering the period 1793-1998. Please note that in many cases BRs are not continuous around the stem appearing only in one of the pair of cores, in other cases BR intensity varies around the stem with BRs of higher intensity class in one core than in the second

Publication 2 - An 1100-year record of blue rings in Bristlecone pine provides new insights into volcanic forcing.

A 1100-year record of blue rings in Bristlecone pine provides new insights into volcanic forcing

Liliana Siekacz [a]

Charlotte Pearson [b,c]

Matthew Salzer [b]

Jakub Wojtasik [d]

Marcin Koprowski [a,e]

[a] Department of Ecology and Biogeography, Nicolaus Copernicus University, Lwowska 1, 87-100, Toruń, Poland

[b] Laboratory of Tree-Ring Research, The University of Arizona, 1215 E. Lowell St., Tucson, AZ, 85721, USA

[c] Geosciences, The University of Arizona, 1040 E. 4th Street, Tucson, AZ, 85721, USA

[d] Centre for Statistical Analysis, Nicolaus Copernicus University, Chopina 12/18, 87-100, Toruń, Poland

[e] Centre for Climate Change Research, Nicolaus Copernicus University, Lwowska 1, 87-100 Torun, Poland

Corresponding author email: lilsie@doktorant.umk.pl

Key words:

blue rings, frost rings, lignification, dendroclimatology, *Pinus longaeva*, volcanism, wood anatomy

Highlights:

- Developed a 1100-year blue ring chronology from bristlecone pine in California.

- Found strong correlation between blue ring formation and volcanic eruptions, particularly of tropical origin.

- Blue rings indicate volcanic cooling effects earlier than traditional ring width measurements.

- Demonstrated that blue rings are more sensitive indicators of late-season cold spells than frost rings.

- Provided new insights into spatial signatures of cooling events linked to major volcanic eruptions.

Abstract

The study of blue rings (underlignified rings) has recently attracted significant interest due to their potential to provide more insights into past cooling episodes, complementing other tree ring-derived data. This research developed a blue ring chronology from bristlecone pine over the past 1100 years, based on 83 cores collected from a tree line site in California's White Mountains. This chronology, the most extensive and well-replicated to date, reveals a strong correlation between BRs and volcanic eruptions, especially those of tropical origin. The study demonstrates that blue rings can indicate the climatic effects of volcanic activity earlier than traditional ring width measurements and are more sensitive and reliable indicators of late growing season cold spells than frost rings. This record, in conjunction with other discrete indicators of historical cooling from various regions, is used to evaluate the extent and spatial signatures of cooling events linked to major volcanic eruptions over the past millennium. These findings underscore the value of BRs in reconstructing high-resolution climate histories and improving the dating of past volcanic episodes.

1. Introduction

Volcanoes are one of the dominant contributors to natural climate variability on interannual to decadal timescales (Crowley, 2000; Mann et al., 2005). By injecting sulfate into the atmosphere they can cause sudden, short-term reductions in solar radiation reaching the Earth's surface (Robock, 2000). This can cause rapid onset of short-term changes in climate, which can have significant impacts for human society (Oppenheimer, 2003). Beyond the written record, tree rings offer means to capture and document such annual and sub-annual changes. They are therefore particularly useful in the study of past volcanism both in terms of dating past events via climatic causal connections, and in understanding subsequent climatic forcing (Briffa et al., 2004). In particular, wood anatomical abnormalities such as frost rings (Barbosa et al., 2019; Brunstein, 1996, 1995; Glerum and Farrar, 1966; Gurskaya and Shiyatov, 2006; Hadad et al., 2020; LaMarche Jr, 1970; LaMarche and Hirschboeck, 1984; Payette et al., 2010), light rings (Tardif et al., 2011; Wang et al., 2000) and blue rings (Greaves et al., 2022; Matisons et al., 2020; Montwé et al., 2018; Piermattei et al., 2020, 2015; Tardif et al., 2020) have been utilized as anatomical markers of adverse growth conditions, which allow a more detailed exploration of sub-annual response to volcanic forcing in addition to constructing long annually resolved records.

Frost rings are caused by a combination of dehydration and the pressure of ice formation (Glerum and Farrar, 1966; Schweingruber, 2007) from sudden and unexpected frosts and occur while the cambium is still active and the xylem mother cells are dividing. They are characterized by structural damage that can clearly be observed under a microscope as, collapsed/crushed/abnormal tracheids with lateral expansion and displacement of the rays (Glerum and Farrar, 1966; Schweingruber, 2007). The connection between frost rings (as well as growth minima) with volcanic eruptions was first demonstrated in studies on bristlecone pine (*Pinus longaeva* D.K. Bailey), which show a strong correlation with volcanic sulfate deposition in polar ice-core records (Baillie, 2010; Baillie and McAneney, 2015; LaMarche and Hirschboeck, 1984; McAneney and Baillie, 2019; Salzer and Hughes, 2007; M. Sigl et al., 2015). Bristlecone pine is the longest living tree species currently known and offers an invaluable archive of past climatic change thanks to its annual resolution, secure dating, and temporal coverage (Bale et al., 2011; Bruening et al., 2018; Brunstein, 1996, 1995; Bunn et al., 2018, 2011; Ferguson, 1979, 1969; LaMarche and Stockton, 1974; Salzer et al., 2014a, 2009; Salzer and Hughes, 2007;

Schulman, 1958; Tran et al., 2017). Recent work on ice-core records has utilized bristlecone data to constrain the dating accuracy of volcanic eruptive history over the course of the Holocene (Sigl et al., 2015, 2022), underlining the value of further exploration of the bristlecone record to develop more detailed and well-replicated histories of sudden, short-term climatic response to volcanic eruptions.

In this study, we explore the potential of blue rings (so called as they are revealed as blue-stained bands of cell walls by the double staining of wood thin-sections with safranin and astra blue dyes) as a means to further augment the volcanic signal in bristlecone pine. Blue rings (BRs) have already been observed to be caused by the type of sudden, short-term cooling resulting from volcanic forcing (Büntgen et al., 2022; Piermattei et al., 2020; Tardif et al., 2020). Unlike frost rings, however, which are formed only when cambial activity continues, blue rings have the capacity to record cooling episodes outside of the growing period. This is because they reflect the incomplete lignification of the tracheid walls, a process that continues outside of the phase of radial growth (Donaldson, 1992, 1991; Piermattei et al., 2015). This is particularly relevant for further studies utilizing ice-core data and other records to fine-tune our understanding of the climatic impacts of past volcanism. Ice-core based volcanic activity reconstructions are subject to dating uncertainties due to potential errors in annual layer interpretation and time lags between stratospheric injection at the source and deposition at the ice-core site. Eruption characteristics such as particle size, latitude, season, injection height, and atmospheric circulation pattern also contribute to different atmospheric residence times of volcanic ejecta and gasses affecting the eruption-deposition time lag. BRs offer the potential to better constrain the dating of volcanic episodes and help paint a more accurate picture of regionally diverse patterns of climatic system response.

Here we present a blue ring chronology from bristlecone pine for the last 1100 years based on 83 cores from trees growing in the White Mountains of California. The aims were to comprehensively explore this newly created dataset in order to establish the full potential of blue rings in bristlecone pine as a proxy for sub-annual ephemeral cooling in association with volcanic eruptions.

2. Materials and methods

This study used bristlecone pine samples collected over multiple field campaigns in the Sheep Mountain and Patriarch Grove area of the Ancient Bristlecone Pine Forest in the White Mountains of California (37.5 W 118.2 N, see fig. S1). Trees sampled were situated in a rough, mountainous terrain with a dolomitic substrate, and covered an elevational transect between 3512 and 3320 m a.s.l. l, with a vertical distance of 192 m from the highest to the lowest situated tree. Samples used to develop the blue ring record came from five locations within this transect, north and south facing slopes (SF and NF from Salzer et al., (2014b)) and sites named Cottonwood Upper (CWU), Sheep Mountain (SHP) and Patriarch Lower (PAL). From these locations, 83 cores were selected for preparation and analysis for blue rings (tab. S1)

2.1 Laboratory preparation

Samples had previously been air-dried, glued into wooden mounts, sanded and measured using standard dendrochronological procedures (Stokes, 1996). To prepare them for analysis in this study, they were separated from their mounts by soaking in near-boiling water. Each core was then divided into 4-6 cm long overlapping segments, diagonally cut to allow for easy reassembly and accurate cross-dating of the finished sections. The segments were not of equal length, as each core was assessed individually under a microscope to ensure maximum ring overlap on both sides of the split. The order of the sectioned pieces was documented for final reassembly of each core. The core elements were cut into thin sections approximately 10-15µm thick using a GSL1 microtome (Gärtner et al., 2014).

To reveal lignified cell walls in red and underlignified cell walls in blue, thin sections were stained using a mixture of Safranine and Astrablue. The stains were prepared according to the procedure outlined by (Gärtner and Schweingruber, 2013) which involved dissolving 0.5 g of Astra Blue powder in 100 ml of distilled water and 2 ml of acetic acid, and 0.1 g of Safranin powder in 100 ml of distilled water. The two solutions were then mixed in a 1:1 ratio. Each thin section was immersed in the stain bath for 3-4 minutes, followed by a wash in ethanol at progressively increasing concentrations of 50%, 75%, and 99.8% to remove excess stain and dehydrate the section. Finally, each section was embedded in Canada Balsam, covered with a cover glass, and oven dried at 60°C for 24 hours.

The 83 cores yielded 612 permanent thin-sections, which were digitized to facilitate ring width measurement and cross-dating. Photographs of each thin-section were taken using a binocular microscope coupled with a CANON EOS 700D camera under 40x magnification. To ensure accuracy, control photos of a scale were taken for each microscope magnification. The pictures were stitched together in PTGui software to create high-resolution images of the entire thin-sections, taking care to achieve a representative overlap of 20-30% between individual photos. The ring widths were then measured in ImageJ software (https://imagej.nih.gov/ij/index.html), and visually cross-dated and dating confirmed using CDendro software (http://www.cybis.se/forfun/dendro/). The cell structure of the sections was surveyed at 40x and 100x magnification using both high-resolution digital images and stained slides. Underlignified tracheids were noted and calendar dates assigned to rings containing them. EWFR and LWFR were also observed and dated accordingly. Blue rings were assigned intensity classes decreasing from BR1 to BR4 following the classification described in Siekacz et al., (2024).

2.2 Data preparation and statistical analysis

The complete BR chronology covers 164-2014 CE with varying sample depth (fig.S2). However, we restricted our analysis to the period 900-2014 CE (fig.1) during which the sample depth reaches at least 10 cores. To assess the association between volcanic eruptions and BR occurrence, we used the time series of Global volcanic forcing (GVF) in W/m-2 established by Sigl et al., (2015) a record of past eruptions and their influence on climate. This data was selected because it is currently the most accurate and securely dated volcanic forcing record over the past two millennia due to the secure alignment of independent age markers in ice-cores (10Be) to precisely dated markers in tree rings (14C) caused by solar particle events. This synchronization of the existing bipolar ice-core chronologies improved dating accuracy to annual resolution, which is critical for our purpose in this study where we seek to compare tree ring evidence and ice-core evidence of the same volcanic events. Although this work was extended to cover the Holocene (Sigl et al., 2022) the authors recommend using the 2015 version in studies concentrating on the common era.

We used a 3 year time window to investigate correlations between the ice core sulfate signal and BR occurrence, allowing for time-lags in ice-core sulfate deposition

(Sigl et al., 2015) and the various timing and scale of climatic impacts following eruptions. These impacts depend on several factors, including season, latitude, magnitude, altitude, particle size and stratospheric residence time of the ejected materials etc. (Cole-Dai, 2010; Dutton and Christy, 1992; Timmreck, 2012). Indeed considerable evidence exists for delayed or extended, regionally variable cooling responses to volcanic eruptions (Fang et al., 2023; Vidal et al., 2016).

We performed a chi-squared test of independence to examine the relationship between our BR record and the record of volcanic forcing derived from ice-core data (Sigl et al., 2015). The test was performed in two steps, first considering only direct year-year matches, second allowing a 3 year window of co-occurrence. These steps were performed in 4 iterations: for all eruptions, and separately for eruptions classified as tropical, northern hemisphere extratropical (NH) and southern hemisphere extratropical (SH), to determine whether the association was dependent on the location of the volcanic eruption.

To quantitatively analyze these associations we fitted a generalized linear mixed-effects model (GLMM), with a binary response variable representing the absence (0) or presence (1) of a BR in a given year, in a particular sample. The independent variables included GVF in W/m-2 (Sigl et al., 2015) and distance from upper treeline (DTL) as previous analysis (Siekacz et al., 2024) demonstrated that BR formation is modulated by DTL in this temperature limited treeline ecotone, with BR formation probability decreasing as DTL increases. The model was fit to data covering 1115 years (900-2014 CE), where sample depth was at least 10 cores. The complete dataset included a minimum and maximum sample depth of 10 and 83 cores respectively, with 22 cases involving two samples per tree. However to account for independence of observations we included only one sample per tree in our model, reducing the maximum sample depth to 61 individual cores. Each core was treated as a random effect, allowing the model's intercept to vary among cores. Data analysis was conducted in R, v. 4.1.3 (R Core Team, 2022), using the package "lme4" for mixed modeling (Bates et al., 2015). The model specification was as follows: BR_event ~ GVF + DTL + (1|core) and it was estimated using ML and BOBYQA optimizer.

RW measurements of the sectioned cores were conservatively standardized to remove trends related to age and size. This is a fundamental procedure in dendrochronology, that aims to eliminate long-term non-climatic factors associated with the growth of trees as they age and increase in size (Cook and Kairiukstis, 1990; Fritts, 1976). The dplR package (Bunn, 2008) was utilized to standardize the data, which included

fitting a negative exponential curve, a linear fit line, or a horizontal line, since high elevation bristlecone pine stands are open and non-competitive. The raw data was then divided by the fitted curve. the mean (Std dev) series intercorrelation and mean (Std dev) first-order auto-correlation coefficient were calculated on the detrended data for each tree and averaged to be 0.5940249 (0.1244917) and 0.6625052 (0.1580373) respectively. To create a standard site chronology, the annual standardized indices of tree growth were averaged by year using a bi-weighted robust mean. We aimed to evaluate if the BR chronology brings new independent information as compared to the ring widths of the trees. High autocorrelation prevented the use of standard statistical tests that require independence of observations. To overcome this issue two standard dendrochronological methods were deployed: Pointer Year analysis (Becker et al., 1994) and Superposed Epoch Analysis (SEA). Respective functions from dplR package (Bunn, 2008) were used for the analysis.

To test whether BRs showed any association with trends in individual ring width index (RWI) series, Pointer Year analysis was performed on the standardized RWI series. Pointer years were defined as those calendar years in which at least 75% of the cross-dated trees presented an RWI variation higher than 10% (Becker et al., 1994). The radial growth variation represents the extent to which the ring of the current year is narrower (negative value) or wider (positive value) than the previous one. A further Chi-squared test of independence was performed to check for evidence of any association between BRs and neutral, positive or negative classifications of a tree ring.

SEA was performed to determine if the association observed at the individual tree level is retained in the standardized chronology of the site and remains statistically significant across the range of BR years. We also examined how this association varies for sets of years with different number of BRs. The stability of this association was tested across all BR event years, as well as subsets of years with at least 5, 10, 15, 20, 25, or more BRs.

To further explore the BR record in terms of response to specific volcanic eruptions, we compared it to the following tree ring derived datasets (tab. 4):

- Bristlecone pine frost rings and growth minima (Salzer and Hughes, 2007): To examine whether the blue ring record could complement and expand these data in inferring the timing of climatic impacts caused by volcanic forcing.

- Growth minima in chronologies from the Yamal Peninsula and Finland (Hantemirov and Shiyatov, 2002; Helama et al., 2002) - as reported by Salzer and Hughes, (2007): To assess whether the growth minima in these regions were present,synchronous, or delayed compared to our BR chronology, yielding insights into the timing, onset and extent of volcanogenic climatic effects.

- Northern hemisphere MXD series from 1400 to 1998 CE (Briffa et al., 1998) based on a network of circum-hemispheric temperature sensitive tree ring density chronologies: To explore whether the BR record can offer further insights into cooling than these data, which are already considered more immediately responsive and sensitive to temperature than RWs, the MXD data were ranked and the lowest 5 percent of values compared with BR years in our record.

- The two longest state of the art northern hemisphere temperature anomaly reconstructions. The first, based on a circum-hemispheric network of mixed RW, MXD and blue-intensity (BI) temperature sensitive data (Wilson et al., 2016) covering 750-2011 CE. The second, based purely on a network of MXD data (Schneider et al., 2015) spanning 600-2000 CE: To further explore the potential of the BR record for enhanced temperature sensitivity, these records were restricted to 900-2000 CE, ranked, and the lowest 5 percent compared to our BR record.

- BR record from *Pinus uncinata* from Pyrenees (Piermattei et al., 2020): To explore the spatial signatures of volcanically induced cooling episodes in BRs of these two geographically distant regions.

3. Results and discussion

3.1 Blue ring and Frost ring chronology

Over the entire chronology length (164-2014, 57816 rings) we identified 1271 BRs (0.022 of all rings), These were subdivided into the intensity classes (1-4 from strongest to weakest) of Siekacz et al. (2024), as follows: BR-1, 98 (0.002), BR-2, 183 (0.003), BR-3, 442(0.008) and BR-4, 557 (0.01). We also identified frost damage in 152 rings, with 43 latewood frost rings (LW_FR (0.001), and 109 earlywood frost rings (EW_FR 0.002). Fig. 1 presents the chronology from 600 CE onwards illustrating the observed BR and FR types, along with sample depth (for the full chronology see fig. S2).

A clear pattern emerged where the number and intensity of BRs decreased with increasing distance below the treeline (fig. 2). The most intense BRs (BR-1, BR-2) tend to occur in the higher portion of the analyzed transect. However, during particularly strong BR years such as 1601, BRs spread across almost the entire elevational transect, appearing in 53 out of 64 samples (83%) with 29 classified as BR-1 and 12 as BR-2.

In this case, BRs are found through almost the entire elevational transect, with a significant proportion of high intensity BRs indicating the severity of the event. Four more years show a BR frequency higher than 50%: 1200 (BRn=18, n =32, 56%), 1453 (BRn=45, n=51, 88%), 1860 (BRn=43, n=82, 52%), 1884 (BRn=56, n=81, 69%). However, 1601 remains the year with the highest share of BR-1 class. Taking into account that the highest section of elevational transect is only partially covered in 1601 (fig.2), it is by far the strongest BR event of the last eleven centuries.

LW_FR occurrences are always associated with BRs, but not all BRs are associated with LW_FRs (fig. 3). In fact, LW_FR occurred only in years of high BR frequency and in much lower numbers. LW_FRs were observed in the following years: 1100 (LW_FRn=1, BRn=5), 1200 (LW_FRn=1 , BRn=18), 1453 (LW_FRn=4, BRn=45), 1601 (LW_FRn=23, BRn=53), 1680 (LW_FRn=1, BRn=26), 1725 (LW_FRn=1, BRn=16), 1732 (LW_FRn=1, BRn=8), 1760 (LW_FRn=1, BRn=28), 1789 (LW_FRn=1, BRn=10), 1884 (LW_FRn=8, BRn=56), 1978 (LW_FRn=1, BRn=25).

The fact that BRs occur in a higher number of years than LW_FRs suggests that BRs respond to subtler temperature declines than LW_FRs, which require subfreezing temperatures to form (Glerum and Farrar, 1966; Schweingruber, 2007). BRs can form in response to temperature declines occurring later in the year, beyond the period when LW_FRs can form. LW_FRs form under sub-freezing temperatures and develop when the cambium is still active, and xylem mother cells are undergoing division and growth (Glerum and Farrar, 1966; Schweingruber, 2007). In contrast, blue rings, characterized by incomplete lignification of tracheid walls, can form even after the cambial activity and radial growth have ceased. This is because cell wall lignification continues and may sometimes persist into the winter or even the following spring in some species (Donaldson, 1992, 1991).

These data indicate that blue rings serve as more sensitive indicators of low temperatures, with their formation documented during colder conditions, although not necessarily below freezing (Siekacz et al., 2024; Piermattei et al., 2015). Unfortunately

estimates of a more precise temperature threshold for blue ring formation have not yet been determined in the literature, and further experimental studies aimed at its estimation are required.

The formation of both BRs and LW_FRs in the listed years, but BRs in a larger number of trees, demonstrates not only that BR are more sensitive to subtle temperature declines, but also how even relatively small changes in elevation and topography can affect the temperatures experienced by individual trees. It shows that a subset of trees located in the higher part of the transect experienced temperatures that dropped below freezing, while others at lower elevations experienced a decline large enough for BRs to form, but not sufficiently cold to cause LW_FR formation. This observation aligns with earlier studies (Bunn et al., 2018, 2011, Salzer 2014b) that analyzed the influence of fine-scale elevation and topography variations on RW patterns in bristlecone pine, where authors showed that temperature differences experienced by individual trees are larger than can be explained by a dry adiabatic lapse rate, underlining the importance of fine-scale topography.

3.2 Blue ring association with volcanic eruption signals in ice-cores

During the period from 900 to 2014, 220 BRs and 133 volcanic ice-core signals occurred (fig. 4). The expected frequency of joint occurrences of events in two random, independent series is equal to the product of their individual probabilities. For all volcanic events listed in Sigl et al., (2015) 29 exact joint occurrences with BRs were observed (fig. 4, tab. 1), which is not significantly higher than the 26 that would be expected by chance $X^2 = 0.40884$, $p = .5226$., However, when accounting for a 3 year window (including exact matches, and BRs occurring a year before or a year after ice-core volcanic signal), joint occurrences increased to 87, which is more than 3 times what would be expected by chance $X^2 = 201.62$, $p < 0.0001$. Over the analyzed period, 65% of volcanic eruptions can be matched with BR events either in the same year, the year before or the year after. For tropical volcanic events, exact matches are already two times higher than what would be expected by chance $X^2 = 5.491$, $p = 0.0191$. In the 3 year window 34 joint occurrences are almost five times higher than expected: $X^2 = 110.09$, $p < 2.2e\text{-}16$. In the case of tropical eruptions 85% can be matched with BRs within the 3-year window. For southern hemisphere extratropical eruptions, neither direct nor 3 year widow joint occurrences are significantly higher than random co-occurrences. However, for northern hemisphere extratropical eruptions, joint occurrences in the 3 year window (41) are 3 times higher than

expected randomly $X^2 = 77$, $p < 2.2e\text{-}16$, and 61% of these eruptions can be matched with BR event.

Model input for the period 900-2014 includes 61 samples from independent trees, in total 39383 observations (tab. 2). Conditional R2 of 0.393 and a marginal R2 of 0.134 suggest that the model explains a moderate proportion of the variance in the response variable, with both fixed and random effects contributing to the explanatory power of the model.

Global volcanic forcing (fig. 4a) has a statistically significant negative effect (beta = -0.03, p = 0.01), the stronger volcanic forcing (represented by negative values) the higher the probability of BR formation. Among the source variables (fig. 4c) tropical eruptions exert the strongest influence, significantly increasing the likelihood of a BR event (beta = 1.81, $p < 0.0001$). Northern hemisphere extratropical eruptions also have a positive, but lower, effect on BR formation (beta = 0.34, p = 0.008). In contrast, southern hemisphere extratropical eruptions have a negative effect on BR formation probability (beta = -1.45, p = 0.003). These findings are consistent with the contingency testing, where we observed the most matches between BRs and tropical eruptions, followed by northern hemisphere extratropical eruptions, and no association between BRs and southern hemisphere eruptions. Additionally, increasing DTL (fig. 4b) decreases (beta = -0.02, $p < 0.0001$) the probability of BR occurrence.

These results indicate a non-random association (through a causal climatic link) between BR formation and volcanic eruptions. The location of the source volcano significantly influences an eruption's potential to cause BR formation (cooling), with eruptions of tropical origin having the strongest association with BRs. However, it should be noted that in the dataset used (Sigl et al., 2015), the attribution of eruptions to specific latitudinal bands is somewhat flexible except in cases where the source volcano is known. More recent studies have shown that bi-polar sulfur deposition (hitherto used as an indication of eruption location) is no longer exclusively indicative of a tropical eruption (Abbott et al., 2021; Pearson et al., 2022). Large enough northern hemisphere extratropical eruptions can cause sulfur deposition in ice of both polar regions and also have a marked influence on climate. When attributing source to an ice-core sulfur signal and associated cooling episode multiple lines of evidence must be considered. Only a historic record or geochemical evidence can definitively pinpoint the latitudinal source of an eruption. Therefore, while a strong cooling signal recorded by BRs indicates a significant climatic impact, it cannot conclusively determine whether the eruption was of tropical origin.

3.3 Blue ring versus ring width information

During the period 900-2014, 131 years were classified as negative pointer years, 836 as neutral, and 148 as positive pointer years (tab. 3, fig. 6). Out of the 216 BR events 41 occurred in years classified as positive pointer years which is 1.5 times more frequent than expected by chance ($X^2 = 12.909$, p = 0. 001573). Conversely, only 14 BR years were associated with negative pointer years. This shows that BRs are less frequently associated with narrow rings suggesting that BRs provide information about cooling episodes that is in most cases independent from RWs.

Visual inspection (fig. 6) of the standardized chronology displaying BR events and negative pointer years, confirms that BRs more frequently occur in wider or neutral growth rings. Only 14 BR events coincide with negative pointer years, and only 2 BR events fall within 5% of lowest RWI values. However 43 BR years precede negative pointer years and 14 BR events occur the year before a year within 5% of lowest RWI values.

Previous analyses have shown that BR formation in bristlecone pine is most strongly associated with thermal conditions in September (Siekacz et al.,2024, Tardif et al., 2020). This suggests that BRs may provide higher time-resolution information about cooling episodes at the end of the growing season and possibly into the dormant season, as lignification continues after the radial growth phase of xylogenesis has concluded. For some species, lignification is documented to continue even during winter and up to the following spring (Donaldson, 1992, 1991). This is consistent with our results which show that BRs form not only significantly more frequently in wider or neutral rings, but also in many cases precede a negative pointer year or a growth minimum. Our findings suggest that BR occurrence may contain additional insights about ephemeral cooling events late in the growing season or after it, when radial growth of a particular year has concluded. During such periods, cooling events can no longer directly impact the radial growth of the current year. However, protracted cooling episodes, such as those linked to climatically effective volcanic eruptions, could still affect climatic conditions after radial growth has ceased, with their effects manifesting in the ring widths of subsequent years. In this context, BR chronologies, which as our results show consistently provide information distinct from ring widths, can offer additional details regarding ephemeral cooling events occurring post the radial growth completion of a given year. Moreover, they may provide early indications of volcanically induced cooling, thus offering more precise dating of

climatically effective eruptions compared to those recorded in traditional tree ring parameters.

Superposed epoch analysis supports this inference at a stand level and as being consistent in time, showing that in BR years, RWs are significantly wider, consistently across all BR number groups (fig. 5). This consistency is important, as the subjective definition of what constitutes an event is a source of uncertainty in SEA and can affect the SEA response (Rao et al., 2019). For example, here the threshold used to define a BR event (the number of BRs per year) is a subjective choice. Furthermore although RWs of the year following a BR event tends to be narrower on average, this difference is not significant. This is likely because the cooling episodes captured by BRs are often ephemeral in nature and do not consistently affect the following year's RWs, leading to an averaging between ephemeral and protracted cooling events across the BR years analyzed.

Ultimately, our results both at individual tree level, at a stand level and across a range of observed BR years in time, support the hypothesis that BRs can indicate cooling events occuring after growth completion in a given year. These events may be ephemeral in nature or could go on to impact RWs of the following years. Furthermore, in our chronology, out of 87 BR years associated with an eruption in the 3-year window, 25 occurred a year before volcanic ice-core signal (fig. 4), showing that in some cases they have a capacity to capture volcanically induced cooling even before sulfur ice-core deposition occurs, offering an alternative earlier dating of some eruptions.

Tree ring width based temperature reconstructions were initially conceived to better understand low resolution (multidecadal and longer) climatic variability (D'Arrigo et al., 2013) and in many respects are less reliable in making inferences at annual and interannual timescales such as abrupt consequences of volcanic eruptions. This reduced sensitivity to high-frequency events such as volcanic eruptions results from RW formation more likely to draw on stored reserves from the prior growing season and to reflect the cumulative cambial activity over the growing season, as well as needle retention in conifers (LaMarche Jr, 1974). As a result, due to the persistent presence of biological memory, treeline conifers tend to exhibit a high year-to-year autocorrelation in ring widths (Anchukaitis et al., 2012; Frank et al., 2010). Consequently, the cooling effects of volcanic eruptions may appear to persist for multiple years in RW-based temperature reconstructions. It's well recognized in the literature that this can lead to an underestimation of the abruptness and severity of climatic extremes resulting from volcanic cooling in RW-based reconstructions which can exhibit a lag over several years

(D'Arrigo et al., 1992; D'Arrigo and Jacoby, 1999; Frank et al., 2010; Krakauer and Randerson, 2003). Previous studies (Wilson et al. 2016) show that RW-based temperature reconstructions (D'Arrigo et al., 2006), show peak post volcanic cooling in 5-6 years after the event, in contrast to MXD-based reconstructions (Schneider et al., 2015) with peak cooling a year after the event. The magnitude and lag of peak cooling reconstructed by RW-based, MXD-based and mixed reconstructions (Wilson et al., 2016) seems to be variable between reconstructions and different sets of volcanic events. These differences might arise from different spectral properties of reconstructions, varying representation of different regions in source chronologies and temporal and spatial dynamical response of the climate system to volcanic cooling as well as its record in different tree ring parameters. While RWs remain valuable for examining the impacts of volcanism on historical climate in various capacities, it may not be the most suitable parameter for quantitative, large-scale analyses of volcanic cooling and associated estimates of Earth's climate sensitivity on interannual time scales (Anchukaitis et al., 2012; D'Arrigo et al., 2009).

BRs on the other hand, are better suited to record high resolution cooling events as essentially they are a record of a cessation of lignification process, which seems to be stopped by abrupt temperature drops, and which does not resume later and so leaves a permanent effect on growth ring structure in the form of underligified bands of cells. Mechanistically, this immediate cessation of the continuous lignification process creates a discrete record of a particular cooling event, independent of long-term growth trends and unaffected by biological memory. Additional evidence supporting this assertion is provided by the comparison of BR years frequency with long term trends in bristlecone pine growth and derived temperature reconstruction (Salzer et al., 2014a). Figure S2 presents the RW chronology developed in the course of this work (fig. S3a), the master Sheep mountain chronology (fig. S3b), (Salzer et al., 2014a), and the temperature anomaly reconstruction based on five bristlecone pine chronologies (Salzer et al., 2014a) (fig. S3c). The strong correlation $r^2 = 0.88$ ($p < 2.2e\text{-}16$) between our chronology based on a limited number of samples, with the full Sheep Mountain chronology is very high which demonstrates its representativeness of overall growth trends from the site. Furthermore, the high correlation of a 20 year smoothing spline of our chronology with the Salzer et al., (2014a) temperature anomaly reconstruction $r^2 = 0.82$ ($p < 2.2e\text{-}16$) shows that a large proportion of the reconstructed temperature trends is retained in our chronology. Visual inspection of BR years spread across the range of reconstructed temperature anomalies shows that BRs tend

to occur uniformly and are not particularly associated with gradual negative temperature anomaly trends (fig. S3c). The calculated BR year frequency during the current warming trend (c. 1850-2000) is equal to that during the Little Ice Age (c. 1400-1850), both at 0,23. Lower BR frequency during Medieval Climate Anomaly (c. 950-1250) -0,13 is most likely associated with lower sample depth during that earlier period of our chronology, and the fact that trees representing that earlier part of the chronology come from the lower section of the analyzed transect (fig. 3), so BR years for this period are likely underrepresented in the current study. This evidence shows that BRs form a discrete record of abrupt cooling episodes at the end and after the growing season, and their formation is not modified by long term growth and temperature trends. As evidenced in our BR – volcanic eruptions analysis (fig.3), a large number of BRs are associated with cooling episodes resulting from volcanic eruptions. However, BRs also record ephemeral cooling episodes not associated with volcanic eruptions, just as not all cooling episodes result from volcanic eruptions and not all volcanic eruptions produce a cold summer (D'Arrigo et al., 2013; Schneider, 1983).

3.4 Blue ring contributions to volcanic case studies

We selected the 20 largest Global volcanic forcing (GVF) estimates (Sigl et al., 2015) 900-2014 CE and explored these with our BR sequence and other tree-ring derived data.

1601 stands out as the strongest BR year in our chronology (fig. 3, fig. 4, tab. 4), with 83% (53 BRs in 64 samples) of samples containing BRs, including 29 classified as the strongest class (BR-1) and 23 LW_FRs. Notably, strong BRs were formed even in the lowest situated trees of the elevational transect. It corresponds to the 9th largest GVF estimate of the period, with ice-core evidence dated to 1601 (Sigl et al., 2015) attributed to the 1600 eruption of Huaynaputina (Peru). Historical sources suggest this eruption occurred in February and March of that year (De Silva and Zielinski, 1998) MXD and mixed RW-MXD-based evidence (Briffa et al., 1998; Schneider et al., 2015; Wilson et al., 2016) all classify the 1601 as the largest negative anomaly but the reconstructed temperatures quickly return to normal values in 1602 (ranked as 357 coolest anomaly in Wilson et al., (2016). In bristlecone pine ring 1602 is among the 5% lowest ring widths of the past 5000 years. This one year delay aligns with the widely accepted phenomenon of lagged RW response to volcanic eruptions due to biological memory (Anchukaitis et al.,

2012) supporting the idea that BRs can provide an earlier indication of volcanically induced cooling than RWs. The strongest BR signal in bristlecone pine in 1601 clearly points to low temperatures at this site, with FRs indicating that some trees experienced freezing conditions while the cambium was still active. BRs were also recorded for 1601 in the Pyrenees (Piermattei et al., 2020) confirming that low temperatures were synchronous between the American south-west and the Iberian peninsula at this time.

1453 is the strongest (by percentage) BR year in our record of the last eleven centuries (fig. 3, fig. 4, tab. 4), 88% (45 BRs in 51 samples) of samples recorded BR and 4 LW_FR. However, the lower number of the strongest class of BR (BR-1), with only 10 occurrences, makes it the second strongest BR event overall. Sigl et al., (2015) ranks it as the 19th largest estimated GVF of the past 1100 years. In our chronology it represents a prolonged BR occurrence, with 3 more BRs in 1454 CE. The MXD data of Briffa et al., (1998) and JJA MXD-based northern hemisphere temperature anomaly (Schneider et al., 2015) rank 1453 as the 4th and 5th lowest respectively. Mixed MXD and RW MJJA temperature anomaly reconstruction (Wilson et al., 2016) ranks 1453, 1454 and 1455 as the 6th, 49th and 37th coldest years respectively, but this apparent extended cooling might also be a result of mixed sources of the reconstruction retaining some of the RW lagged cooling. In the 5000 year bristlecone pine chronology (Salzer and Hughes, 2007) 1453 doesn't fall within lowest 5% RW values, however a FR was noted. Salzer and Hughes, (2007) also report that in Yamal and Finland chronologies 1453, 1454, and 1456 are among the 5% lowest RW values. BRs were not formed in the Pyrenees (Piermattei et al., 2020) that year. Strong BR signal in 1453 followed by a weaker one in 1454 indicate that bristlecone pine experienced significant cooling at the end of the 1453 growing season and a lesser one the following year.

1458 was the second largest GVF over the study period (Sigl et al., 2015), but only weakly registered in bristlecone pine BRs in 4 out of 51 samples in 1457. The BR signal a year before the ice-core sulfur deposit may suggest an earlier date of the eruption. Salzer also recorded FR in 1457 and an extended growth minimum over 1458-1462 suggesting an prolonged climatic impact possibly accentuated by a combined effect of earlier 1453 eruption, but also characteristic of a lagged RW response. Piermattei et al., (2020) didn't note BR for that year in their chronology. However, MJJA temperature anomaly reconstruction (Wilson et al., 2016) lists the 15th and 19th coolest conditions in 1457 and 1459 respectively. Interestingly neither Briffa et al., (1998) nor Schneider et al., (2015) record this period among low values. This diverse response in hemispheric scale

reconstructions indicates that, even these based on MXD, which carry a stronger temperature signal (D'Arrigo et al., 2013; Esper et al., 2015; Frank et al., 2007) and are better suited to accurately resolve rapid temperature changes associated with volcanic eruptions may be biased. This likely results from temporal and spatial dynamics of the climate system response to volcanic cooling and uneven representation of different regions in the source chronologies building the hemispheric mean. Moreover, our BR record with a much stronger BR signal in 1453 than 1457 (45 vs 4 BRs) provides further support to the argument made by Esper et al., (2017) that 1453, rather than 1458, should be the correct date of the stronger of the two 1450s sulphate singlas in ice-cores. This challenges the redating of its earlier placement in 1453 (Gao et al., 2008, 2006) to 1458 by Sigl et al., (2015).

The 1883 Krakatoa eruption, ranked as the 24th largest eruption of the past 1100 years (Sigl et al., 2015), is reflected in the bristlecone pine BR chronology, which records 56 BRs across 80 cores and 8 LW_FRs in 1884. This indicates cooling a year after the eruption's climactic phase in august 1883. Piermattei et al., (2020) also reported BR in 1884, although this year is not represented by a RW minimum in bristlecone pine (Salzer and Hughes, 2007), nor it is among the 5% lowest RW values in Yamal and Finland chronologies. However, other studies (Briffa et al., 1998; Schneider et al., 2015; Wilson et al., 2016) report 1884 as a year with cool conditions ranked as 13th, 61st and 11th, respectively and 1885 as 41st in Schneider et al., (2015).

The major unknown eruption in 1809 and the famous Tambora eruption in 1815 (followed by 1816 – the so called "year without a summer" (Oppenheimer, 2003)) rank as the 6th and 3rd largest GVF respectively (Sigl et al., 2015). This double event sequence is evidenced by BRs in 1809, 1810 and 1811 with 22, 13 and 10 BRs out of 80 samples respectively. Salzer and Hughes, (2007) reported FR in 1809 and 1810, but no growth minima related to 1809 or 1815 eruptions. Piermattei et al., (2020) reported BRs in 1809 and Schneider et al., (2015) classified 1813 as the 21st largest negative anomaly in MXD-based JJA temperature reconstruction. The lack of immediate response to the 1809 volcanic episode, even in MXD-based reconstruction, which is not burdened with biological memory artifacts, indicates a complex climate response. We can clearly identify a protracted BR signal in our chronology pointing to cooler conditions experienced by

bristlecone pine over 3 seasons, however the RWs do not reflect a significant negative response, suggesting that the low temperatures were experienced after the growing season window, while lignification continued. The BR recorded in 1809 in the Pyrenees (Piermattei et al., 2020) is evidence to synchronous conditions there. Response to the Tambora eruption seems to be even more enigmatic. Despite being widely regarded as one of the largest eruption of the last millennium (Oppenheimer, 2003) we find no BRs related to this eruption. Salzer and Hughes, (2007) report lower RW for 1815 but not low enough to fall into 5% lowest values. In the reconstructions we compare (Briffa et al., 1998; Schneider et al., 2015; Wilson et al., 2016) the period 1816 to 1819 and inSchneider et al., (2015) even 1815, all rank among the 30 largest negative deviations (tab. 4).Anchukaitis et al., (2012) however, calculating spatial anomaly maps of reconstructed April-September mean temperature using the Briffa et al., (1998) MXD network, shows regionally variable climatic response to the double volcanic event, with cooling in western United States in 1810 and warming in 1815, which aligns with our BR evidence. Similarly, Esper et al., (2013) noted different climate regimes governing weather in central and northern Europe, with MXD data showing different patterns between central European and Scandinavian chronologies. Four most negative deviations for northern Europe occurred in 1453, 1614, 1632/33 and 1812, in central Europe these are 1258, 1698, 1816, 1912. This suggests that the reconstructed cooling strength depends on the proximity and density of proxy data. For example Briffa et al., (1998) NH extratropical MXD network, compared with Esper et al., (2013) findings from Europe, suggests that spatially heterogeneous temperature patterns mitigate post-volcanic effects at the hemispheric scale. Cooling patterns are regionally variable, and connecting distant proxy sources might smear and dampen the overall cooling reconstructed. D'Arrigo et al., (2006) concluded that the reconstructing a single large-scale parameter like annual or seasonal hemispheric temperature does not provide any valid spatial climatic information.

A protracted BR signal appears related to the 1640 eruption attributed to Parker volcano (Toohey and Sigl, 2017). This eruption is estimated to be 6th largest GVF of the last 1100 years and corresponds with BRs in 1640-1644 (16, 9, 7, 9, 2 BRs out of 65 samples respectively). Salzer and Hughes, (2007) also reported FR in 1640 and RW minima in 1641, 1644-1647. This is another case where the climate pattern does not appear to be replicated in the Pyrenees (Piermattei et al., 2020). The MXD data and temperature reconstructions (Briffa et al., 1998; Schneider et al., 2015; Wilson et al., 2016) all classify

years 1641-1643 as falling into 30 largest negative deviations. A bristlecone pine BR and FR signal in 1640 suggests cooling had already begun late in the growing season of 1640, demonstrating the capacity of BRs to record volcanically induced cooling even before highly temperature sensitive MXD data.

An intriguing case is the unattributed volcanic eruption recorded in the ice-cores in 1695. The MXD and temperature anomaly data (Briffa et al., 1998; Schneider et al., 2015; Wilson et al., 2016) all indicate protracted cooling episode starting in 1695 (tab. 4), with negative deviations falling within lowest 5% up to 1699. However, our BR signal in 1694-1695 though weak, points to the onset of cooler conditions already in 1694.Piermattei et al., (2020) reported BR in 1698 and Salzer and Hughes, (2007) frost ring in 1699. RW minima were also reported in Finland and Yamal chronologies in 1696 and 1698 respectively, confirming cooling in those regions with characteristic to RWs delayed response.

The unattributed ice-core signal in 1191 (Sigl et al., 2015; Toohey and Sigl, 2017) is associated with BRs already in 1190 (tab. 4) suggesting an earlier date for the eruption. Schneider et al., (2015) MXD-based JJA temperature anomaly reconstruction ranks 1190 as the 47th largest negative anomaly, however this cooling signal is missing from other reconstructions analyzed (Briffa et al., 1998; Wilson et al., 2016). This illustrates how lower sample depth in earlier periods of the reconstructions and underrepresentation of some regions in the source chronologies can result in an underestimation of cooling in hemispheric scale reconstructions. This regionally variable climate system response is exemplified by a lack of BRs in the Pyrenees (Piermattei et al., 2020) for that eruption.

The largest GVF of the last millennium, the 1257 Samalas eruption (Sigl et al., 2015; Toohey and Sigl, 2017) shows up in our BR chronology with a delay and to a very limited extent. Only one BR was recorded in 1259 followed by two in both 1260 and 1261, and seven in 1262. There is no associated RW minimum, but FRs were noted in 1257 and 1259 (Salzer and Hughes, 2007). Piermattei et al., (2020) reported BRs in 1258, and only the JJA MXD-based temperature reconstruction (Schneider et al., 2015) rank 1258 and 1259 as among the 5% coldest years (9th, 29th respectively). This suggests that the

magnitude of the estimated GVF does not directly translate to the magnitude of climatic response. Multiple lines of tree ring evidence show that some of the lower magnitude eruptions might have had a larger climatic impact than Samalas. To more accurately assess volcanic impact on climate it is important not only to consider the size and extent of the volcanic sulfur signal in ice-core records, but to also include tree ring evidence of cooling episodes from various regions. Anchukaitis et al., (2012) demonstrated that General Circulation Models (GCMs) may exhibit distinct patterns of summer warming across regions following seemingly significant eruptions, such as the one in 1258, despite the overall trend toward global and hemispheric summer cooling. The extent of these temperature changes depends on various factors including the eruption's characteristics, resulting changes in solar radiation, prevailing background climatic conditions, internal climate variability, season, latitude of the eruption and other relevant factors. Consequently, atmospheric wave patterns may be perturbed, causing cooling in certain regions, while others may experience minimal change or even warming (Robock and Mao, 1992). Furthermore, factors such as seasonal growth patterns and climate response, the geographical distribution of tree ring chronologies, biological persistence, autocorrelation, divergence and the increasing scarcity of chronologies further back in time, all add complexity to analyzing the climate impact of volcanic eruptions in the proxy record.

4. Conclusions

Our results indicate that BRs are very temperature-sensitive, high-time resolution indicators of ephemeral cooling. We demonstrated a clear association between large climatically effective volcanic eruptions and BRs in bristlecone pine, with the strongest effect of tropical eruptions. We illustrate how a multiproxy approach combining BRs, FRs, RW minima, MXD minima and hemispheric scale temperature reconstructions can enhance our understanding of climate system response to specific volcanic eruptions. In some cases, BRs provide earlier evidence of cooling onset than RWs due to their ability to capture cooling episodes after the radial growth phase in a particular year is complete. This ability makes BRs valuable in overcoming the limitations of RWs in capturing sudden and short-term cooling episodes, which are often impacted by biological persistence and autocorrelation. In certain instances, BRs have the capacity to capture some of the volcanically induced cooling episodes earlier than RW and even MXD-based temperature anomaly reconstructions because cooling patterns are regionally variable and connecting

distant proxy sources in hemispheric scale reconstructions can smear and dampen the overall cooling (Esper et al., 2013). This is particularly evident in the earlier part of hemispheric scale reconstructions (Briffa et al., 1998; Schneider et al., 2015; Wilson et al., 2016), when a limited number of source chronologies and their geographic representation can delay and average out the reconstructed cooling. We have also shown that certain BR event years can suggest an earlier date for an eruption than the ice-core record, responding to the cooling effect of the stratospheric sulfate before it is deposited.

Overall, we have demonstrated that BR chronologies can provide an additional line of evidence for past cooling episodes, some of ephemeral and more localized nature, some related to large volcanic eruptions with quick rebound to neutral conditions (eg. 1601) and some with more persistent consequences manifested in cooler conditions for a number of years (eg. 1640-1644, 1809-1811). However, not all BR signals are associated with large volcanic eruptions, just as not all MXD minima occur associated with identified volcanic eruptions (Briffa et al., 1995; Hughes et al., 1999). This is because not every cold summer in a specific location can be attributed to a volcanic event, and likewise, not all volcanic eruptions result in cooler summers. BRs offer a highly sensitive record of local thermal conditions, but are a noisy proxy. Many years with a low BR signal may reflect localized coldsnaps rather than large-scale cooling. In mountainous areas, diverse topography can influence BR formation, so a relatively large sample depth is required to discern between the evidence of localized cold snaps present in some trees, and signatures of regional cooling episodes. However, we advocate for development of more BR chronologies in long tree ring records from various regions. This approach will help build a more accurate picture of spatial climatic signatures of past volcanic eruptions and enable better evaluation of the influence of explosive volcanic events on regional and global climates.

5. Figures and tables

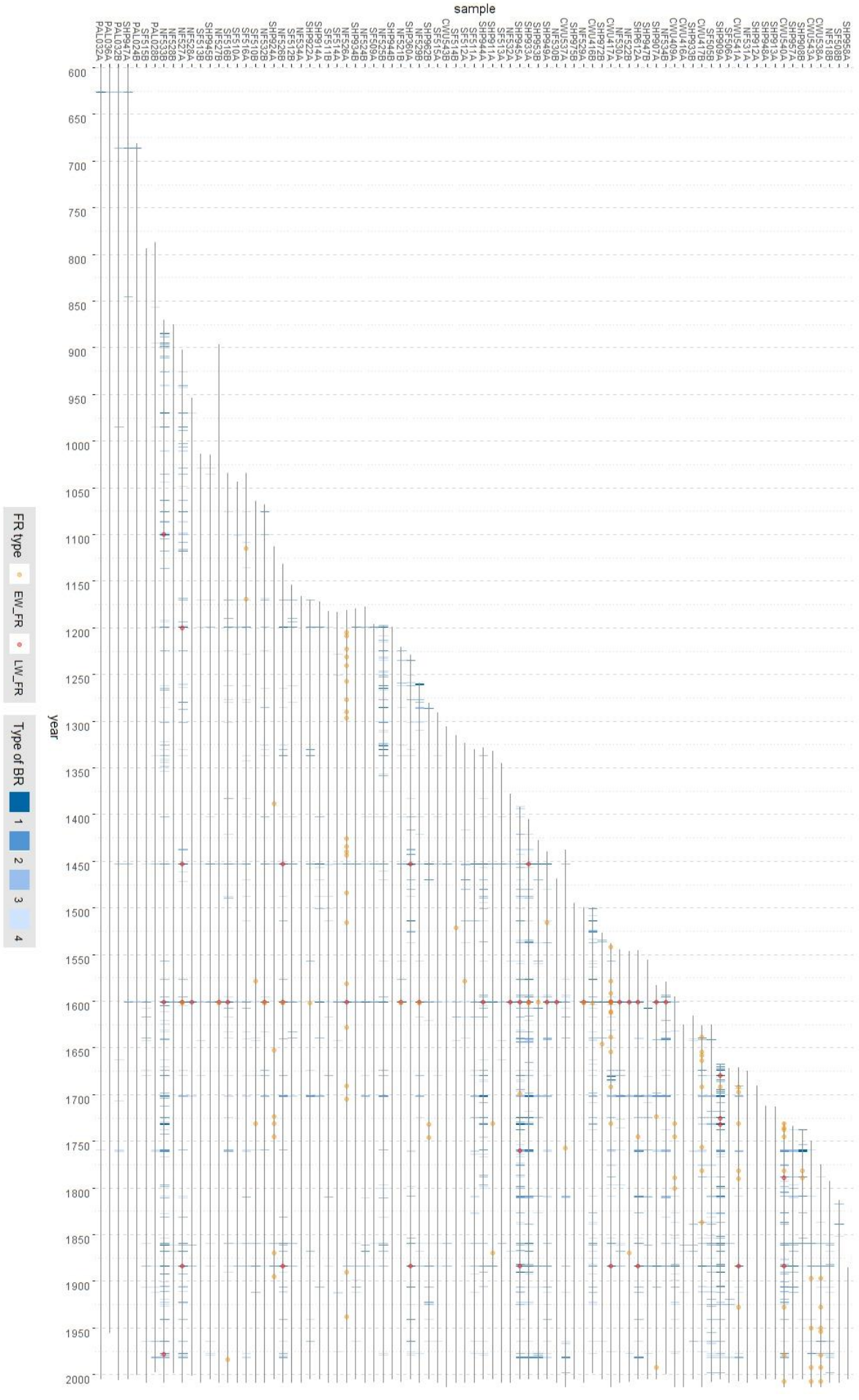
sample
year
FR type
EW_FR
LW_FR
Type of BR
1
2
3
4

Figure 1 Blue ring and frost ring chronology for period 600-2014 sorted by sample depth.

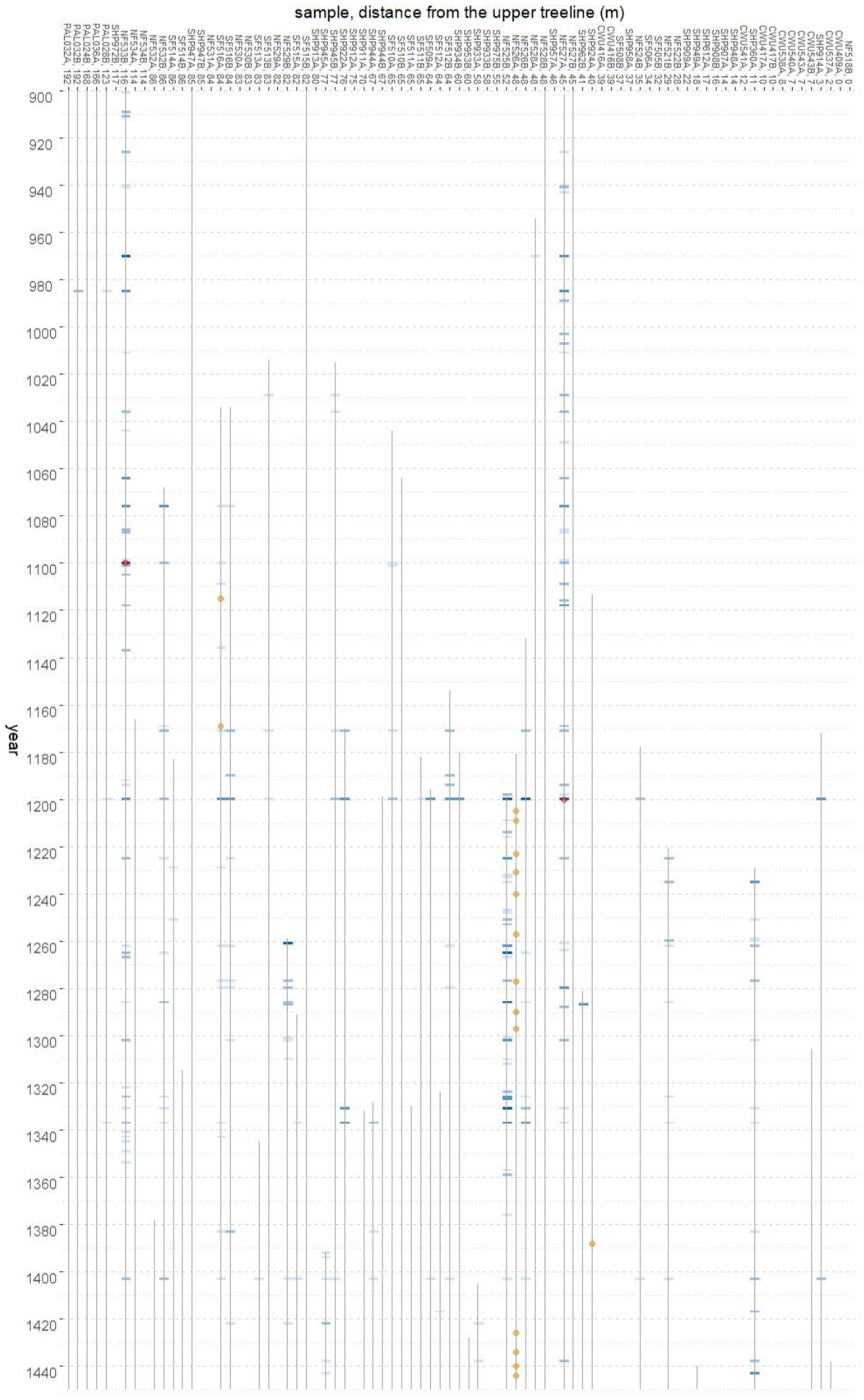
sample, distance from the upper treeline (m)
year
PAL032A, 192
PAL032B, 192
PAL024B, 168
PAL036A, 166
PAL028B, 123
SHP972B, 117
NF539A, 116
NF534A, 114
NF532A, 88
NF532B, 86
SF514B, 86
SF514A, 86
SHP947B, 85
SHP947A, 85
NF531A, 84
SF516A, 84
SF516B, 84
NF530A, 83
NF530B, 83
SF513B, 83
NF529A, 82
NF529B, 82
SF515A, 82
SF515B, 82
SHP913A, 80
SHP945A, 77
SHP945B, 77
SHP922A, 76
SHP912A, 75
SHP911A, 70
SHP944A, 67
SHP944B, 67
SF510B, 65
SF510A, 65
SF511A, 65
SF511B, 65
SF509A, 64
SF512A, 64
SF512B, 64
SHP934B, 60
SHP953B, 60
SHP933A, 58
SHP933B, 58
SHP975B, 55
NF526B, 52
NF526A, 48
NF528A, 48
NF528B, 48
SHP957A, 46
NF527A, 45
NF527B, 45
SHP962B, 41
SHP924A, 40
CWU416A, 39
CWU416B, 39
SF508B, 37
SHP958A, 37
NF524B, 35
SF506A, 32
SF506B, 32
NF521B, 29
NF522B, 28
SHP909A, 22
SHP949A, 18
SHP612A, 17
SHP908B, 16
SHP907A, 14
SHP948A, 14
CWU541A, 12
SHP960A, 11
CWU417A, 10
CWU417B, 10
CWU538A, 10
CWU540A, 8
CWU543A, 7
CWU543B, 7
SHP914A, 3
CWU537A, 2
CWU409A, 0
NF518B, 0
900
920
940
960
980
1000
1020
1040
1060
1080
1100
1120
1140
1160
1180
1200
1220
1240
1260
1280
1300
1320
1340
1360
1380
1400
1420
1440

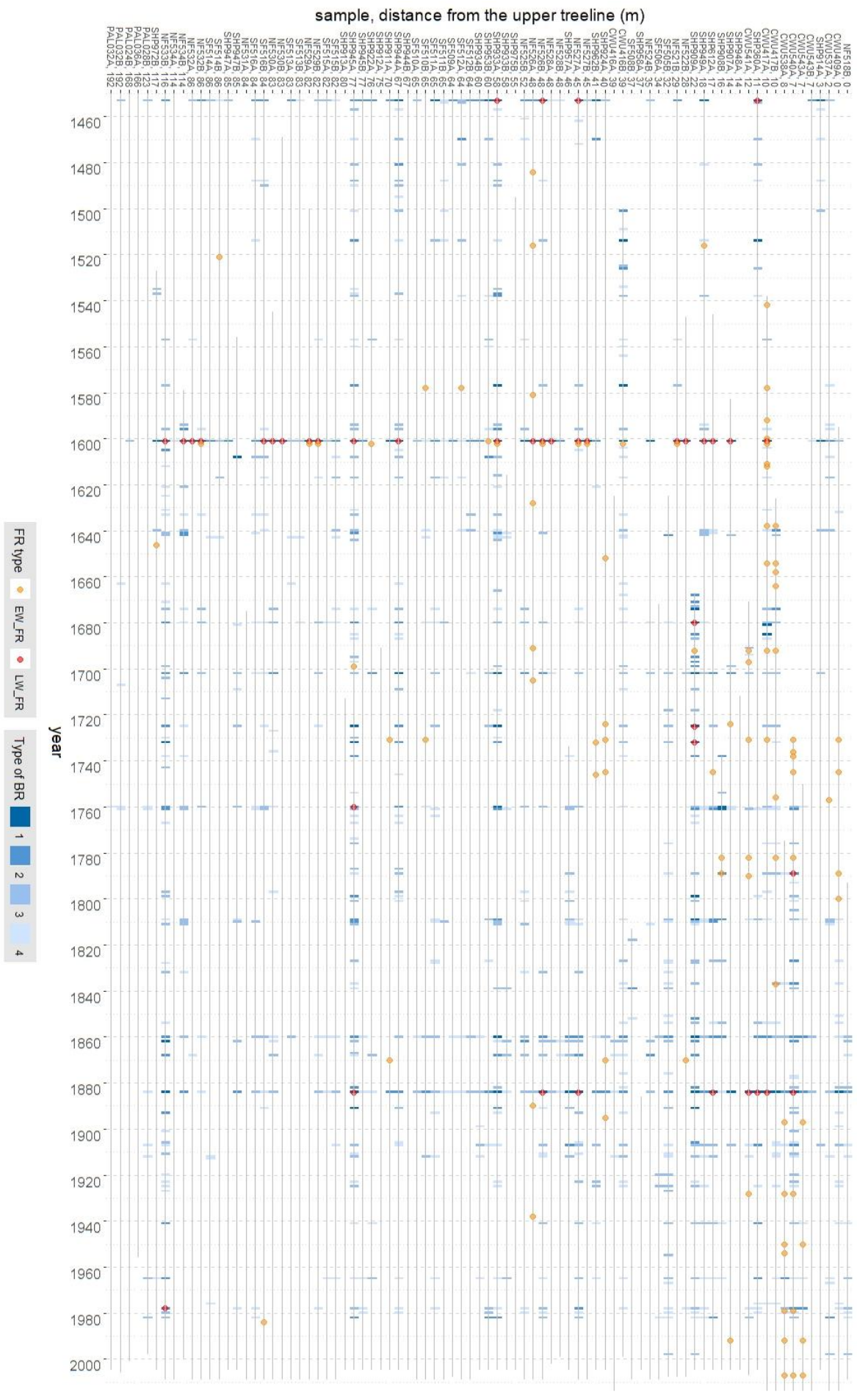
sample, distance from the upper treeline (m)
year
FR type
EW_FR
LW_FR
Type of BR
1
2
3
4

Figure 2 Blue ring and frost ring chronology for the period 900-2014 sorted by distance from upper treeline. This figure illustrates the developed chronology showing how blue ring occurrence and intensity class is modified by the distance from upper treeline. Please note how BRs are clearly replicated in the same years between different trees indicating that they respond to the same forcing agent. Also note how blue ring occurrence decreases with increasing distance from upper treeline. And how in the strongest blue ring years (1601) BRs form in almost the entire elevational transect, and how BR intensity class decreases the further below the tree line the tree is situated (eg. 1884). Comparing BR occurrence and intensity between different BR years across the elevational transect qualitatively illustrates the difference in the strength of cooling episodes that led to blue ring formation.

Figure 3 Aggregated BR number of all classes per year versus Global volcanic forcing (GVF) (Sigl et al., 2015). A shows 900-1450 CE, B shows 1450-2000 CE. BR and volcanic eruption cooccurrence (red), BRs a year before or after a volcanic ice-core signal (green), BR with no correlation (blue). GVF tropical (violet), southern hemisphere extratropical (brown) and northern hemisphere extratropical (yellow). Please note the high co occurrence of BRs and volcanic eruptions in the 3-year match window, also direct BR-volcano matches with particularly high BR numbers in 1601, 1809, and 1884 for eruptions of tropical origin. Most very weak BR years (1-2 BR a year) are not associated with volcanic signal and are likely result of a localized cold-air pooling (Bunn et al. 2011). Note also that several strong BR years appear not to be associated with volcanic ice-core signal eg. 1403, 1680, 1702, showing that not all cooling episodes result from volcanic eruptions.

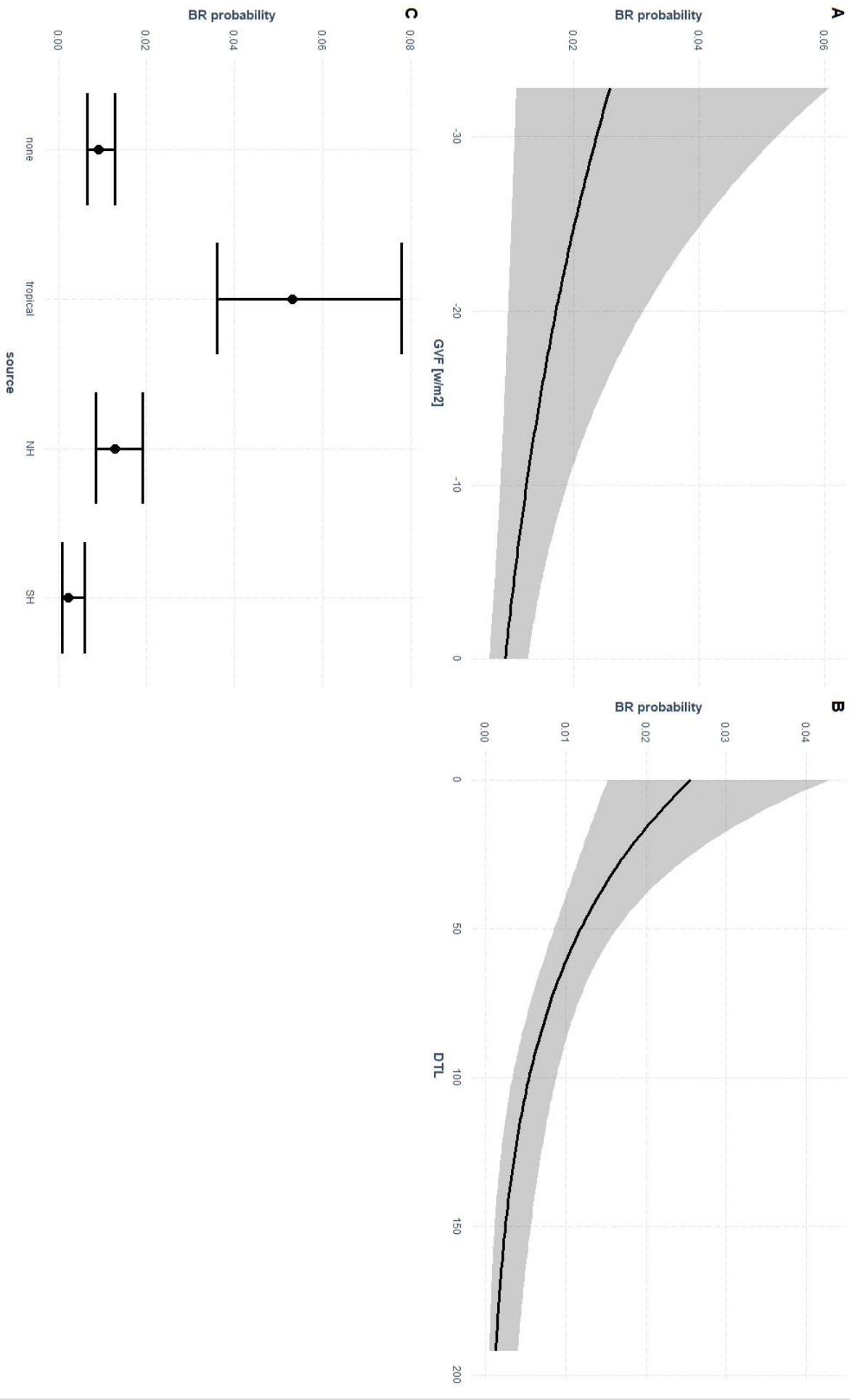
A
BR probability
0.06
0.04
0.02
-30
-20
-10
0
GVF [w/m2]
B
BR probability
0.04
0.03
0.02
0.01
0.00
0
50
100
150
200
DTL
C
BR probability
0.08
0.06
0.04
0.02
0.00
none
tropical
NH
SH
source

Figure 4 Figure 4 Generalized linear mixed-effects model (GLMM) results presented as predicted probability of BR formation for each predictor significant in the model, plotted along observed ranges of predictors. BR probability is shown according to: a) GVF, b) DTL, c) attributed latitudinal band of the eruption. Please note the highest effect of tropical eruptions on BR formation.

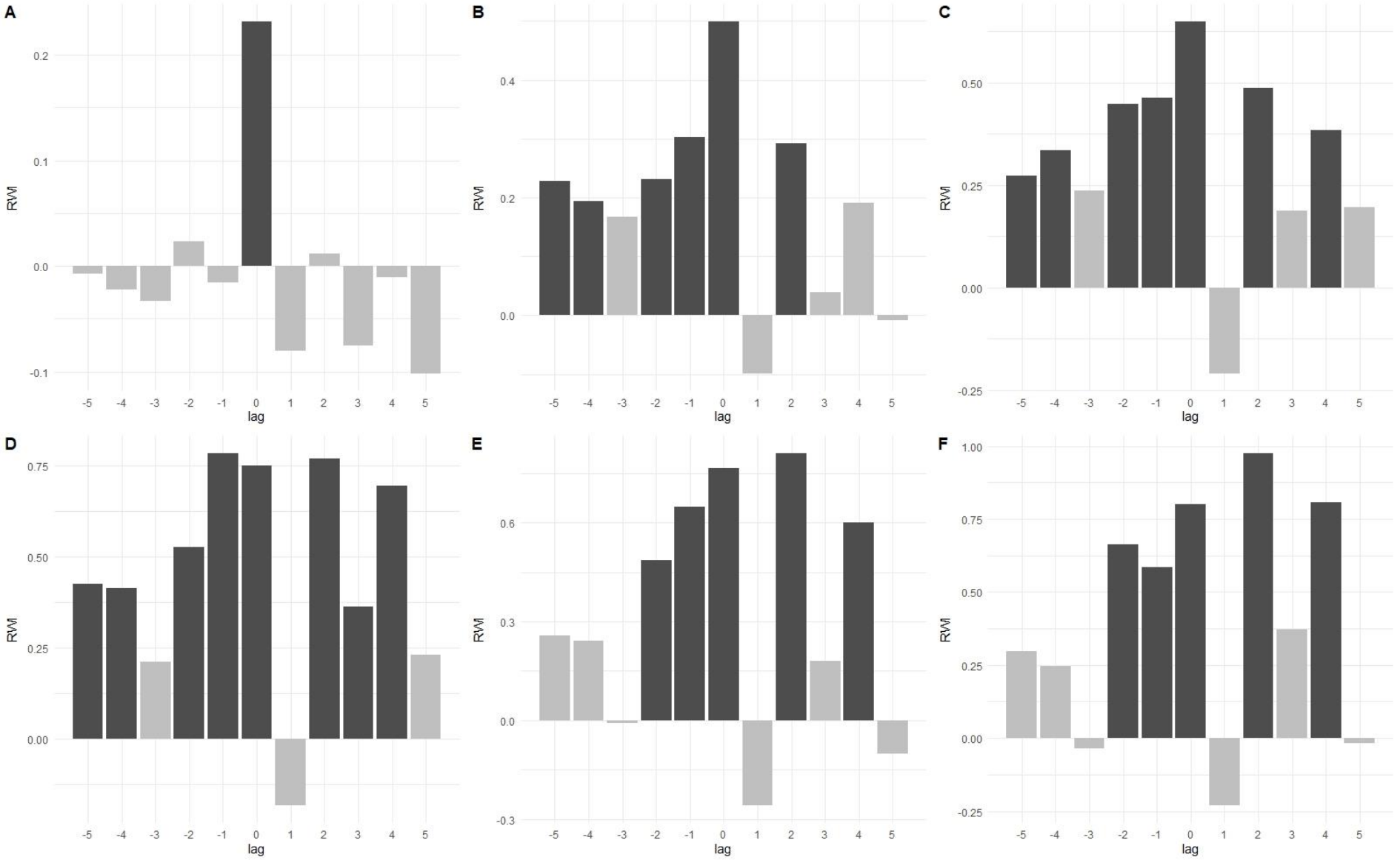
A
B
C
D
E
F
RW
lag

Figure 5 Figure 5 Superposd Epoch Analysis results for 5 years prior to an event, the event and 5 years after the event year. Event years are: A - all BR years, B - BR years with equal to or more than 5 BRs, C - BR years with equal to or more than 10 BRs, D - BR years with equal to or more than 15 BRs, E - BR years with equal to or more than 20 BRs and BR years with equal to or more than 25 BRs. Displayed are scaled departures from the mean RW index values for the 5 years prior to each event, the event year and 5 years immediately after the event. 95%-confidence intervals were computed for the scaled values for each year in the superposed epoch based on 1000 bootstrap resampling of event years; dark gray are significant at $p<0.05$.

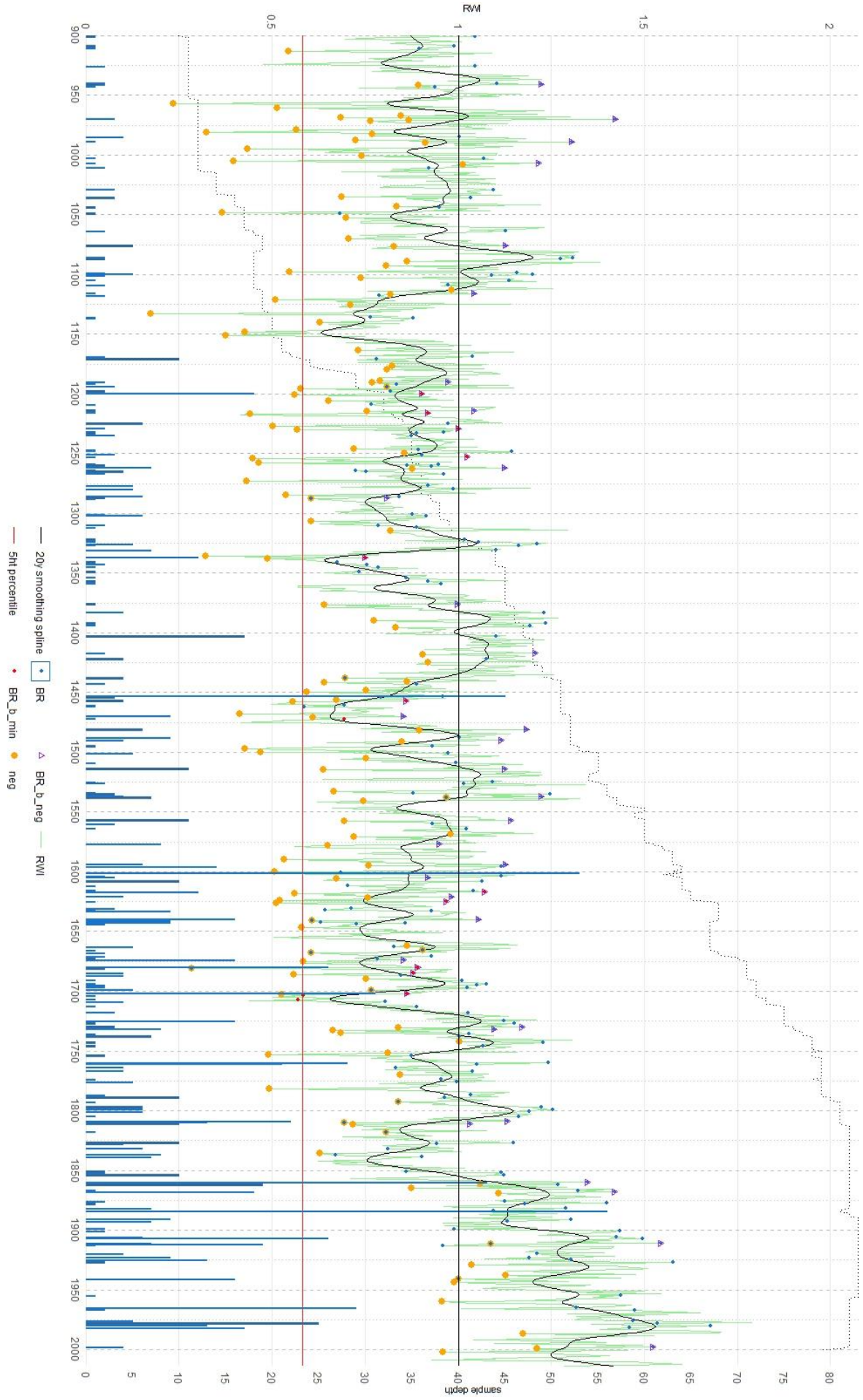
RWI
0.5
1
1.5
2
900
950
1000
1050
1100
1150
1200
1250
1300
1350
1400
1450
1500
1550
1600
1650
1700
1750
1800
1850
1900
1950
2000
0
5
10
15
20
25
30
35
40
45
50
55
60
65
70
75
80
sample depth
20y smoothing spline
BR
BR_b_neg
RWI
5ht percentile
BR_b_min
neg

Figure 6 Relationship between BRs and RW. Standard site chronology calculated for the 83 cores analyzed in this study for the period 900-2000 AD. Larger orange points indicate negative pointer years from the pointer years analysys, red horizontal line delineates the 5th percentile of the chronology, RWI index values below are classified as RW minima. BRs are displayed as finer blue points, BRs a year before a growth minimum are displayed in red, and a year before negative pointer year in purple. BRs coinciding with a pointer year are displayed as finer blue point overlaid on negative pointer year, BRs coinciding with growth minima fall below the 5th percentile line. Grey dotted line represents the sample depth, blue vertical bars display number of BRs in a particular year compared to a sample depth. Left y-axis RW index scale, right y-axis sample depth scale.

Table 1 Results of Chi-squared test of independence between volcanic eruptions chronology (Sigl et al., 2015) and BR chronology for time period 900-2014.

			Vol all		Vol trop		Vol SH		Vol NH	
			1	0	1	0	1	0	1	0
BR	observed	1	29	187	**14**	202	2	214	13	203
		0	104	795	26	873	24	875	54	845
			X2 (1, *N = 1115*) = 0.40884, *p = .5226*		X2 (1, *N = 1115*) = 5.491, *p = .01912*		X2 (1, *N = 1115*) = 1.6225, *p = .2027*		X2 (1, *N = 1115*) = 1.9298e-29 , *p = 1*	
BR-3y	observed	1	**87**	**129**	**34**	182	10	206	**41**	175
		0	**46**	**853**	**6**	893	16	883	**26**	873
			X2 (1, *N = 1115*) = 201,62, *p < **.001***		X2 (1, *N = 1115*) = 110.09, *p < **.001***		X2 (1, *N = 1115*) = 5.0224, *p = .02502*		X2 (1, *N = 1115*) = 77, *p < **.001***	
	expected	1	25.77	190.23	7.75	208.25	5.04	210.96	12.98	203.02
		0	107.23	791.77	32.25	866.75	20.96	878.04	54.02	844.98

Table 2 Parameters of generalized linear mixed-effects model (GLMM).

		BR_event		
Predictors	*Log-Odds*	*CI*	*Statistic*	*p*
(Intercept)	-3.65 ***	-4.18 – -3.12	-13.48	**2.025e-41**
Global volcanic forcing GVF W/m^2	-0.03 *	-0.06 – -0.01	-2.53	**1.125e-02**
tropical	1.81 ***	1.55 – 2.07	13.66	**1.699e-42**
NH	0.34 **	0.09 – 0.60	2.63	**8.431e-03**
SH	-1.45 **	-2.43 – -0.47	-2.91	**3.625e-03**
DTL	-0.02 ***	-0.02 – -0.01	-3.94	**7.990e-05**
Random Effects				
σ^2	3.29			
$\tau_{00\ symbol}$	1.41			
ICC	0.30			
N $_{symbol}$	61			
Observations	39383			
Marginal R^2 / Conditional R^2	0.134 / 0.393			
AIC	7257.409			

** p<0.05 ** p<0.01 *** p<0.001*

Table 3 Results of Chi-squared test of independence between pointer years and BR chronology for time period 900-2014.

			Pointer years		
			-1	0	1
Observed	BR	0	117	675	107
		1	**14**	161	**41**
			X2 (2, *N = 1115*) = 12.909 , ***p = .001573***		
Expected	BR	0	105.6	674	119.3
		1	25.4	162	28.7

Table 4 BR chronolgy comparison with other tree ring proxies for eruptions with Global volcanic forcing larger than or equal to that of Krakatoa (Sigl et. 2015). Underlined are case studies discusses in more detail in the main text. ***Bolded*** *are BR years when BRs formed a year earlier than the ice year for eruption. (1) Source attribution, eruption year and VSSI after Toohey et al. (2017), (2) GVF estimates and ice dates after Sigl et al. (2015), (3) Salzer and Hughes, (2007), (4) Piermattei et al. (2015), (5) Briffa et al. (1998), 5% lowest values of the period 1400-1994, (6) Wilson et al. (2016), 5% lowest values of the period 900-2000, (7) Schneider et al. (2015), 5% lowest values of the period 900-2000.*

Volcano (1)	Ice Year (CE)(2)	Eruption Year (CE)(1)	BR years	BRn/N	BRn in consecutive years	FR (4)	BCP RW minima (4)	FIN RW minima (4)	YAM RW minima (4)	BR (5)	MXD minima (6)	MJJA temp anomaly minima (7)	JJA temp anomaly (8)	GVF [W/m2](2)	VSSI (Tg [S]) (1)
Samalas	1258	1257	1259-1262	1/ 37	1;2;2;7	1257, 1259				1258			(9)1258, (29)1259	-32,79	59,42
Unidentified	1458	1458	**1457**	4/51		1457	1458-1462	1460	1459-1460			(15)1457, (19)1459		-20,55	32,98
Tambora	1815	1815		0/81				1813	1815	1816	(2)1816, (5)1817, (22)1818, (29)1819	(4)1816, (9)1817, (11)1819	(36)1815, (12)1816, (16)1817, (32)1818, (28)1819	-17,2	28,08
Unidentified	1230	1230	**1229**	2/35			1230			1233		(43)1230	(52)1230	-15,9	23,78
Grímsvötn (Laki)	1783	1783		0/78							(26)1783	(12)1783	(4)1783	-15,49	20,81
Unidentified	1809	1809	1809-1811	22/80	22;13;10	1809, 1810				1809			(21)1813	-12,01	19,26
Unidentified	1108	1108	1109	2/18		1109							(8)1109, (38)1110	-11,99	19,16
Parker	1641	1640	**1640-1644**	16/65	16;9;7;9;2	1640	1641, 1644-1647	1641, 1642, 1644	1642, 1644		(3)1641, (28)1642, (10)1643	(8)1641, (14)1642, (7)1643	(3)1641, (18)1642, (7)1643	-11,84	18,68
Huaynaputina	1601	1600	1601	53/63		1601	1602	1601, 1605, 1607-1610	1609	1601	(1)1601	(1)1601	(1)1601	-11,58	18,95
Unidentified	1171	1171	1171	10/23		1171							(20)1172	-11,3	18,05
Unknown	1695	1695	**1694-1695**	1/72	1;2	1699		1696	1698	1698	(6)1695, (9)1698, (11)1699	(44)1695, (46) 1697, (5)1698, (2)1699	(42)1695, (6)1698, (2)1699	-10,24	15,74
Unknown	939	939	940-941	2/11	2;2								(26)940	-10,12	16,23
Unknown	1286	1286	1286-1288	6/37	6;2;1	1287	1288			1288				-9,69	15,06
Unknown	1345	1345	1345	1/45			1348-1350			1345			(45)1446	-9,4	15,11
Unknown	1276	1276	1277	5/36		1277								-7,71	11,53
Cosigüina	1836	1835	1837	8/81			1836, 1838	1837	1834	1835	(21)1836, (15)1837	(12)1835, (3)1836, (18)1837	(51)1835, (35)1836	-6,57	9,48
Pinatubo	1991	–		0/81							1992			-6,49	–
Babuyan Claro	1832	1831	1832	6/81								(17)1832, (25)1833	(24)1832, (10)1833	-6,46	12,98
Unknown/Kuawe	1453	1453	1453-1454	45/51	45;3	1453		1454	1453, 1456		(4)1453	(6)1453, (49)1454, (37)1455	(5)1453	-5,99	9,97
Unknown	916	916		0/11										-5,94	6,08
Unknown	1191	1191	**1190, 1192**	2/29	2;1	1190							(47)1190	-5,86	8,53
Nevado del Ruiz	1595	1595	**1594, 1596**	6/62	6;14	1596							(67)1594	-5,75	8,87
Unknown	1182	1182		0/28										-5,57	10,05
Krakatau	1884	1883	1884	56/80		1884				1884	(13)1884	(61)1884	(11)1884, (47)1885	-5,48	9,34

6. References

Anchukaitis, K.J., Breitenmoser, P., Briffa, K.R., Buchwal, A., Büntgen, U., Cook, E.R., D'Arrigo, R.D., Esper, J., Evans, M.N., Frank, D., Grudd, H., Gunnarson, B.E., Hughes, M.K., Kirdyanov, A. V., Körner, C., Krusic, P.J., Luckman, B., Melvin, T.M., Salzer, M.W., Shashkin, A. V., Timmreck, C., Vaganov, E.A., Wilson, R.J.S., 2012. Tree rings and volcanic cooling. Nat Geosci 5, 836–837. https://doi.org/10.1038/ngeo1645

Baillie, M.G.L., 2010. Volcanoes, ice-cores and tree-rings: One story or two? Antiquity 84, 202–215. https://doi.org/10.1017/S0003598X00099877

Baillie, M.G.L., McAneney, J., 2015. Tree ring effects and ice core acidities clarify the volcanic record of the first millennium. Climate of the Past 11, 105–114. https://doi.org/10.5194/cp-11-105-2015

Bale, R.J., Robertson, I., Salzer, M.W., Loader, N.J., Leavitt, S.W., Gagen, M., Harlan, T.P., McCarroll, D., 2011. An annually resolved bristlecone pine carbon isotope chronology for the last millennium. Quat Res. https://doi.org/10.1016/j.yqres.2011.05.004

Barbosa, A.C., Stahle, D.W., Burnette, D.J., Torbenson, M.C.A., Cook, E.R., Bunkers, M.J., Garfin, G., Villalba, R., 2019. Meteorological Factors Associated With Frost Rings in Rocky Mountain Bristlecone Pine At Mt. Goliath, Colorado. Tree Ring Res 75, 101. https://doi.org/10.3959/1536-1098-75.2.101

Bates, D., Mächler, M., Bolker, B., Walker, S., 2015. Fitting Linear Mixed-Effects Models Using lme4. J Stat Softw 67. https://doi.org/10.18637/jss.v067.i01

Becker, M., Nieminen, T.M., Geremia, F., 1994. Short-term variations and long-term changes in oak productivity in northeastern France. The role of climate and atmospheric CO2. Annales des Sciences Forestieres 51. https://doi.org/10.1051/forest:19940504

Briffa, K.R., Jones, P.D., Schweingruber, F.H., Osborn, T.J., 1998. Influence of volcanic eruptions on Northern Hemisphere summer temperature over the past 600 years. Nature 393, 450–455. https://doi.org/10.1038/30943

Briffa, K.R., Jones, P.D., Schweingruber, F.H., Shiyatov, S.G., Cook, E.R., 1995. Unusual twentieth-century summer warmth in a 1,000-year temperature record from Siberia. Nature 376, 156–159. https://doi.org/10.1038/376156a0

Briffa, K.R., Osborn, T.J., Schweingruber, F.H., 2004. Large-scale temperature inferences from tree rings: a review. Glob Planet Change 40, 11–26. https://doi.org/10.1016/S0921-8181(03)00095-X

Bruening, J.M., Bunn, A.G., Salzer, M.W., 2018. A climate-driven tree line position model in the White Mountains of California over the past six millennia. J Biogeogr 45, 1067–1076. https://doi.org/10.1111/jbi.13191

Brunstein, F.C., 1996. Climatic significance of the bristlecone pine latewood frost-ring record at Almagre Mountain, Colorado, U.S.A. Arct Antarct Alp Res 28, 65–76. https://doi.org/10.2307/1552087

Brunstein, F.C., 1995. Bristlecone pine frost-ring and light-ring chronologies, from 569 BC to AD 1993, Colorado.

Bunn, A.G., 2008. A dendrochronology program library in R (dplR). Dendrochronologia (Verona) 26, 115–124. https://doi.org/10.1016/j.dendro.2008.01.002

Bunn, A.G., Hughes, M.K., Salzer, M.W., 2011. Topographically modified tree-ring chronologies as a potential means to improve paleoclimate inference: A letter. Clim Change 105, 627–634. https://doi.org/10.1007/s10584-010-0005-5

Bunn, A.G., Salzer, M.W., Anchukaitis, K.J., Bruening, J.M., Hughes, M.K., 2018. Spatiotemporal Variability in the Climate Growth Response of High Elevation Bristlecone Pine in the White Mountains of California. Geophys Res Lett 45, 13,312-13,321. https://doi.org/10.1029/2018GL080981

Büntgen, U., Crivellaro, A., Arseneault, D., Baillie, M., Barclay, D., Bernabei, M., Bontadi, J., Boswijk, G., Brown, D., Christie, D.A., Churakova, O. V., Cook, E.R., D'Arrigo, R., Davi, N., Esper, J., Fonti, P., Greaves, C., Hantemirov, R.M., Hughes, M.K., Kirdyanov, A. V., Krusic, P.J., Le Quesne, C., Ljungqvist, F.C., McCormick, M., Myglan, V.S., Nicolussi, K., Oppenheimer, C., Palmer, J., Qin, C., Reinig, F., Salzer, M., Stoffel, M., Torbenson, M., Trnka, M., Villalba, R., Wiesenberg, N., Wiles, G., Yang, B., Piermattei, A., 2022. Global wood anatomical perspective on the onset of the Late Antique Little Ice Age (LALIA) in the mid-6th century CE. Sci Bull (Beijing) 67, 2336–2344. https://doi.org/10.1016/j.scib.2022.10.019

Cole-Dai, J., 2010. Volcanoes and climate. Wiley Interdiscip Rev Clim Change. https://doi.org/10.1002/wcc.76

Cook, E., Kairiukstis, L.A., 1990. Tree-Ring Standardization and Growth-Trend Estimation, Methods of Dendrochronology.

Crowley, T.J., 2000. Causes of climate change over the past 1000 years. Science (1979) 289, 270–277. https://doi.org/10.1126/science.289.5477.270

D'Arrigo, R., Wilson, R., Anchukaitis, K.J., 2013. Volcanic cooling signal in tree ring temperature records for the past millennium. Journal of Geophysical Research: Atmospheres 118, 9000–9010. https://doi.org/10.1002/jgrd.50692

D'Arrigo, R., Wilson, R., Jacoby, G., 2006. On the long-term context for late twentieth century warming. Journal of Geophysical Research: Atmospheres 111. https://doi.org/10.1029/2005JD006352

De Silva, S.L., Zielinski, G.A., 1998. Global influence of the AD 1600 eruption of Huaynaputina, Peru. Nature 393, 455–458. https://doi.org/10.1038/30948

Donaldson, L.A., 1992. Lignin distribution during latewood formation in Pinus radiata D. Don. IAWA J 13, 381–387.

Donaldson, L.A., 1991. Seasonal changes in lignin distribution during tracheid development in Pinus radiata D. Don. Wood Sci Technol 25, 15–24. https://doi.org/10.1007/BF00195553

Dutton, E.G., Christy, J.R., 1992. Solar radiative forcing at selected locations and evidence for global lower tropospheric cooling following the eruptions of El Chichón and Pinatubo. Geophys Res Lett 19. https://doi.org/10.1029/92GL02495

Esper, J., Büntgen, U., Hartl-Meier, C., Oppenheimer, C., Schneider, L., 2017. Northern Hemisphere temperature anomalies during the 1450s period of ambiguous volcanic forcing. Bull Volcanol 79, 41. https://doi.org/10.1007/s00445-017-1125-9

Esper, J., Schneider, L., Krusic, P.J., Luterbacher, J., Büntgen, U., Timonen, M., Sirocko, F., Zorita, E., 2013. European summer temperature response to annually dated volcanic eruptions over the past nine centuries. Bull Volcanol 75, 736. https://doi.org/10.1007/s00445-013-0736-z

Esper, J., Schneider, L., Smerdon, J.E., Schöne, B.R., Büntgen, U., 2015. Signals and memory in tree-ring width and density data. Dendrochronologia (Verona) 35, 62–70. https://doi.org/10.1016/j.dendro.2015.07.001

Fang, S., Sigl, M., Toohey, M., Jungclaus, J., Zanchettin, D., Timmreck, C., 2023. The Role of Small to Moderate Volcanic Eruptions in the Early 19th Century Climate. Geophys Res Lett 50. https://doi.org/10.1029/2023GL105307

Ferguson, C.W., 1979. Dendrochronology of bristlecone pine, Pinus longaeva. Environ Int 2, 209–214. https://doi.org/10.1016/0160-4120(79)90003-5

Ferguson, C.W., 1969. A 7104-Year Annual Tree-Ring Chronology for Bristlecone Pine, Pinus Aristata, from the White Mountains, California. Tree-Ring Bulletin.

Frank, D., Büntgen, U., Böhm, R., Maugeri, M., Esper, J., 2007. Warmer early instrumental measurements versus colder reconstructed temperatures: shooting at a moving target. Quat Sci Rev 26, 3298–3310. https://doi.org/10.1016/j.quascirev.2007.08.002

Fritts, H.C., 1976. Tree Rings and Climate. Academic Press, New York. https://doi.org/10.1126/science.197.4301.361.b

Gao, C., Robock, A., Ammann, C., 2008. Volcanic forcing of climate over the past 1500 years: An improved ice core-based index for climate models. Journal of Geophysical Research: Atmospheres 113. https://doi.org/10.1029/2008JD010239

Gao, C., Robock, A., Self, S., Witter, J.B., Steffenson, J.P., Clausen, H.B., Siggaard-Andersen, M., Johnsen, S., Mayewski, P.A., Ammann, C., 2006. The 1452 or 1453 A.D. Kuwae eruption signal derived from multiple ice core records: Greatest volcanic sulfate event of the past 700 years. Journal of Geophysical Research: Atmospheres 111. https://doi.org/10.1029/2005JD006710

Gärtner, H., Lucchinetti, S., Schweingruber, F.H., 2014. New perspectives for wood anatomical analysis in dendrosciences: The GSL1-microtome. Dendrochronologia (Verona) 32, 47–51. https://doi.org/10.1016/j.dendro.2013.07.002

Gärtner, H., Schweingruber, F., 2013. Microscopic preparation techniques for plant stem analysis. Verlag Dr. Kessel, Remagen-Oberwinter.

Glerum, C., Farrar, J.L., 1966. Frost Ring Formation in the Stems of Some Coniferous Species. Canadian Journal of Botany 44, 879–886. https://doi.org/10.1139/b66-103

Greaves, C., Crivellaro, A., Piermattei, A., Krusic, P.J., Oppenheimer, C., Potapov, A., Hordo, M., Metslaid, S., Kask, R., Kangur, A., Büntgen, U., 2022. Remarkably high blue ring occurrence in Estonian Scots pines in 1976 reveals wood anatomical evidence of extreme autumnal cooling. Trees. https://doi.org/10.1007/s00468-022-02366-1

Gurskaya, M.A., Shiyatov, S.G., 2006. Distribution of frost injuries in the wood of conifers. Russ J Ecol 37, 7–12. https://doi.org/10.1134/S1067413606010024

Hadad, M., Tardif, J.C., Conciatori, F., Waito, J., Westwood, A., 2020. Climate and atmospheric circulation related to frost-ring formation in Picea mariana trees from the Boreal Plains, interior North America. Weather Clim Extrem 29, 100264.

Hantemirov, R.M., Shiyatov, S.G., 2002. A continuous-multimillennial ring-width chronology in Yamal, northwestern Siberia. Holocene 12, 717–726. https://doi.org/10.1191/0959683602hl585rp

Helama, S., Lindholm, M., Timonen, M., Meriläinen, J., Eronen, M., 2002. The supra-long Scots pine tree-ring record for Finnish Lapland: Part 2, interannual to centennial variability in summer temperatures for 7500 years. Holocene 12, 681–687. https://doi.org/10.1191/0959683602hl581rp

Hughes, M.K., Vaganov, E.A., Shiyatov, S., Touchan, R., Funkhouser, G., 1999. Twentieth-century summer warmth in northern Yakutia in a 600-year context. Holocene 9, 629–634. https://doi.org/10.1191/095968399671321516

LaMarche Jr, V.C., 1970. Frost-damage rings in subalpine conifers and their application to tree-ring dating problems. Smith, JH G., and Worrall, J.(eds.), Tree-ring Analysis with Special Reference to Northwest America. University of British Columbia Faculty of Forestry Bulletin 99–100.

LaMarche, V.C., Hirschboeck, K.K., 1984. Frost rings in trees as records of major volcanic eruptions. Nature. https://doi.org/https://doi.org/10.1038/307121a0

LaMarche, V.C., Stockton, C.W., 1974. Chronologies from temperature-sensitive bristlecone pines at upper treeline in western United States. Tree-Ring Bulletin 34, 21–45.

Mann, M.E., Cane, M.A., Zebiak, S.E., Clement, A., 2005. Volcanic and Solar Forcing of the Tropical Pacific over the Past 1000 Years. J Clim 18, 447–456. https://doi.org/10.1175/JCLI-3276.1

Matisons, R., Gärtner, H., Elferts, D., Kārkliņa, A., Adamovičs, A., Jansons, Ā., 2020. Occurrence of ‘blue’ and ‘frost’ rings reveal frost sensitivity of eastern Baltic provenances of Scots pine. For Ecol Manage 457, 117729. https://doi.org/https://doi.org/10.1016/j.foreco.2019.117729

McAneney, J., Baillie, M., 2019. Absolute tree-ring dates for the Late Bronze Age eruptions of Aniakchak and Thera in light of a proposed revision of ice-core chronologies. Antiquity 93, 99–112. https://doi.org/10.15184/aqy.2018.165

Montwé, D., Isaac-Renton, M., Hamann, A., Spiecker, H., 2018. Cold adaptation recorded in tree rings highlights risks associated with climate change and assisted migration. Nat Commun 9, 1–7. https://doi.org/10.1038/s41467-018-04039-5

Oppenheimer, C., 2003. Climatic, environmental and human consequences of the largest known historic eruption: Tambora volcano (Indonesia) 1815. Progress in Physical Geography: Earth and Environment 27, 230–259. https://doi.org/10.1191/0309133303pp379ra

Payette, S., Delwaide, A., Simard, M., 2010. Frost-ring chronologies as dendroclimatic proxies of boreal environments. Geophys Res Lett 37, 1–6. https://doi.org/10.1029/2009GL041849

Piermattei, A., Crivellaro, A., Carrer, M., Urbinati, C., 2015. The “blue ring”: anatomy and formation hypothesis of a new tree-ring anomaly in conifers. Trees 29, 613–620. https://doi.org/10.1007/s00468-014-1107-x

Piermattei, A., Crivellaro, A., Krusic, P.J., Esper, J., Vítek, P., Oppenheimer, C., Felhofer, M., Gierlinger, N., Reinig, F., Urban, O., Verstege, A., Lobo, H., Büntgen, U., 2020. A millennium-long ‘Blue Ring’ chronology from the Spanish Pyrenees reveals severe ephemeral summer cooling after volcanic eruptions. Environmental Research Letters 15, 124016. https://doi.org/10.1088/1748-9326/abc120

Robock, A., 2000. Volcanic eruptions and climate. Reviews of geophysics 38, 191–219.

Robock, A., Mao, J., 1992. Winter warming from large volcanic eruptions. Geophys Res Lett 19, 2405–2408.

Salzer, M.W., Bunn, A.G., Graham, N.E., Hughes, M.K., 2014a. Five millennia of paleotemperature from tree-rings in the Great Basin, USA. Clim Dyn 42, 1517–1526.

Salzer, M.W., Hughes, M.K., 2007. Bristlecone pine tree rings and volcanic eruptions over the last 5000 yr. Quat Res 67, 57–68. https://doi.org/10.1016/j.yqres.2006.07.004

Salzer, M.W., Hughes, M.K., Bunn, A.G., Kipfmueller, K.F., 2009. Recent unprecedented tree-ring growth in bristlecone pine at the highest elevations and possible causes. Proc Natl Acad Sci U S A 106, 20348–20353. https://doi.org/10.1073/pnas.0903029106

Salzer, M.W., Larson, E.R., Bunn, A.G., Hughes, M.K., 2014b. Changing climate response in near-treeline bristlecone pine with elevation and aspect. Environmental Research Letters 9, 114007. https://doi.org/10.1088/1748-9326/9/11/114007

Schneider, L., Smerdon, J.E., Büntgen, U., Wilson, R.J.S., Myglan, V.S., Kirdyanov, A. V., Esper, J., 2015. Revising midlatitude summer temperatures back to A.D. 600 based on a wood density network. Geophys Res Lett 42, 4556–4562. https://doi.org/10.1002/2015GL063956

Schulman, E., 1958. Bristlecone pine, oldest known living thing. Nat Geogr Mag 113, 355–372.

Schweingruber, F.H., 2007. Wood structure and environment. Springer Science \& Business Media.

Siekacz, L., Pearson, C., Salzer, M., Soja-Kukieła, N., Koprowski, M., 2024. Blue rings in Bristlecone pine as a high resolution indicator of past cooling events. Clim Change 177, 123. https://doi.org/10.1007/s10584-024-03773-8

Sigl, M., Toohey, M., McConnell, J.R., Cole-Dai, J., Severi, M., 2022. Volcanic stratospheric sulfur injections and aerosol optical depth during the Holocene (past 11 500 years) from a bipolar ice-core array. Earth Syst Sci Data 14, 3167–3196. https://doi.org/10.5194/essd-14-3167-2022

Sigl, M., Winstrup, M., McConnell, J.R., Welten, K.C., Plunkett, G., Ludlow, F., Büntgen, U., Caffee, M., Chellman, N., Dahl-Jensen, D., Fischer, H., Kipfstuhl, S., Kostick, C., Maselli, O.J., Mekhaldi, F., Mulvaney, R., Muscheler, R., Pasteris, D.R., Pilcher, J.R., Salzer, M., Schüpbach, S., Steffensen, J.P., Vinther, B.M., Woodruff, T.E., 2015. Timing and climate forcing of volcanic eruptions for the past 2,500 years. Nature 523, 543–549. https://doi.org/10.1038/nature14565

Stokes, M.A., 1996. An introduction to tree-ring dating. University of Arizona Press.

Tardif, J.C., Girardin, M.P., Conciatori, F., 2011. Light rings as bioindicators of climate change in Interior North America. Glob Planet Change 79, 134–144.

Tardif, J.C., Salzer, M.W., Conciatori, F., Bunn, A.G., Hughes, M.K., 2020. Formation, structure and climatic significance of blue rings and frost rings in high elevation bristlecone pine (Pinus longaeva D.K. Bailey). Quat Sci Rev 244, 106516. https://doi.org/https://doi.org/10.1016/j.quascirev.2020.106516

Timmreck, C., 2012. Modeling the climatic effects of large explosive volcanic eruptions. WIREs Climate Change 3, 545–564. https://doi.org/10.1002/wcc.192

Toohey, M., Sigl, M., 2017. Volcanic stratospheric sulfur injections and aerosol optical depth from 500 BCE to 1900 CE 809–831.

Tran, T.J., Bruening, J.M., Bunn, A.G., Salzer, M.W., Weiss, S.B., 2017. Cluster analysis and topoclimate modeling to examine bristlecone pine tree-ring growth signals in the Great Basin, USA. Environmental Research Letters 12. https://doi.org/10.1088/1748-9326/aa5388

Vidal, C.M., Métrich, N., Komorowski, J.-C., Pratomo, I., Michel, A., Kartadinata, N., Robert, V., Lavigne, F., 2016. The 1257 Samalas eruption (Lombok, Indonesia): the single greatest stratospheric gas release of the Common Era. Sci Rep 6, 34868. https://doi.org/10.1038/srep34868

Wang, L., Payette, S., Bégin, Y., 2000. A Quantitative Definition of Light Rings in Black Spruce (Picea mariana) at the Arctic Treeline in Northern Québec, Canada . Arct Antarct Alp Res 32, 324–330. https://doi.org/10.1080/15230430.2000.12003370

Wilson, R., Anchukaitis, K., Briffa, K.R., Büntgen, U., Cook, E., D'Arrigo, R., Davi, N., Esper, J., Frank, D., Gunnarson, B., Hegerl, G., Helama, S., Klesse, S., Krusic, P.J., Linderholm, H.W., Myglan, V., Osborn, T.J., Rydval, M., Schneider, L., Schurer, A., Wiles, G., Zhang, P., Zorita, E., 2016. Last millennium northern hemisphere summer temperatures from tree rings: Part I: The long term context. Quat Sci Rev 134, 1–18. https://doi.org/10.1016/j.quascirev.2015.12.005

Supplementary data

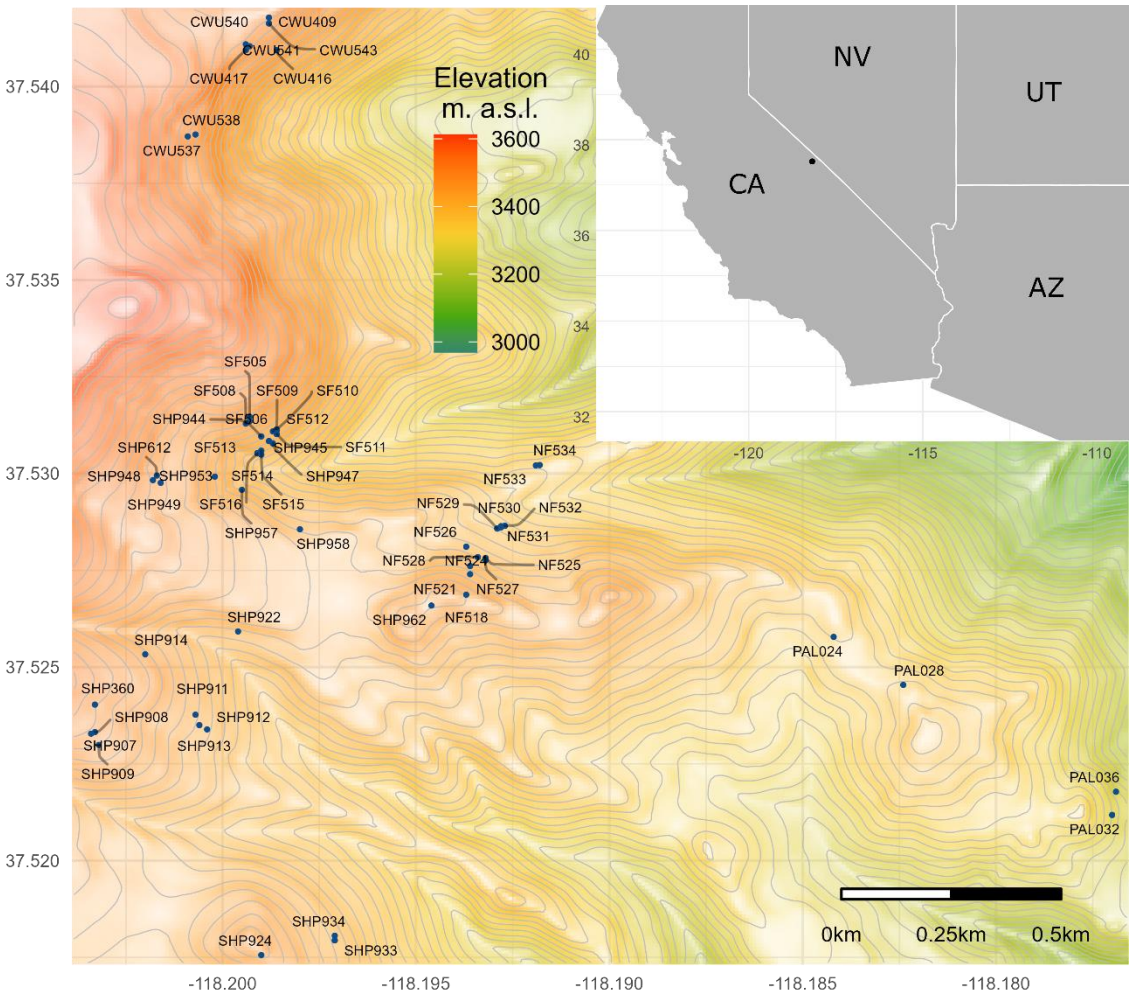

Figure S 1 Locations of sampled bristlecone pine specimens on a relief map of the study area and inset map showing the location of the study area in the south-western United States.

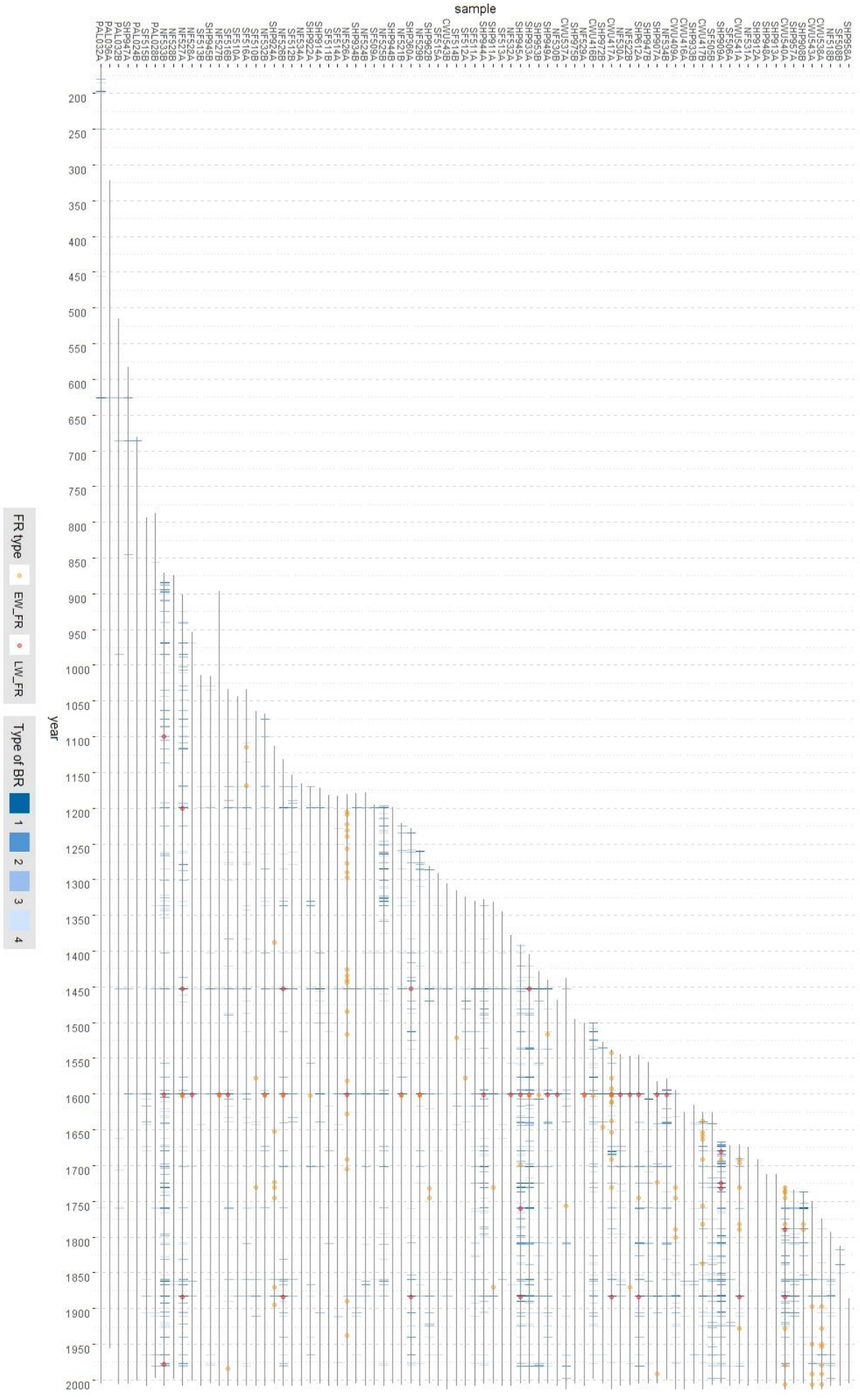
sample
year
FR type
EW_FR
LW_FR
Type of BR
1
2
3
4

Figure S 2 Blue ring and frost ring chronology for period 164-2014 (full chronology lenght) sorted by sample depth.

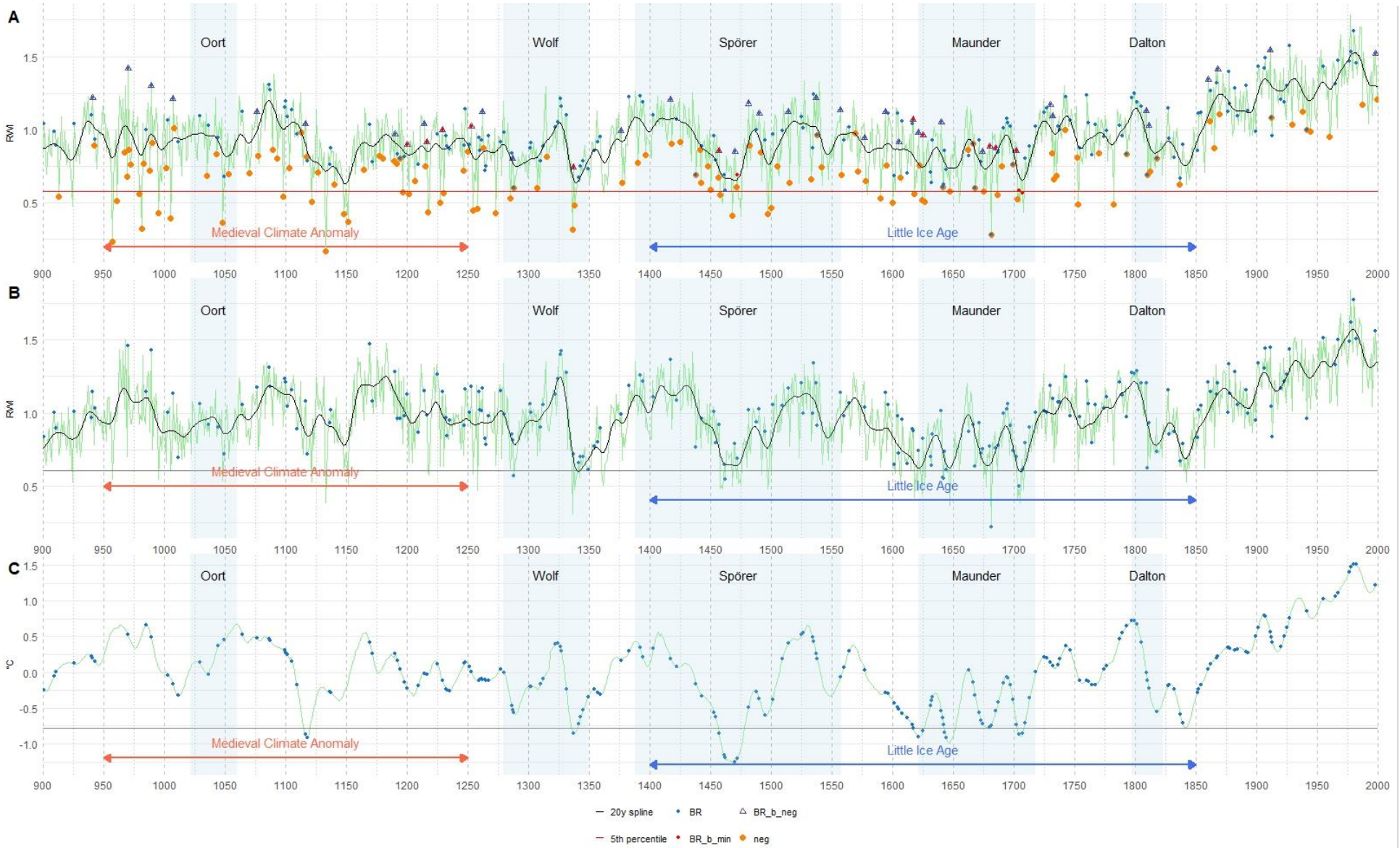
A
B
C
Oort
Wolf
Spörer
Maunder
Dalton
RWI
°C
Medieval Climate Anomaly
Little Ice Age
20y spline
BR
BR_b_neg
5th percentile
BR_b_min
neg

Figure S 3 Standard site chronology calculated for the 83 cores analyzed in this study for the period 900-2000 CE, B - Master Sheep mountain chronology (Salzer et al., 2014a), C - the temperature anomaly reconstruction based on five bristlecone pine chronologies (Salzer et al., 2014a). Please note high correlation between each.

Summary

Our study constitutes the largest and most comprehensive investigation of blue rings (BRs) to date. We have developed a BR chronology from bristlecone pine, spanning 164-2014 AD, with an increasingly robust sample depth from 10 samples in 900 AD to 83 in the most recent period. In total, we analyzed 57816 rings and identified 1271 BRs.

The results are presented in two thematically coherent articles. The first article, focuses on the classification of BRs and analyzes the influence of thermal and topographic factors on their formation. The second article, establishes a clear relationship between the occurrence of BRs and climatically effective volcanic eruptions over the past eleven centuries. Moreover, it explores the relationship between BRs and the widths of annual rings in bristlecone pine, demonstrating the potential of BRs to reveal short-term cooling episodes not recorded in traditional chronologies of annual ring widths and maximum latewood density.

Based on the observed variability, BRs were classified into four intensity levels, ranging from BR-1 to BR-4 (the strongest to the weakest). The classification of BR intensity was developed based on several factors, including the number of rows of under-lignified tracheids, the degree of lignification of tracheid walls, the thickness of latewood cell walls compared to surrounding rings, and the overall intensity of the blue color resulting from the proportion of underlignified cell walls. Our study assessed the full variability of BR intensity in bristlecone pine over the past 18 centuries, showing that BRs appeared exclusively in the latewood, predominantly in the outermost cells of the radial file. We found that the weaker BR classes (BR-3 and BR-4) are the most abundant types of this generally rare phenomenon, they contain significant information and should not be overlooked in future studies. We also identified and analyzed the occurrence of frost damage, classifying these as latewood frost rings (LW_FRs) and earlywood frost rings (EW_FRs).

Using a generalized linear mixed-effects model, we demonstrated that mean monthly temperatures significantly influence BR formation. We identified a complex interplay of mean monthly temperatures of several months affecting BR formation, with the strongest relationship with lower temperatures in September, followed by June, August, and April. We also found a positive relationship with temperatures in February and October. Although our analysis of available daily temperature data over 1981-2014 was limited to only two BR years, we were able to show a connection between short-term temperature decreases (at the

scale of several days) at the end of the growing season and the occurrence of BRs, based on our analysis of the 1982 and 1998 BR events.

Topographic factors affecting BR formation were also explored. The model revealed a significant negative relationship with distance from the upper tree line, indicating that trees located further below the tree line exhibit fewer and lower intensity classes of BR. No evidence was found that exposure affects BR formation. Our study highlights the complex interplay between temperature, topography, and BR formation, with low temperatures as the primary driver, modified by elevation due to the adiabatic lapse rate. We observe a buffering effect with distance below the upper treeline, which is balanced against the severity of the cold snap. More extreme low-temperature departures result in more BRs of higher intensity, occurring further down the transect than less severe cooling events. Consequently, BR classification and sampling strategy across a larger elevational transect, rather than only near the upper tree line, provide valuable paleoclimatic insights and should be implemented in future studies.

A more detailed analysis of previously developed monthly topoclimate indices revealed no consistent significant differences between the topoclimate variables of trees that recorded BRs and those that did not. This finding suggests that the BR sensitivity of a specific tree cannot be fully explained by current topoclimate variables, raising the possibility that trees may experience more significant microsite-induced temperature variations than previously documented, or that genetic susceptibility at the individual tree level may play a role in BR formation.

The study offers an in-depth analysis of the factors leading to blue ring formation in bristlecone pine trees. It concludes that BRs are sensitive indicators of late-season cooling events, with their formation influenced by both temperature and topography. However, the BR sensitivity of specific trees in topographically variable mountainous environments are influenced by multiple factors making them a complex but valuable proxy for reconstructing past climatic conditions.

In the second article, we demonstrated based on the full temporal span of our dataset that BRs are more sensitive indicators of past cooling episodes than latewood frost rings. This conclusion is supported by the fact that while all LWFR occurrences are accompanied by BRs, the reverse is not true, BRs are more numerous than LWFRs. BRs are more frequent both over time and within a single year's elevational transect. This suggests that BRs can record cooling episodes that: 1) are of lower intensity, since LW_FRs require subfreezing

temperatures to form, and 2) occur later in the season, since while LW_FRs form during periods of cambial activity, BRs can form even after cambial activity has ceased but when the last-formed tracheids are still lignifying. This enables BRs to capture cooling episodes that frequently are not reflected in the LW_FR record.

We established a strong, statistically significant connection between BR formation and volcanic activity. Between 900 and 2014 CE, 220 BR events and 133 volcanic signals from ice cores were recorded. Contingency tests show that 65% of ice core volcanic sulfate signals can be matched with BR events within a three-year window, indicating a strong non-random association between volcanic eruptions and BR formation. Tropical eruptions showed the strongest correlation with BRs, with exact matches twice as high as expected randomly, and joint occurrences within the three-year window nearly five times higher. Specifically, 85% of tropical eruptions match BRs within the three-year window. Conversely, southern hemisphere extratropical eruptions showed no significant association with BRs, while northern hemisphere extratropical eruptions had joint occurrences three times higher than expected, with 61% matching BR events.

A statistical model analyzing data from 61 tree samples and 39383 observations supported these findings, showing that global volcanic forcing significantly increases the likelihood of BR formation, with tropical eruptions having the strongest influence. These results indicate a causal link between volcanic eruptions and BR formation, influenced significantly by the eruption's geographical origin.

Analysis of pointer years and growth minima reveals that BRs tend to form significantly more often in wider or neutral rings, and frequently preceding a negative pointer year or growth minimum. As such we conclude that BRs may provide additional insights into ephemeral cooling events occurring late in the growing season or after it, when radial growth of a particular year has concluded. During such periods, cooling events are no longer able to influence the current year's radial growth directly. However, protracted cooling events, such as those linked with climatically effective volcanic eruptions, could influence climatic conditions post the completion of radial growth of a specific year and into the following growing season. As a result, the effects of these events may manifest with a delay in the ring widths formed in subsequent years. In this context, BR chronologies, which as our results show consistently provide distinct information independent of ring widths, can offer additional details regarding ephemeral cooling events that occur after the completion of radial growth of a given year. Moreover, they may serve as early indications of cooling

induced by volcanic activity, thus providing more precise dating of climatically effective eruptions compared to other tree ring parameters.

Superposed epoch analysis further reinforces this conclusion at both the stand level and across different event years, demonstrating that in BR years, ring widths are consistently and significantly wider across all BR frequency categories. Our findings across individual trees, at the stand level, and over a range of BR years, consistently support the hypothesis that BRs can signal cooling events occurring after a year's growth has concluded, these cooling events may be ephemeral, or more lasting and affect the ring widths in the following years, constituting a valuable proxy complementing climate reconstructions.

Furthermore our chronology reveals that out of 87 BR years linked to volcanic eruptions within a three-year match window, 25 of these occurred a year before the corresponding volcanic ice-core signal was detected. This suggests that BRs may sometimes capture evidence of volcanically induced cooling before sulfur deposition in ice cores, offering an alternative earlier dating of some eruptions.

It is widely recognized that tree ring based temperature reconstructions suffer from biological memory and autocorrelation issues, which makes them less reliable in making inferences at sub-annual and interannual timescales as relevant to the sudden consequences of volcanic eruptions. This can lead to an underestimation of the abruptness and severity of climatic extremes resulting from volcanic cooling in RW based reconstructions which can exhibit a lag over several years. In contrast, BRs are better suited to record cooling episodes. BR formation results from the immediate cessation of the lignification process in tree rings, triggered by sudden temperature drops. This process does not resume, leaving a permanent record of the event in the form of bands of under-lignified cells. Unlike RWs, BR formation is not influenced by long-term growth trends or biological memory, making them a more reliable indicator of specific cooling events.

Utilizing a set of 24 volcanic eruptions with Global volcanic forcing larger than or equal to that of Krakatoa, we demonstrated that a multiproxy approach integrating BRs, frost rings, growth minima, maximum latewood density (MXD), and hemispheric temperature reconstructions—can significantly enhance our understanding of climate system responses to volcanic eruptions.

BRs can provide earlier evidence for the onset of cooling compared to RWs, capturing cooling episodes after the annual radial growth phase has concluded. This ability allows BRs to address limitations in RWs, which may fail to accurately reflect sudden, short-

term cooling due to biological persistence and autocorrelation effects. BRs can sometimes indicate volcanically induced cooling earlier than both RW and MXD-based temperature reconstructions. This is because cooling patterns can vary regionally, so when combining distant proxy sources in hemispheric reconstructions the overall cooling signal (even in temperature sensitive MXD based reconstructions) can become diluted and smoothed out. This issue is especially pronounced in the earlier segments of hemispheric reconstructions, where a limited number of source chronologies and their geographic representation can delay and average out the recorded cooling. Furthermore, some BR event years may suggest an earlier timing for volcanic eruptions than indicated by ice-core records, reflecting the climate's response to stratospheric sulfate before its deposition. While 40% of BR events are associated with volcanic cooling episodes, BRs also record ephemeral cooling episodes not associated with volcanic eruptions. Not all BR signals are linked to significant volcanic eruptions, just as not all MXD minima correspond to known volcanic events. This is because not every cold summer in a particular location can be attributed to volcanic activity, and similarly, not all eruptions lead to cooler summers.

BRs offer a sensitive record cooling episodes but can be a noisy proxy, with many low BR signal years reflecting localized cold snaps rather than large-scale cooling. In mountainous regions, diverse topography can influence BR formation, necessitating a relatively large sample depth to distinguish between localized cold snaps reflected in some trees and regional cooling episodes. Future work should focus on the development of more high-resolution records of past cooling events, such as BR chronologies from long tree-ring records in various regions. This approach will help build a more accurate understanding of the spatial climatic signatures of past volcanic eruptions, enabling us to better evaluate their influence on both regional and global climates.

Future outlooks

We identify three main areas of further development of our study:

1) To further explore the lignification classes developed in this study in two directions: a) quantitative wood anatomy (QWA) to characterize the dimensional parameters of cell walls specific for each BR class and b) to establish a quantitative interpretation of the present qualitative BR classification.

Earlier explorations (Piermattei et al., 2020, 2015) noted that the cell lumen area and cell wall thickness in the latewood during BR years are reduced compared to fully lignified rings, which is in agreement with our visual characteristic of the BR-1 intensity class. However more detailed exploration of tracheid dimensional characteristics of all four BR intensity classes is merited. Confocal Raman Spectroscopy will be used to complement these cellular analyses and provide detailed higher resolution insights targeting and studying the composition of specific cell wall layers (Zhang, 2021). Traditionally, the lignin content in plant cell walls is determined through wet chemical analysis, a method that offers only average compositional data and lacks the resolution to examine lignin distribution at the micro-level within cell walls. Initial exploration of Confocal Raman Spectroscopy in comparative studying of BRs and normally lignified rings (Piermattei et al., 2020) showed lignin depletion in BRs compared to normally lignified rings. We plan to target specific blue rings from our dataset representing varying BR intensity classes and perform a comparative analysis between stained thin-sections and spectral maps of the same rings in spectral bands representative of lignin, cellulose, and hemiceluloses (Agarwal, 2006; Gierlinger et al., 2012; Gierlinger and Schwanninger, 2006; Piermattei et al., 2020; Zhang, 2021). The Raman spectra are often complex, with overlapping peaks from cellulose, hemicellulose, and lignin. Spectral deconvolution techniques, such as curve fitting or multivariate analysis and calibration techniques can be used to accurately quantify the lignin content. Comparative analysis between double stained thin-sections and Raman lignin spectra imaging will help further develop a more representative BR classification, qualifying the actual lignin content in specific BR intensity classes. We will investigate to what extent the qualitative BR classification developed in this study represents different levels of lignin content. Eventually, through comparative analysis of double-stained thin-sections and Raman spectroscopy results, we will aim to provide an

approximate calibration method for lignin quantification to be further implemented in double-stained thin-section BR studies.

2) The dataset of double-stained thin-sections of 83 bristlecone pine samples covering the period 164-2014 AD should be explored at quantitative wood anatomy (QWA) level. Roxas software (von Arx and Carrer, 2014) can be used for the automatic identification and measurement of anatomical structures across all tracheid cells in the digitized thin-sections and the boundaries of annual rings. The measured anatomical parameters can further be used to calculate dendroanatomical density, i.e., the percentage of the wall area of each cell in relation to the full cell area, and integrated into density profiles from which the anatomical maximum latewood density (aMXD the highest value of the anatomical density of a tree ring defined as the proportion of cell wall area (CWA) in relation to the full tracheid area (TA). The TA is the area sum of the CWA and the lumen area (LA)) can be calculated.

Upper tree line chronologies from bristlecone pine have been utilized to reconstruct temperature over the past 4500 years however this TRW based temperature reconstruction retains temperature variability over decadal to centennial timescales (Salzer et al., 2014a). At interannual timescales, MXD is proven to be a supreme parameter for temperature reconstruction since it is considered to be less burdened by biological memory and the year-to-year autocorrelation issues and more directly responsive to late growing season temperature as they affect cell wall thickening and therefore density of latewood (D'Arrigo et al., 2013; Esper et al., 2015; Frank et al., 2007).

Based on our thin-sections dataset we want to develop aMXD chronology and perform temperature reconstruction for the period 1400-2005. Within that period the largest BR signals related to volcanic eruptions occur in 1453, 1601, and 1884 along with a series of less pronounced BR signals related and unrelated to identified volcanic sulfur deposition in ice cores. We want to further explore how BR chronology can enhance the information that comes from direct aMXD measurements from the same cores analyzed. In our study so far we have already established how BRs can bring additional information about ephemeral cooling episodes compared to bristlecone pine RWs, and that BRs can bring an additional layer of information to MXD chronologies from other species and regions, and TRW and MXD-based hemispheric temperature reconstructions. Björklund et al., (2021) revealed that BRs are characterized by low aMXD, however, not all low aMXD values are associated with BRs. Furthermore, we want to explore if and what footprints different classes of BR intensity leave in aMXD profiles. Björklund et al., (2021) focused

on studying the differences between different approaches to obtaining maximum latewood density signals (X-ray, Blue Intensity, and aMXD) and showed that incomplete lignification (as represented by BR years) is not captured in traditional X-ray and Blue Intensity methods. Bristlecone pine trees are characterized by very narrow growth rings, their iconic gnarly shapes, and the twisted internal structure of tracheids, which made it impossible so far to measure MXD with traditional X-ray MXD technique that requires the X-ray beams to be parallel to the tracheids in the analyzed sample. However recent improvements with the development X-ray Computed Tomography (X-ray CT) made it possible to measure MXD from challenging wood samples (De Mil et al., 2016; Van den Bulcke et al., 2014) as this new technique allows to correct for grain angle enabling extraction of MXD information from irregular wood structure. These advances led to the very recent development of X-ray CT-based MXD chronology for bristlecone pine (De Mil et al. 2024, preprint), which is reported to correlate significantly with a wide seven-month (March-September) warm season temperature window. This allowed further development of warm season X-ray CT-based MXD temperature reconstruction which is reported to retain high frequency interannual temperature variability. We want to further compare aMXD and X-ray CT-based MXD records and temperature reconstructions. aMXD data can be aggregated at various resolution levels, even higher than X-ray CT-based MXD records. We want to compare information coming from X-ray CT-based MXD records and different resolution levels of aMXD data and investigate if finer resolution aMXD could provide even more skilled temperature reconstruction than X-ray CT-based MXD records. Such studies for bristlecone pine so far were impossible due to methodological challenges and lack of datasets however soon to be published X-ray CT based MXD record (De Mil et al. 2024, preprint) and aMXD dataset (that we're currently developing) will enable this detailed analysis of bristlecone pine record. Furthermore, we want to explore how and if specific BR intensity classes can be captured by X-ray CT-based MXD and aMXD data.

3) Continued development of the BR record to cover the full timespan of the existing bristlecone pine record. Bristlecone pines are recognized as the longest-living trees and serve as a vital record of historical climate variations. Their ability to provide data of annual resolution, secure dating, and temporal coverage makes them exceptionally valuable for studying past environmental change (Bale et al., 2011; Bruening et al., 2018; Brunstein, 1996, 1995; Bunn et al., 2018, 2011; Ferguson, 1979, 1969; LaMarche and Stockton, 1974; Salzer et al., 2014a, 2009; Salzer and Hughes, 2007; Schulman, 1958; Tran et al., 2017). Recently the discovery of so called Miyake events (Miyake et al., 2012)

has allowed to tie precise 10Be markers in ice cores and 14C spikes in bristlecone pine to constrain the dating of ice core records and utilized growth anomalies and frost ring records to secure timelines of volcanic eruptive history during the Holocene (Sigl et al., 2022, 2015). Our study has demonstrated that BR chronology provides information about cooling episodes not captured or captured with higher time resolution than RW and FR chronologies. This underscores the importance of further developing continuous BR record for the full extent of bristlecone pine archives to develop more comprehensive and reliable histories of abrupt, short-term climate responses to volcanic events. A long BR record could considerably enhance paleoclimatic and cultural histories related to eruptive events (Büntgen et al., 2022; Piermattei et al., 2020) as well as understanding of their influence on regional circulation patterns.

Furthermore, we expect that the scientific interest in the significant paleoclimatic potential of BRs is going to increase and result in the development of more BR chronologies from different regions and species (Büntgen et al. 2022). We have demonstrated how comparison of such records from distant sources is going to help better constrain the spatial and temporal footprints of past climatically effective volcanic eruptions.

References

Abe, H., Nakai, T., Utsumi, Y., Kagawa, A., 2003. Temporal water deficit and wood formation in Cryptomeria japonica. Tree Physiol. https://doi.org/10.1093/treephys/23.12.859

Agarwal, U.P., 2006. Raman imaging to investigate ultrastructure and composition of plant cell walls: distribution of lignin and cellulose in black spruce wood (Picea mariana). Planta 224, 1141–1153. https://doi.org/10.1007/s00425-006-0295-z

Anchukaitis, K.J., Breitenmoser, P., Briffa, K.R., Buchwal, A., Büntgen, U., Cook, E.R., D'Arrigo, R.D., Esper, J., Evans, M.N., Frank, D., Grudd, H., Gunnarson, B.E., Hughes, M.K., Kirdyanov, A. V., Körner, C., Krusic, P.J., Luckman, B., Melvin, T.M., Salzer, M.W., Shashkin, A. V., Timmreck, C., Vaganov, E.A., Wilson, R.J.S., 2012. Tree rings and volcanic cooling. Nat Geosci 5, 836–837. https://doi.org/10.1038/ngeo1645

Arzac, A., Tabakova, M.A., Khotcinskaia, K., Koteneva, A., Kirdyanov, A. V, Olano, J.M., 2021. Linking tree growth and intra-annual density fluctuations to climate in suppressed and dominant Pinus sylvestris L. trees in the forest-steppe of Southern Siberia. Dendrochronologia (Verona) 67, 125842.

Atalla, R.H., Agarwal, U.P., 1985. Raman microprobe evidence for lignin orientation in the cell walls of native woody tissue. Science (1979) 227, 636–638.

Baayen, R.H., 2008. Analyzing Linguistic Data: A Practical Introduction to Statistics using R. Cambridge University Press. https://doi.org/10.1017/CBO9780511801686

Baillie, M.G.L., 2010. Volcanoes, ice-cores and tree-rings: One story or two? Antiquity 84, 202–215. https://doi.org/10.1017/S0003598X00099877

Baillie, M.G.L., McAneney, J., 2015. Tree ring effects and ice core acidities clarify the volcanic record of the first millennium. Climate of the Past 11, 105–114. https://doi.org/10.5194/cp-11-105-2015

Bale, R.J., Robertson, I., Salzer, M.W., Loader, N.J., Leavitt, S.W., Gagen, M., Harlan, T.P., McCarroll, D., 2011. An annually resolved bristlecone pine carbon isotope chronology for the last millennium. Quat Res. https://doi.org/10.1016/j.yqres.2011.05.004

Barbosa, A.C., Stahle, D.W., Burnette, D.J., Torbenson, M.C.A., Cook, E.R., Bunkers, M.J., Garfin, G., Villalba, R., 2019. Meteorological Factors Associated With Frost Rings in Rocky Mountain Bristlecone Pine At Mt. Goliath, Colorado. Tree Ring Res 75, 101. https://doi.org/10.3959/1536-1098-75.2.101

Barnett, J.R., Jeronimidis, G., 2003. Wood quality and its biological basis. CRC Press.

Bates, D., Mächler, M., Bolker, B., Walker, S., 2015. Fitting Linear Mixed-Effects Models Using lme4. J Stat Softw 67. https://doi.org/10.18637/jss.v067.i01

Becker, M., Nieminen, T.M., Geremia, F., 1994. Short-term variations and long-term changes in oak productivity in northeastern France. The role of climate and

atmospheric CO2. Annales des Sciences Forestieres 51. https://doi.org/10.1051/forest:19940504

Begum, S., Nakaba, S., Yamagishi, Y., Oribe, Y., Funada, R., 2013. Regulation of cambial activity in relation to environmental conditions: understanding the role of temperature in wood formation of trees. Physiol Plant 147, 46–54.

Björklund, J., Fonti, M. V, Fonti, P., den Bulcke, J., von Arx, G., 2021. Cell wall dimensions reign supreme: cell wall composition is irrelevant for the temperature signal of latewood density/blue intensity in Scots pine. Dendrochronologia (Verona) 65, 125785.

Bollhöner, B., Prestele, J., Tuominen, H., 2012. Xylem cell death: emerging understanding of regulation and function. J Exp Bot 63, 1081–1094.

Bollschweiler, M., Stoffel, M., Schneuwly, D.M., Bourqui, K., 2008. Traumatic resin ducts in Larix decidua stems impacted by debris flows. Tree Physiol 28, 255–263. https://doi.org/10.1093/treephys/28.2.255

Boyce, R.L., Lubbers, B., 2011. Bark-stripping patterns in bristlecone pine (Pinus aristata) stands in Colorado, USA1. J Torrey Bot Soc 138, 308–321.

Briffa, K.R., Jones, P.D., Schweingruber, F.H., Osborn, T.J., 1998. Influence of volcanic eruptions on Northern Hemisphere summer temperature over the past 600 years. Nature 393, 450–455. https://doi.org/10.1038/30943

Briffa, K.R., Jones, P.D., Schweingruber, F.H., Shiyatov, S.G., Cook, E.R., 1995. Unusual twentieth-century summer warmth in a 1,000-year temperature record from Siberia. Nature 376, 156–159. https://doi.org/10.1038/376156a0

Briffa, K.R., Melvin, T.M., Osborn, T.J., Hantemirov, R.M., Kirdyanov, A. V., Mazepa, V.S., Shiyatov, S.G., Esper, J., 2013. Reassessing the evidence for tree-growth and inferred temperature change during the Common Era in Yamalia, northwest Siberia. Quat Sci Rev 72, 83–107. https://doi.org/10.1016/j.quascirev.2013.04.008

Briffa, K.R., Osborn, T.J., Schweingruber, F.H., 2004. Large-scale temperature inferences from tree rings: a review. Glob Planet Change 40, 11–26. https://doi.org/10.1016/S0921-8181(03)00095-X

Bruening, J.M., Bunn, A.G., Salzer, M.W., 2018. A climate-driven tree line position model in the White Mountains of California over the past six millennia. J Biogeogr 45, 1067–1076. https://doi.org/10.1111/jbi.13191

Bruening, J.M., j., T.T., Bunn, A.G., Weiss, S.B., Salzer, M.W., 2017. Fine-scale modeling of bristlecone pine treeline position in the Great Basin, USA. Environmental Research Letters 12, 14008.

Bruening, J.M., 2016. Fine-scale topoclimate modeling and climatic treeline prediction of Great Basin bristlecone pine (Pinus longaeva) in the American southwest.

Brunstein, F.C., 2006. Growth-form characteristics of ancient Rocky Mountain bristlecone pines (Pinus aristata), Colorado. https://doi.org/https://doi.org/10.3133/sir20065219

Brunstein, F.C., 1996. Climatic significance of the bristlecone pine latewood frost-ring record at Almagre Mountain, Colorado, U.S.A. Arct Antarct Alp Res 28, 65–76. https://doi.org/10.2307/1552087

Brunstein, F.C., 1995. Bristlecone pine frost-ring and light-ring chronologies, from 569 BC to AD 1993, Colorado.

Bunn, A.G., 2008. A dendrochronology program library in R (dplR). Dendrochronologia (Verona) 26, 115–124. https://doi.org/10.1016/j.dendro.2008.01.002

Bunn, A.G., Hughes, M.K., Salzer, M.W., 2011. Topographically modified tree-ring chronologies as a potential means to improve paleoclimate inference: A letter. Clim Change 105, 627–634. https://doi.org/10.1007/s10584-010-0005-5

Bunn, A.G., Salzer, M.W., Anchukaitis, K.J., Bruening, J.M., Hughes, M.K., 2018. Spatiotemporal Variability in the Climate Growth Response of High Elevation Bristlecone Pine in the White Mountains of California. Geophys Res Lett 45, 13,312-13,321. https://doi.org/10.1029/2018GL080981

Büntgen, U., Crivellaro, A., Arseneault, D., Baillie, M., Barclay, D., Bernabei, M., Bontadi, J., Boswijk, G., Brown, D., Christie, D.A., Churakova, O. V., Cook, E.R., D'Arrigo, R., Davi, N., Esper, J., Fonti, P., Greaves, C., Hantemirov, R.M., Hughes, M.K., Kirdyanov, A. V., Krusic, P.J., Le Quesne, C., Ljungqvist, F.C., McCormick, M., Myglan, V.S., Nicolussi, K., Oppenheimer, C., Palmer, J., Qin, C., Reinig, F., Salzer, M., Stoffel, M., Torbenson, M., Trnka, M., Villalba, R., Wiesenberg, N., Wiles, G., Yang, B., Piermattei, A., 2022. Global wood anatomical perspective on the onset of the Late Antique Little Ice Age (LALIA) in the mid-6th century CE. Sci Bull (Beijing) 67, 2336–2344. https://doi.org/10.1016/j.scib.2022.10.019

Büntgen, U., Frank, D.C., Nievergelt, D., Esper, J., 2006. Summer temperature variations in the European Alps, A.D. 755-2004. J Clim 19, 5606–5623. https://doi.org/10.1175/JCLI3917.1

Castagneri, D., Fonti, P., von Arx, G., Carrer, M., 2017. How does climate influence xylem morphogenesis over the growing season? Insights from long-term intra-ring anatomy in Picea abies. Ann Bot 119, 1011–1020.

Cole-Dai, J., 2010. Volcanoes and climate. Wiley Interdiscip Rev Clim Change. https://doi.org/10.1002/wcc.76

Cook, E., Kairiukstis, L.A., 1990. Tree-Ring Standardization and Growth-Trend Estimation, Methods of Dendrochronology.

Cosgrove, D.J., 2005. Growth of the plant cell wall. Nat Rev Mol Cell Biol 6, 850–861.

Crivellaro, A., Piermattei, A., Dolezal, J., Dupree, P., Büntgen, U., 2022. Biogeographic implication of temperature-induced plant cell wall lignification. Commun Biol 5, 767. https://doi.org/10.1038/s42003-022-03732-y

Crivellaro, A., Reverenna, M., Ruffinatto, F., Urbinati, C., Piermattei, A., 2018. The anatomy of »blue ring« in the wood of Pinus nigra. Les/Wood 67, 21–28. https://doi.org/10.26614/les-wood.2018.v67n02a02

Crowley, T.J., 2000. Causes of climate change over the past 1000 years. Science (1979) 289, 270–277. https://doi.org/10.1126/science.289.5477.270

Cuny, H.E., Rathgeber, C.B.K., Frank, D., Fonti, P., Fournier, M., 2014. Kinetics of tracheid development explain conifer tree-ring structure. New Phytologist 203, 1231–1241. https://doi.org/10.1111/nph.12871

D'Arrigo, R., Wilson, R., Anchukaitis, K.J., 2013. Volcanic cooling signal in tree ring temperature records for the past millennium. Journal of Geophysical Research: Atmospheres 118, 9000–9010. https://doi.org/10.1002/jgrd.50692

D'Arrigo, R., Wilson, R., Jacoby, G., 2006. On the long-term context for late twentieth century warming. Journal of Geophysical Research: Atmospheres 111. https://doi.org/10.1029/2005JD006352

De Mil, T., Matskovskiy, V., Salzer, M., Corluy, L., Verschuren, L., Pearson, C., Van Hoorebeke, L., Trouet, V., Van den Bulcke, J., 2024. Bristlecone Pine Maximum Latewood Density as a Superior Proxy for Millennium-length Temperature Reconstructions. Authorea Preprints.

De Mil, T., Vannoppen, A., Beeckman, H., Van Acker, J., Van den Bulcke, J., 2016. A field-to-desktop toolchain for X-ray CT densitometry enables tree ring analysis. Ann Bot 117, 1187–1196. https://doi.org/10.1093/aob/mcw063

De Silva, S.L., Zielinski, G.A., 1998. Global influence of the AD 1600 eruption of Huaynaputina, Peru. Nature 393, 455–458. https://doi.org/10.1038/30948

Delpierre, N., Lireux, S., Hartig, F., Camarero, J.J., Cheaib, A., Čufar, K., Cuny, H., Deslauriers, A., Fonti, P., Gričar, J., others, 2019. Chilling and forcing temperatures interact to predict the onset of wood formation in Northern Hemisphere conifers. Glob Chang Biol 25, 1089–1105.

Donaldson, L.A., 2001. Lignification and lignin topochemistry - An ultrastructural view. Phytochemistry 57, 859–873. https://doi.org/10.1016/S0031-9422(01)00049-8

Donaldson, L.A., 1994. Mechanical constraints on lignin deposition during lignification. Wood Sci Technol 28, 111–118.

Donaldson, L.A., 1993. Lignin distribution in wood from a progeny trial of genetically selected Pinus radiata D. Don. Wood Sci Technol 27, 391–395. https://doi.org/10.1007/BF00192226

Donaldson, L.A., 1992. Lignin distribution during latewood formation in Pinus radiata D. Don. IAWA J 13, 381–387.

Donaldson, L.A., 1991. Seasonal changes in lignin distribution during tracheid development in Pinus radiata D. Don. Wood Sci Technol 25, 15–24. https://doi.org/10.1007/BF00195553

Du, J., Groover, A., 2010. Transcriptional regulation of secondary growth and wood formation. J Integr Plant Biol 52, 17–27.

Dutton, E.G., Christy, J.R., 1992. Solar radiative forcing at selected locations and evidence for global lower tropospheric cooling following the eruptions of El Chichón and Pinatubo. Geophys Res Lett 19. https://doi.org/10.1029/92GL02495

Eckstein, D., 2013. 'A new star'--but why just parenchyma for dendroclimatology? New Phytologist 198, 328–330.

Esper, J., Büntgen, U., Hartl-Meier, C., Oppenheimer, C., Schneider, L., 2017. Northern Hemisphere temperature anomalies during the 1450s period of ambiguous volcanic forcing. Bull Volcanol 79, 41. https://doi.org/10.1007/s00445-017-1125-9

Esper, J., Büntgen, U., Timonen, M., Frank, D.C., 2012. Variability and extremes of northern Scandinavian summer temperatures over the past two millennia. Glob Planet Change 88–89, 1–9. https://doi.org/10.1016/j.gloplacha.2012.01.006

Esper, J., Schneider, L., Krusic, P.J., Luterbacher, J., Büntgen, U., Timonen, M., Sirocko, F., Zorita, E., 2013. European summer temperature response to annually dated volcanic eruptions over the past nine centuries. Bull Volcanol 75, 736. https://doi.org/10.1007/s00445-013-0736-z

Esper, J., Schneider, L., Smerdon, J.E., Schöne, B.R., Büntgen, U., 2015. Signals and memory in tree-ring width and density data. Dendrochronologia (Verona) 35, 62–70. https://doi.org/10.1016/j.dendro.2015.07.001

Fang, S., Sigl, M., Toohey, M., Jungclaus, J., Zanchettin, D., Timmreck, C., 2023. The Role of Small to Moderate Volcanic Eruptions in the Early 19th Century Climate. Geophys Res Lett 50. https://doi.org/10.1029/2023GL105307

Ferguson, C.W., 1979. Dendrochronology of bristlecone pine, Pinus longaeva. Environ Int 2, 209–214. https://doi.org/10.1016/0160-4120(79)90003-5

Ferguson, C.W., 1969. A 7104-Year Annual Tree-Ring Chronology for Bristlecone Pine, Pinus Aristata, from the White Mountains, California. Tree-Ring Bulletin.

Fonti, P., Bryukhanova, M. V., Myglan, V.S., Kirdyanov, A. V., Naumova, O. V., Vaganov, E.A., 2013. Temperature-induced responses of xylem structure of *Larix sibirica* (Pinaceae) from the Russian Altay. Am J Bot 100, 1332–1343. https://doi.org/10.3732/ajb.1200484

Frank, D., Büntgen, U., Böhm, R., Maugeri, M., Esper, J., 2007. Warmer early instrumental measurements versus colder reconstructed temperatures: shooting at a moving target. Quat Sci Rev 26, 3298–3310. https://doi.org/10.1016/j.quascirev.2007.08.002

Fritts, H.C., 1976. Tree Rings and Climate. Academic Press, New York. https://doi.org/10.1126/science.197.4301.361.b

Fujino, T., Itoh, T., 1998. Changes in the three dimensional architecture of the cell wall during lignification of xylem cells in Eucalyptus tereticornis.

Gao, C., Robock, A., Ammann, C., 2008. Volcanic forcing of climate over the past 1500 years: An improved ice core-based index for climate models. Journal of Geophysical Research: Atmospheres 113. https://doi.org/10.1029/2008JD010239

Gao, C., Robock, A., Self, S., Witter, J.B., Steffenson, J.P., Clausen, H.B., Siggaard-Andersen, M., Johnsen, S., Mayewski, P.A., Ammann, C., 2006. The 1452 or 1453 A.D. Kuwae eruption signal derived from multiple ice core records: Greatest volcanic sulfate event of the past 700 years. Journal of Geophysical Research: Atmospheres 111. https://doi.org/10.1029/2005JD006710

Gao, J., Yang, B., Peng, X., Rossi, S., 2021. Tracheid development under a drought event producing intra-annual density fluctuations in the semi-arid China. Agric For Meteorol 308, 108572.

Gärtner, H., Lucchinetti, S., Schweingruber, F.H., 2014. New perspectives for wood anatomical analysis in dendrosciences: The GSL1-microtome. Dendrochronologia (Verona) 32, 47–51. https://doi.org/10.1016/j.dendro.2013.07.002

Gärtner, H., Schweingruber, F., 2013. Microscopic preparation techniques for plant stem analysis. Verlag Dr. Kessel, Remagen-Oberwinter.

Gerlach, D., 1969. Botanische mikrotechnik. Georg Thieme Verlag.

Gierlinger, N., Keplinger, T., Harrington, M., 2012. Imaging of plant cell walls by confocal Raman microscopy. Nat Protoc 7, 1694–1708. https://doi.org/10.1038/nprot.2012.092

Gierlinger, N., Schwanninger, M., 2006. Chemical Imaging of Poplar Wood Cell Walls by Confocal Raman Microscopy. Plant Physiol 140, 1246–1254. https://doi.org/10.1104/pp.105.066993

Gindl, W., 2001. CELL-WALL LIGNIN CONTENT RELATED TO TRACHEID DIMENSIONS IN DROUGHT-SENSITIVE AUSTRIAN PINE (PINUS NIGRA). IAWA J 22, 113–120. https://doi.org/10.1163/22941932-90000272

Gindl, W., Grabner, M., Wimmer, R., 2001. Effects of altitude on tracheid differentiation and lignification of Norway spruce. Canadian Journal of Botany 79, 815–821. https://doi.org/10.1139/b01-060

Gindl, W., Grabner, M., Wimmer, R., 2000. The influence of temperature on latewood lignin content in treeline Norway spruce compared with maximum density and ring width. Trees - Structure and Function 14, 409–414. https://doi.org/10.1007/s004680000057

Glerum, C., Farrar, J.L., 1966. Frost Ring Formation in the Stems of Some Coniferous Species. Canadian Journal of Botany 44, 879–886. https://doi.org/10.1139/b66-103

Greaves, C., Crivellaro, A., Piermattei, A., Krusic, P.J., Oppenheimer, C., Potapov, A., Hordo, M., Metslaid, S., Kask, R., Kangur, A., Büntgen, U., 2022. Remarkably high blue ring occurrence in Estonian Scots pines in 1976 reveals wood anatomical evidence of extreme autumnal cooling. Trees. https://doi.org/10.1007/s00468-022-02366-1

Gurskaya, M.A., 2014. Temperature conditions of the formation of frost damages in conifer trees in the high latitudes of Western Siberia. Biology Bulletin 41, 187–196.

Gurskaya, M.A., Shiyatov, S.G., 2006. Distribution of frost injuries in the wood of conifers. Russ J Ecol 37, 7–12. https://doi.org/10.1134/S1067413606010024

Hadad, M., Tardif, J.C., Conciatori, F., Waito, J., Westwood, A., 2020. Climate and atmospheric circulation related to frost-ring formation in Picea mariana trees from the Boreal Plains, interior North America. Weather Clim Extrem 29, 100264.

Hantemirov, R.M., Shiyatov, S.G., 2002. A continuous-multimillennial ring-width chronology in Yamal, northwestern Siberia. Holocene 12, 717–726. https://doi.org/10.1191/0959683602hl585rp

Helama, S., Lindholm, M., Timonen, M., Meriläinen, J., Eronen, M., 2002. The supra-long Scots pine tree-ring record for Finnish Lapland: Part 2, interannual to centennial variability in summer temperatures for 7500 years. Holocene 12, 681–687. https://doi.org/10.1191/0959683602hl581rp

Helama, S., Saranpää, P., Pearson, C.L., Arppe, L., Holopainen, J., Mäkinen, H., Mielikäinen, K., Nöjd, P., Sutinen, R., Taavitsainen, J.P., Timonen, M., Uusitalo, J., Oinonen, M., 2019. Frost rings in 1627 BC and AD 536 in subfossil pinewood from Finnish Lapland. Quat Sci Rev 204, 208–215. https://doi.org/10.1016/j.quascirev.2018.11.031

Huang, J.-G., Ma, Q., Rossi, S., Biondi, F., Deslauriers, A., Fonti, P., Liang, E., Mäkinen, H., Oberhuber, W., Rathgeber, C.B.K., Tognetti, R., Treml, V., Yang, B., Zhang, J.-L., Antonucci, S., Bergeron, Y., Camarero, J.J., Campelo, F., Čufar, K., Cuny, H.E., De Luis, M., Giovannelli, A., Gričar, J., Gruber, A., Gryc, V., Güney, A., Guo, X., Huang, W., Jyske, T., Kašpar, J., King, G., Krause, C., Lemay, A., Liu, F., Lombardi, F., del Castillo, E., Morin, H., Nabais, C., Nöjd, P., Peters, R.L., Prislan, P., Saracino, A., Swidrak, I., Vavrč\'\ik, H., Vieira, J., Yu, B., Zhang, S., Zeng, Q., Zhang, Y., Ziaco, E., 2020. Photoperiod and temperature as dominant environmental drivers triggering secondary growth resumption in Northern Hemisphere conifers. Proceedings of the National Academy of Sciences 117, 20645–20652. https://doi.org/10.1073/pnas.2007058117

Hughes, M.K., Vaganov, E.A., Shiyatov, S., Touchan, R., Funkhouser, G., 1999. Twentieth-century summer warmth in northern Yakutia in a 600-year context. Holocene 9, 629–634. https://doi.org/10.1191/095968399671321516

Hughes, M.K., Funkhouser, G., 1998. Extremes of moisture availability reconstructed from tree rings for recent millennia in the Great Basin of western North America. The impacts of climate variability on forests 99–107. https://doi.org/https://doi.org/10.1007/BFb0009768

Kidd, K.R., Copenheaver, C.A., Zink-Sharp, A., 2014. Frequency and factors of earlywood frost ring formation in jack pine (Pinus banksiana) across northern lower Michigan. Ecoscience 21, 157–167.

Kipfmueller, K.F., Salzer, M.W., 2010. Linear trend and climate response of five-needle pines in the western United States related to treeline proximity. Canadian Journal of Forest Research 40, 134–142.

Kozlowski, T.T., Pallardy, S.G., 1997. Growth control in woody plants. Elsevier.

LaMarche Jr, V.C., 1970. Frost-damage rings in subalpine conifers and their application to tree-ring dating problems. Smith, JH G., and Worrall, J.(eds.), Tree-ring Analysis with

Special Reference to Northwest America. University of British Columbia Faculty of Forestry Bulletin 99–100.

LaMarche Jr, V.C., 1974. Paleoclimatic Inferences from Long Tree-Ring Records: Intersite comparison shows climatic anomalies that may be linked to features of the general circulation. Science (1979) 183, 1043–1048. https://doi.org/DOI: 10.1126/science.183.4129.1043

LaMarche, V.C., Hirschboeck, K.K., 1984. Frost rings in trees as records of major volcanic eruptions. Nature. https://doi.org/https://doi.org/10.1038/307121a0

LaMarche, V.C., Stockton, C.W., 1974. Chronologies from temperature-sensitive bristlecone pines at upper treeline in western United States. Tree-Ring Bulletin 34, 21–45.

Mann, M.E., Cane, M.A., Zebiak, S.E., Clement, A., 2005. Volcanic and Solar Forcing of the Tropical Pacific over the Past 1000 Years. J Clim 18, 447–456. https://doi.org/10.1175/JCLI-3276.1

Matisons, R., Gärtner, H., Elferts, D., Kārkliņa, A., Adamovičs, A., Jansons, Ā., 2020. Occurrence of 'blue' and 'frost' rings reveal frost sensitivity of eastern Baltic provenances of Scots pine. For Ecol Manage 457, 117729. https://doi.org/https://doi.org/10.1016/j.foreco.2019.117729

Matulewski, P., Buchwal, A., Zielonka, A., Wrońska-Wałach, D., Čufar, K., Gärtner, H., 2021. Trampling as a major ecological factor affecting the radial growth and wood anatomy of Scots pine (Pinus sylvestris L.) roots on a hiking trail. Ecol Indic 121, 107095. https://doi.org/10.1016/j.ecolind.2020.107095

McAneney, J., Baillie, M., 2019. Absolute tree-ring dates for the Late Bronze Age eruptions of Aniakchak and Thera in light of a proposed revision of ice-core chronologies. Antiquity 93, 99–112. https://doi.org/10.15184/aqy.2018.165

Miyake, F., Nagaya, K., Masuda, K., Nakamura, T., 2012. A signature of cosmic-ray increase in ad 774"775 from tree rings in Japan. Nature 486. https://doi.org/10.1038/nature11123

Montwé, D., Isaac-Renton, M., Hamann, A., Spiecker, H., 2018. Cold adaptation recorded in tree rings highlights risks associated with climate change and assisted migration. Nat Commun 9, 1–7. https://doi.org/10.1038/s41467-018-04039-5

Morino, K., Minor, R.L., Barron-Gafford, G.A., Brown, P.M., Hughes, M.K., 2021. Bimodal cambial activity and false-ring formation in conifers under a monsoon climate. Tree Physiol.

Mutwil, M., Debolt, S., Persson, S., 2008. Cellulose synthesis: a complex complex. Curr Opin Plant Biol 11, 252–257.

Nabais, C., Campelo, F., Vieira, J., Cherubini, P., 2014. Climatic signals of tree-ring width and intra-annual density fluctuations in Pinus pinaster and Pinus pinea along a latitudinal gradient in Portugal. Forestry. https://doi.org/10.1093/forestry/cpu021

Oppenheimer, C., 2003. Climatic, environmental and human consequences of the largest known historic eruption: Tambora volcano (Indonesia) 1815. Progress in Physical

Geography: Earth and Environment 27, 230–259. https://doi.org/10.1191/0309133303pp379ra

Panyushkina, I.P., Hughes, M.K., Vaganov, E.A., Munro, M.A.R., 2003. Summer temperature in northeastern Siberia since 1642 reconstructed from tracheid dimensions and cell numbers of Larix cajanderi. Canadian Journal of Forest Research. https://doi.org/10.1139/x03-109

Payette, S., Delwaide, A., Simard, M., 2010. Frost-ring chronologies as dendroclimatic proxies of boreal environments. Geophys Res Lett 37, 1–6. https://doi.org/10.1029/2009GL041849

Perrot-Rechenmann, C., 2010. Cellular responses to auxin: division versus expansion. Cold Spring Harb Perspect Biol 2, a001446.

Piermattei, A., Crivellaro, A., Carrer, M., Urbinati, C., 2015. The "blue ring": anatomy and formation hypothesis of a new tree-ring anomaly in conifers. Trees 29, 613–620. https://doi.org/10.1007/s00468-014-1107-x

Piermattei, A., Crivellaro, A., Krusic, P.J., Esper, J., Vítek, P., Oppenheimer, C., Felhofer, M., Gierlinger, N., Reinig, F., Urban, O., Verstege, A., Lobo, H., Büntgen, U., 2020. A millennium-long 'Blue Ring' chronology from the Spanish Pyrenees reveals severe ephemeral summer cooling after volcanic eruptions. Environmental Research Letters 15, 124016. https://doi.org/10.1088/1748-9326/abc120

Proseus, T.E., Boyer, J.S., 2006. Periplasm turgor pressure controls wall deposition and assembly in growing Chara corallina cells. Ann Bot 98, 93–105.

Rathgeber, C.B.K., Cuny, H.E., Fonti, P., 2016. Biological basis of tree-ring formation: a crash course. Front Plant Sci 7, 734.

Ren, P., Rossi, S., Gricar, J., Liang, E., Cufar, K., 2015. Is precipitation a trigger for the onset of xylogenesis in Juniperus przewalskii on the north-eastern Tibetan Plateau? Ann Bot 115, 629–639.

Robock, A., 2000. Volcanic eruptions and climate. Reviews of geophysics 38, 191–219.

Robock, A., Mao, J., 1992. Winter warming from large volcanic eruptions. Geophys Res Lett 19, 2405–2408.

Rossi, S., Deslauriers, A., Anfodillo, T., Carraro, V., 2007. Evidence of threshold temperatures for xylogenesis in conifers at high altitudes. Oecologia 152, 1–12.

Saleh, T.M., Leney, L., Sarkanen, K. V, 1967. Radioautographic studies of cottonwood, Douglas fir and wheat plants.

Salzer, M.W., Bunn, A.G., Graham, N.E., Hughes, M.K., 2014a. Five millennia of paleotemperature from tree-rings in the Great Basin, USA. Clim Dyn 42, 1517–1526.

Salzer, M.W., Hughes, M.K., 2007. Bristlecone pine tree rings and volcanic eruptions over the last 5000 yr. Quat Res 67, 57–68. https://doi.org/10.1016/j.yqres.2006.07.004

Salzer, M.W., Hughes, M.K., Bunn, A.G., Kipfmueller, K.F., 2009. Recent unprecedented tree-ring growth in bristlecone pine at the highest elevations and possible causes. Proc Natl Acad Sci U S A 106, 20348–20353. https://doi.org/10.1073/pnas.0903029106

Salzer, M.W., Kipfmueller, K.F., 2005. Reconstructed temperature and precipitation on a millennial timescale from tree-rings in the southern Colorado Plateau, U.S.A. Clim Change 70, 465–487. https://doi.org/10.1007/s10584-005-5922-3

Salzer, M.W., Larson, E.R., Bunn, A.G., Hughes, M.K., 2014b. Changing climate response in near-treeline bristlecone pine with elevation and aspect. Environmental Research Letters 9, 114007. https://doi.org/10.1088/1748-9326/9/11/114007

Saranpää, P., 2003. Wood density and growth. Wood quality and its biological basis 87–117.

Schneider, L., Smerdon, J.E., Büntgen, U., Wilson, R.J.S., Myglan, V.S., Kirdyanov, A. V., Esper, J., 2015. Revising midlatitude summer temperatures back to A.D. 600 based on a wood density network. Geophys Res Lett 42, 4556–4562. https://doi.org/10.1002/2015GL063956

Schulman, E., 1958. Bristlecone pine, oldest known living thing. Nat Geogr Mag 113, 355–372.

Schulman, E., Ferguson, C., 1956. Millenia-old pine trees sampled in 1954 and 1955, in: Schulman, E. (Ed.), Dendroclimatic Changes in Semiarid America. University of Arizona Press, Tucson AZ, pp. 136–138.

Schweingruber, F.H., 2007. Wood structure and environment. Springer Science \& Business Media.

Siekacz, L., Pearson, C., Salzer, M., Soja-Kukieła, N., Koprowski, M., 2024. Blue rings in Bristlecone pine as a high resolution indicator of past cooling events. Clim Change 177, 123. https://doi.org/10.1007/s10584-024-03773-8

Sigl, M., Toohey, M., McConnell, J.R., Cole-Dai, J., Severi, M., 2022. Volcanic stratospheric sulfur injections and aerosol optical depth during the Holocene (past 11 500 years) from a bipolar ice-core array. Earth Syst Sci Data 14, 3167–3196. https://doi.org/10.5194/essd-14-3167-2022

Sigl, M., Winstrup, M., McConnell, J.R., Welten, K.C., Plunkett, G., Ludlow, F., Büntgen, U., Caffee, M., Chellman, N., Dahl-Jensen, D., Fischer, H., Kipfstuhl, S., Kostick, C., Maselli, O.J., Mekhaldi, F., Mulvaney, R., Muscheler, R., Pasteris, D.R., Pilcher, J.R., Salzer, M., Schüpbach, S., Steffensen, J.P., Vinther, B.M., Woodruff, T.E., 2015. Timing and climate forcing of volcanic eruptions for the past 2,500 years. Nature 523, 543–549. https://doi.org/10.1038/nature14565

Stoffel, M., 2008. Dating past geomorphic processes with tangential rows of traumatic resin ducts. Dendrochronologia (Verona) 26, 53–60.

Stoffel, M., Schneuwly, D., Bollschweiler, M., Lièvre, I., Delaloye, R., Myint, M., Monbaron, M., 2005. Analyzing rockfall activity (1600–2002) in a protection forest—a case study using dendrogeomorphology. Geomorphology 68, 224–241. https://doi.org/10.1016/j.geomorph.2004.11.017

Stokes, M.A., 1996. An introduction to tree-ring dating. University of Arizona Press.

Tardif, J.C., Girardin, M.P., Conciatori, F., 2011. Light rings as bioindicators of climate change in Interior North America. Glob Planet Change 79, 134–144.

Tardif, J.C., Salzer, M.W., Conciatori, F., Bunn, A.G., Hughes, M.K., 2020. Formation, structure and climatic significance of blue rings and frost rings in high elevation bristlecone pine (Pinus longaeva D.K. Bailey). Quat Sci Rev 244, 106516. https://doi.org/https://doi.org/10.1016/j.quascirev.2020.106516

Timmreck, C., 2012. Modeling the climatic effects of large explosive volcanic eruptions. WIREs Climate Change 3, 545–564. https://doi.org/10.1002/wcc.192

Toohey, M., Sigl, M., 2017. Volcanic stratospheric sulfur injections and aerosol optical depth from 500 BCE to 1900 CE 809–831.

Touchan, R., Meko, D.M., Aloui, A., 2008. Precipitation reconstruction for Northwestern Tunisia from tree rings. J Arid Environ 72, 1887–1896. https://doi.org/10.1016/j.jaridenv.2008.05.010

Tran, T.J., Bruening, J.M., Bunn, A.G., Salzer, M.W., Weiss, S.B., 2017. Cluster analysis and topoclimate modeling to examine bristlecone pine tree-ring growth signals in the Great Basin, USA. Environmental Research Letters 12. https://doi.org/10.1088/1748-9326/aa5388

Trendelenburg, 1939. Das Holz als Rohstoff. Lehmanns, Munich.

Ursache, R., Nieminen, K., Helariutta, Y., 2013. Genetic and hormonal regulation of cambial development. Physiol Plant 147, 36–45.

Van den Bulcke, J., Wernersson, E.L.G., Dierick, M., Van Loo, D., Masschaele, B., Brabant, L., Boone, M.N., Van Hoorebeke, L., Haneca, K., Brun, A., Luengo Hendriks, C.L., Van Acker, J., 2014. 3D tree-ring analysis using helical X-ray tomography. Dendrochronologia (Verona) 32, 39–46. https://doi.org/10.1016/j.dendro.2013.07.001

Vanholme, R., Demedts, B., Morreel, K., Ralph, J., Boerjan, W., 2010. Lignin biosynthesis and structure. Plant Physiol 153, 895–905.

Versace, S., Battipaglia, G., Tognetti, R., Garf\`\i, V., Gianelle, D., Cherubini, P., 2021. Intra-annual density fluctuations in silver fir are triggered by drought conditions. Trees 1–15.

Vidal, C.M., Métrich, N., Komorowski, J.-C., Pratomo, I., Michel, A., Kartadinata, N., Robert, V., Lavigne, F., 2016. The 1257 Samalas eruption (Lombok, Indonesia): the single greatest stratospheric gas release of the Common Era. Sci Rep 6, 34868. https://doi.org/10.1038/srep34868

von Arx, G., Carrer, M., 2014. ROXAS – A new tool to build centuries-long tracheid-lumen chronologies in conifers. Dendrochronologia (Verona) 32, 290–293. https://doi.org/10.1016/j.dendro.2013.12.001

Wang, L., Payette, S., Bégin, Y., 2000. A Quantitative Definition of Light Rings in Black Spruce (Picea mariana) at the Arctic Treeline in Northern Québec, Canada . Arct Antarct Alp Res 32, 324–330. https://doi.org/10.1080/15230430.2000.12003370

Wilson, R., Anchukaitis, K., Briffa, K.R., Büntgen, U., Cook, E., D'Arrigo, R., Davi, N., Esper, J., Frank, D., Gunnarson, B., Hegerl, G., Helama, S., Klesse, S., Krusic, P.J., Linderholm, H.W., Myglan, V., Osborn, T.J., Rydval, M., Schneider, L., Schurer, A.,

Wiles, G., Zhang, P., Zorita, E., 2016. Last millennium northern hemisphere summer temperatures from tree rings: Part I: The long term context. Quat Sci Rev 134, 1–18. https://doi.org/10.1016/j.quascirev.2015.12.005

Zhang, X., 2021. Visualising lignin quantitatively in plant cell walls by micro-Raman spectroscopy. RSC Adv 11, 13124–13129. https://doi.org/10.1039/D1RA01825F

Zhong, R., Ye, Z.-H., 2015. Secondary cell walls: biosynthesis, patterned deposition and transcriptional regulation. Plant Cell Physiol 56, 195–214.

Zhong, R., Ye, Z.-H., 2009. Secondary cell walls. eLS.

Ziaco, E., Truettner, C., Biondi, F., Bullock, S., 2018. Moisture-driven xylogenesis in Pinus ponderosa from a Mojave Desert mountain reveals high phenological plasticity. Plant Cell Environ 41, 823–836.

Ziaco, E., Biondi, F., Rossi, S., Deslauriers, A., 2016. Environmental drivers of cambial phenology in Great Basin bristlecone pine. Tree Physiol 36, 818–831. https://doi.org/10.1093/treephys/tpw006